1999

Determination of failure mode and efficiency for single angles in tension.

James M. Dunlop
University of Windsor

INFORMATION TO USERS

This manuscript has been reproduced from the microfilm master. UMI films the text directly from the original or copy submitted. Thus, some thesis and dissertation copies are in typewriter face, while others may be from any type of computer printer.

The quality of this reproduction is dependent upon the quality of the copy submitted. Broken or indistinct print, colored or poor quality illustrations and photographs, print bleedthrough, substandard margins, and improper alignment can adversely affect reproduction.

In the unlikely event that the author did not send UMI a complete manuscript and there are missing pages, these will be noted. Also, if unauthorized copyright material had to be removed, a note will indicate the deletion.

Oversize materials (e.g., maps, drawings, charts) are reproduced by sectioning the original, beginning at the upper left-hand corner and continuing from left to right in equal sections with small overlaps.

Photographs included in the original manuscript have been reproduced xerographically in this copy. Higher quality 6" x 9" black and white photographic prints are available for any photographs or illustrations appearing in this copy for an additional charge. Contact UMI directly to order.

Bell & Howell Information and Learning
300 North Zeeb Road, Ann Arbor, MI 48106-1346 USA
800-521-0600

Determination of Failure Mode and Efficiency

For Single Angles In Tension

by
James Dunlop B.A.Sc.

A Thesis
submitted to the College of Graduate Studies and Research
through the Civil and Environmental Engineering Department
in Partial Fulfillment
of the Requirements for the degree of
Master of Applied Science
at the University of Windsor

Windsor, Ontario, Canada
1999

900209

I hereby declare that I am the sole author of this document.

I authorize the University of Windsor to lend this document to other institutions or individuals for the purpose of scholarly research.

James Dunlop

I further authorize the University of Windsor to reproduce the document by photocopying or by other means, in total or in part, at the request of other institutions or individuals for the purpose of scholarly research.

James Dunlop

The UNIVERSITY OF WINDSOR requires the signatures of all persons using or photocopying this document.

Please sign below, and give address and date.

ABSTRACT

A number of tensile tests were performed in order to determine if the formulae in the Canadian Standards Association CSA-S16.1-94, are valid for single angles. The experiments consisted of applying a tension load to a single angle specimen while recording strain distribution at mid-span, elongation, yielding pattern, failure load and the mode of failure. Length and connection size are the two variables considered in this research.

Failure of all the specimens tested was by net-section through the bolt hole closest to the mid-span. This result was predicted by the equation developed by Temple. Limitations in the design apparatus excluded all angles which were predicted to fail across the gross cross-section. Sample calculations predicting the gross-cross sectional failure were completed.

Angle efficiency calculated using Kulak and Wu's equation provide excellent results when compared with efficiencies in S16.1.

ACKNOWLEDGEMENTS

The author wishes to express his sincere gratitude to his advisor Dr. M.C Temple, who supervised the research of this thesis, and for his guidance throughout this research. Special thanks are also due to Mr. Richard Clark and Mr. Dieter Liebsch and all the technicians at the Technical Support Centre for their assistance in the preparation of the test specimens and test apparatus.

TABLE OF CONTENTS

LIST OF FIGURES

LIST OF TABLES

LIST OF SYMBOLS

A_{cn} = the area of the connected leg

A_g = gross area

A_n = the critical net area

A'_{ne} = effective net area reduced for shear lag

A_o = area of unconnected leg

F_y = yield stress

F_u = ultimate tensile stress

P_u = the maximum load from testing

T_R = the factored tensile resistance

β = 1.0 for members with four or more fasteners, 0.5 or members with fewer than four

ϕ = resistance factor

CHAPTER I

INTRODUCTION

1.1 General

Angles in tension are used widely in the construction industry as bracing members in buildings, to support members in transmission towers, etc. In the design of these members, whatever the use may be, a set of equations governs the maximum load the angle can carry. These equations can be found in Clause 13.2 (a) of CAN/CSA-S16.1-94, "Limit States Design of Steel Structures" (CSA 94). The equations that set the limits for gross cross-sectional failure, net-section failure and for shear lag failure are:

[1] $T_R = \phi A_g F_y$
[2] $T_R = 0.85\phi A_{ne} F_u$
[3] $T_R = 0.85\phi A'_{ne} F_u$

where T_R = the tensile resistance, F_y = yield stress, F_u = ultimate tensile stress A_g = gross area, A_n = the critical net area, A'_{ne} = effective net area reduced for shear lag

It is the first failure mode that is of interested in this research. It is the objective of this research to determine if the first equation, should be considered as a failure mode. At the last revision of the Standard there was considerable debate by the CSA-S16.1 Committee as to whether or not the gross section failure equation should be used for the design of angles. Some believed it should be considered while others thought otherwise. The reason for the debate is that for the first equation to be a failure mode it is assumed that there is a constant state of stress across the entire section of the angle. When angles have only one leg connected the stress does not develop equally across the section. This is why the other equations in Clause 13.2 (a) are required. From this debate questions arise, which are, "How do we know whether the angle will fail by gross-section failure or

by net-section failure?" and " Are there angles that fail by gross-section but have been designed for net-section failure?" If the structure was designed for net-section failure when it actually fails by gross-section, failure is not a problem from a load carrying point a view. It means the structure will be able to carry a higher load safely. The issue is that if the structure has been over designed then it is not the most economical design and money has been wasted in this structure. This leads us to the objectives of this research.

1.2 Objective

The objective of this research is to study the behaviour of single angles in tension. The research will include the study of the mode of failure, effect of length and connection size on: (a) ultimate load; (b) efficiency of the angles; (c) strain distribution at mid section; (d) total elongation; and (e) start point of yielding and its propagation along the member. Through this research it is hoped to predict the failure mode (gross-section or net-section failure), and thus determine if the gross-section failure equation can be considered a failure mode.

1.3 Research Overview

The experimental research included the testing of single angles under tension loads. The angles are connected to gusset plates using a single line of bolts. The test members had two different lengths and two connection sizes. All specimens tested had three strain gauges placed at mid-span and a dial gauge to measure total elongation. The strain gauges where placed to determine strain distribution at mid-span as load was increased to specimen failure. The dial gauge was placed to determine how the elongation varied as the load was increased to member failure.

CHAPTER II

LITERATURE REVIEW

2.1 Previous Studies

In completing a literature review on research involving tension test on angles several papers were studied that are related to the topic of this research. They are summarized in the following paragraphs.

Kulak and Wu (1997) completed research on net-section properties of tension angles. They found that the net section strength of a single angle member is not affected by changes in member length. Also the angle thickness has little effect on net-section efficiency. The net-section efficiency of single and double angles can be treated as practically the same. Net-section efficiencies with three or fewer fasteners per line are significantly lower than members with four or more fasteners per line. They also found that the degree of end restraint applied to the end of single angles by gusset plates has little effect on net-section strength. From their research they developed the efficiency equation,

[4] $U = \{A_{cn} + \beta(F_y/F_u)A_o\} / A_n$

β = 1.0 for members with four or more fasteners, 0.5 or members with fewer than four,
A_{cn} = the area of the connected leg, A_o = area of unconnected leg

Temple (1998) has raised the question of whether or not some angles are being designed for net section failure when gross cross sectional failure should be considered as a failure mode. In this discussion it is proposed that an equation be used that should predict whether the angle member will fail through the net section or across the gross cross section. The equation is as follows:

[5] $A_g \leq A'_{ne}(F_u / F_y)$

The explanation as to where this equation comes from is done in Chapter IV.

In 1906 McKibben tested single and double angles to determine the ultimate strength of the angles in tension. He discovered that double angles with net and gross sectional area less than that of the single angle with dimensions twice the size had failure loads that were greater in every case. In 1907 McKibben noted that the efficiency is better when the center of pull coincides with the center of gravity instead of the gauge line.

Research done in 1953 by Nelson, tested eighteen angles where the length and connections varied. He developed equations based on three stages of loading. The three stages are identified by elongation and guided by the strain readings. The first stage had small overall elongations and uniform rate of deflection suggesting the elastic range. The first stage ends when the critical section has yielded. The second stage has elongations in the inelastic range. This stage ends when centroid of the angle lines up with the line of pull. The third stage starts when the centroid and the line of pull coincide and ends when the angle fails. He concluded that the strength design should be based on the first stage equation. This equation is based on the product of the yield strength and the net-section area.

CHAPTER III

EXPERIMENTAL PROCEDURE

3.1 General

Experimental testing was performed to obtain data on the strain distribution at mid-span of all the specimens. As well, data on the total elongation and yield propagation was recorded. All specimens were designed in accordance with CSA S16.1. In order to collect the data required two lengths and two connection sizes were used. Bolt size was held constant at 19 mm (3/4 in) for all specimens tested. The first specimen length was 5000 mm. The other specimen length was 1000 mm. The connections used were either 3 or 4-bolt.

3.2 Test Specimens

The test group consisted of single angles of size 64x64x6.4 mm. This test group consisted of twelve angles. Half of the specimens had a length measuring 5000 mm, while the remaining had a length of 1000 mm. The specimens were used to determine the strain distribution at mid-span, total elongation, starting point of yielding, propagation of yielding and to determine failure mode.

3.3 Preparation of Test Specimens

In testing angles each specimen requires a certain amount of preparation before testing occurs. The first three specimens tested were angles with dimensions 64x64x6.4 mm, 5000 mm in length with a 3-bolt connection. The next three specimens tested were angles with dimensions 64x64x6.4 mm, 5000 mm in length with a 4-bolt connection.

The remaining six angles were similar to the first six, the length being the only difference. For the remaining six the length was reduced to 1000 mm. Table 1 gives a summary of the angle dimensions. On all of the specimens tested the strain gauges were placed in the same area. All gauges were located at mid-span. This area where the gauge was to be placed had to be prepared so that it was totally smooth and free of any kind of dirt. Two of the gauges were placed on the connected leg such that they divided the angle leg into three equal sections. The remaining gauge was located at the center of the unconnected leg. The connection holes were drilled with a diameter of 22 mm to accommodate 19 mm diameter bolts. The holes had a center-to-center distance of 65 mm, an end distance of 34 mm and were located a distance of 35 mm from the heel. Figure 1 (a) to (d) show the dimension details of the four different angle types.

In order to determine where the test specimen began to yield a layer of white wash was required. All specimens being tested required this white wash coating. The white wash consists of a lime powder mixed with water. The white wash was prepared so that its consistency would allow a coating thick enough to change the colour of the angles to white. The white wash coating was allowed to dry for sixty minutes before testing.

3.4 Test Set-up

Testing was done entirely in the Structural Engineering Laboratory at the University of Windsor. The testing apparatus was built to accommodate a maximum load of 400 kN and a maximum length of 5000 mm. The apparatus could be arranged to accommodate a length of 1000 mm. Figure 2 shows the apparatus as it was built. The remainder of this section describes the parts and equipment used in the apparatus.

3.4.1 End Connection

All specimens were bolted to a gusset plate which had a pin connection to the load cell and the fixed portion of the set-up. The angle specimen was allowed some movement in the y-y axis as well as in the x-x axis. This movement was allowed by the pin connection at the load cell and the result of testing single angles. The end connection detail is shown in Figure 3.

3.4.2 Load Cell and Jack

The load cell and hydraulic jack were able to support and deliver the design load of 400 kN required for testing. The load cell was calibrated using the universal testing machine to obtain the load-strain relationship required for testing. The load cell was wired to a strain indicator box which gave readings in microstrain. The calibration curve is shown in Figure 4.

3.4.3 Test Apparatus

The specimens were tested horizontally in the Civil Engineering Laboratory. At the load cell end the angles were bolted to gusset plates which were connected to the load cell using a pin connection. The load cell was bolted to a support frame. At the other end the angles were bolted to gusset plates which were connected to the support frame using a pin connection. The support frame was bolted to the floor using four bolts. Figure 2 shows an assembly drawing of this system.

3.4.4 Strain Gauges

Showa foil strain gauges were used on all the test specimens. These gauges had a resistance of 120 ohms (Ω) and 5 mm gauge length. Figure 5 shows strain gauge placement.

3.5 Test Procedure

The procedure for testing was to apply load until failure. Load was applied in increments between 5 and 10 kN. At each load increment, elongation and strain was recorded. Observations on yielding and its propagation through the specimen were recorded.

3.6 Data Collection

3.6.1 Load

Results from the calibration test of the load cell were required to convert the microstrain readings of the strain indicator into loads in kiloNewtons. Figure 4 shows this calibration curve.

3.6.2 Elongation

Specimen elongation was recorded using a 0.01 mm dial gauge connected to the floor and placed on the load cell. The elongation dial gauge placement is shown in Figure 6.

3.7 Tension Coupon Tests

Tension tests were prepared for each of the angle specimens tested. Each angle had two coupons cut from its length before the holes were drilled. The coupons were cut from each of the legs. The tension coupons were prepared according to ASTM Standard (1989), a typical specimen is shown in Figure 7.

The coupons were tested using the Universal Testing Machine to determine the tensile yield and ultimate stresses of the material. Strain gauges were applied to two of these coupons to determine the Young's Modulus of the material.

CHAPTER IV

THEORY OF FAILURE MODE

4.1 General

The theory of determining the type of failure mode that should occur in the specimen will be discussed in this chapter. Gross cross-sectional and net section failure are the two failure modes that are of interest. An equation was developed by Temple (1998) that seems to indicate which failure mode will occur. This equation is derived by equating the equation for gross area failure [1] and net section failure [3]. The multiplier of 0.85 in the shear lag failure equation should be set to 1.0 since it is added to the equation to increase the safety index. The resulting equation is as follows:

[5] $A_g \leq A'_{ne} F_u / F_y$

Since this equation is an inequality it means that if A_g is less than the term on the right side of the equation the failure mode should be by gross cross-sectional failure. Reading the equation the opposite way means that the angles should fail by net section failure. The remaining sections in this chapter discuss how to use this equation to predict the failure mode of the specimens.

4.2 Gross cross-sectional Failure

4.2.1 Equation Predicting Failure

Equation [5] governs whether gross cross-sectional failure will occur. Therefore, for gross section failure to occur the gross section area must be less than or equal to the net shear lag area multiplied by the ratio of the material properties. The material properties values can be obtained by performing tension coupon tests. However, in the

design phase these exact values are not available. In Canada the common type of steel used in angles, CSA G40.21-M 300W (CSA 1992), has a guaranteed minimum yield stress of 300 MPa and minimum ultimate tensile strength of 450 MPa. Therefore the ratio of F_u to F_y is 1.5. The shear lag area (A'_{ne}) is calculated using Clause 12.3.3.2(b) of S16.1-94.

4.2.2 Calculations Required

The calculations involved in determining gross cross-sectional failure are simple. The gross sectional area can be found in the commentary on the CAN/CSA-S16.1-94 Standard included in the Handbook of Steel Construction (CISC 1995). If the specimen cannot be found you can calculate the area as the sum of the length of the legs minus the thickness then multiplied by the thickness. Make sure that the area of the heel of the angle has not been accounted for twice in the calculations. The ratio of F_u to F_y is obtained from coupon tests, if available, or can be taken as 1.5 for these calculations. The shear lag area (A'_{ne}) is calculated from Clause 12.3.3.2(b) of S16.1-94. This clause allows the calculation of the area A'_{ne} taking into consideration the size of the connection. When the connection has three or fewer transverse lines of bolts a factor of 0.6 must be multiplied with the net-section area (A_{ne}) to get the net effective area accounting for shear lag. When the connection consists of four or more transverse lines of bolts the factor of 0.8 is used in the calculation of the shear lag area. Once all the values in the equation are calculated the failure mode can be determined. If the above equation is satisfied gross cross-sectional failure should occur.

4.2.3 Process and Examples Satisfying Equation

The process of determining if gross cross-sectional failure occurs can be summarized by the following steps:

Step 1: Select the angle to be studied
Step 2: Obtain gross cross-sectional area $\Rightarrow (A_g)$
Step 3: Calculate the area of the bolt hole $\Rightarrow (A_h)$
Step 4: Calculate the net-section area $\Rightarrow (A_{nc})$
Step 5: Calculate the net section area accounting for shear lag $\Rightarrow (A'_{nc})$
Step 6: Calculate $\Rightarrow A'_{nc} F_u/F_y$
Step 7: Compare gross section area (A_g) to $A'_{nc} F_u/F_y$

When step seven is complete and the result is that $A_g \leq A'_{nc} F_u/F_y$, then the angle should fail by gross cross-sectional failure. If this is not the case then another failure mode must be considered. That failure mode will be discussed later in the chapter. An example of the calculations can be found in Table 2. After the failure mode has been determined the failure load can be calculated.

4.2.4 Loads Required to Test

Once the angles which have gross cross-section failure have been determined the next step is to find out what load the angles can resist. The equation to calculate the failure load is [1] , found in Clause 13.2 (a) of CAN/CSA-S16.1-94. For the purpose of laboratory testing the "ϕ" in that equation can be removed since it is a factor that accounts for several variables. However, this factor must be included when designing angles used in public structures. Testing of angles to prove that [5] governs gross cross-section failure could not be completed due to the failure loads of the angles that must be tested. The loads required for testing exceeded the design loads the set-up apparatus could support.

4.3 Net-section Failure

4.3.1 Equation Predicting Failure

The equation that governs whether net cross-sectional failure occurs is:

[6] $A_g \geq A'_{ne} F_u / F_y$

Therefore, for net-section failure to occur the gross cross-section area must be greater than or equal to the net section area accounting for shear lag multiplied by the ratio of the material properties. The material properties values can be obtained by completing tension coupon tests. Canadian steel CSA G40.21-M 300W, has a guaranteed minimum yield stress of 300 MPa and minimum ultimate tensile strength of 450 MPa. Therefore the ratio of F_u to F_y is 1.5. The shear lag area (A'_{ne}) is calculated using Clause 12.3.3.2(b) of S16.1-94.

4.3.2 Calculation Required

The calculations involved in determining net-section failure are the same as those to calculate gross cross-sectional failure. The gross sectional area can be found in the commentary of the CAN/CSA-S16.1-94 Standard included in the Handbook of Steel Construction (CISC 1995). The ratio of F_u to F_y is taken as 1.5 in the calculations. The shear lag area (A'_{ne}) is calculated from Clause 12.3.3.2(b) of S16.1-94. Once all the values in the equation are calculated they are entered and the failure mode is obtained. If the above equation is satisfied net cross-sectional failure should occur.

4.3.3 Process and Examples Satisfying Equation

The process of determining if net cross-sectional failure occurs can be summarized by the steps found in Section 4.2.3. When step seven is complete and the result is that [6] is satisfied. Then the angle should fail by net cross-sectional failure. An example of the calculations are found in Table 3. After the failure mode has been determined the failure load must calculated.

4.3.4 Loads Required to Test

Once the angles which have net cross-section failure have been determined the next step is to determine the load that angles can resist. The equation to calculated the failure load is found in Clause 13.2 (a)(ii and iii) of CAN/CSA-S16.1-94. The lesser value from these equations will govern the failure load. For the purpose of laboratory testing the "ϕ and 0.85" in the equations can be removed since they are intended to increase the safety index. However, this factor must be included when designing angles used in public structures. Testing done in the laboratory at the University of Windsor has shown that [6] does prove that net-section failure will occur in the specimens tested. The results of the net-section failure testing is the subject of the next chapter.

CHAPTER V

TEST RESULTS

5.1 General

This chapter will show all the results of testing that was preformed. It will include the results of the tension coupon tests, as well as the results from the full scale experiments. The data from the tension tests will give the material properties and the efficiencies of the angles tested. Results of the full scale experiment will include Load vs. Elongation and Strain curves. Observations and failure mode of the angles will also appear in the Section 5.3 of this chapter. When testing is being performed the material properties of the specimens must be determined. This is done to ensure exact values of the material properties are used in any calculations concerning the test specimens.

5.2 Tension Coupons Tests

The material properties of the tension coupon tests are shown in Table 4. These results are averages since two coupons were taken for each angle. From the coupons that were tested, two had strain gauges placed at the center on both sides to obtain average strain values. The strain values were used to check the Modulus of Elasticity of the angles that were tested. The two coupons used were from two different angles in the test group. The average modulus of elasticity of the coupons tested was 196 200 MPa. The average yield stress, average ultimate stress and the average elongation were 320 MPa, 448 MPa, and 32 %, respectively.

The data from the tension coupons can be found in Appendix A, Tables A1 to A12. These tables show the results of the twenty-four tension coupons cut from the twelve angle specimens used in the tests.

5.3 Experimental Results

5.3.1 Failure Mode

The failure mode that occurred for all tests done was net-section failure. When using the equation that was proposed by Temple (1998), and explained in Chapter Four the result is net-section failure. All results and discussion of the result from this point on are based on net-section failure of the specimens.

5.3.2 Section Yielding

Throughout the testing, observations were recorded on the manner in which the angle reacted to the applied loads. The main observation made was the starting point of yielding and how it progressed through the angle. This observation was made possible by observing cracks in the white wash. In all tests performed yielding always began at the first bolt hole in the connection. Figure 8 shows a connection detail which outlines the numbering of the bolt holes. Yielding then progressed to the second and on through the remaining bolt holes (Figure 9). While yielding progressed through the bolt holes it began in the unconnected leg. It started at the heel of the angle below the first bolt hole. It then proceeded towards the edge of the unconnected leg. After reaching the edge of the unconnected leg in front of the first bolt hole yielding of the unconnected leg began in front of the second bolt hole. This pattern continued until the unconnected leg had yielded in front of all bolt holes in the connection. Figure 10 shows the yielding pattern

of the unconnected leg. Once the yielding of the connection on both legs reached a certain point the yielding of the angle towards the center began. The yielding on both legs started at the heel and progressed at approximately 45 degrees towards the edge of the legs. This pattern is shown in Figure 11. As the yielding proceeded towards mid-span the material above the first bolt hole began thinning. The material continued thinning at this point until failure occurred at this point. Figures 12 and 13 show the thinning of the material and the failure of the angle, respectively. The starting point of yielding and its propagation through the angle occurred in the same manner for all specimens tested. The amount of yielding taking place did change with certain parameters. The deformations caused by yielding were permanent and are shown in Figure 14 (a) and (b).

5.3.3 Total Elongation At Failure

The total elongation was measured by a dial gauge located on the load cell face (Figure 6). Total Elongation curves are found in Appendix B, Figures B1 to B12. The final results of the measurements for the 3-bolt 5000 mm specimens was an average elongation of 30.03 mm. The 3-bolt 1000 mm long angles had an average elongation of 28.58 mm. For angles with 4-bolt 5000 mm length the total elongation was 29.30 mm on average. Finally, the specimens of 4-bolt 1000 mm length had an average total elongation of 32.77 mm. Table 5 shows the total elongation of all the specimens.

5.3.4 Loads

5.3.4.1 Approximate Yield Loads

Using the elongation curves in Appendix B the approximate yield loads that occurred during the testing can be determined for each angle. The results of this approximation are found in Table 6. The average yield load for the 3-bolt, 5000 mm specimens, was 90 kN. For 3-bolt, 1000 mm, the average yield load was 93 kN. The specimens with 4-bolt, 5000 mm in length, the average was 117 kN. Finally, specimens with 4-bolt, 1000 mm had an average of 92 kN. Since dial gauges were read at certain intervals, which changed slightly during testing, only an approximation can be made. The procedure in achieving these numbers was to draw a line of best fit along the beginning data points. Another line of best fit was drawn over data points recorded later in the test. The point at which the two line intercept is the approximate yielding load. This load was compared to the loads at which the yielding at the first bolt was observed. The two values are close to each other. This is only an approximation since strain gauges were not placed at the connection. There are no strain values to determine the exact yield load of the specimen.

5.3.4.2 Failure Loads

Unlike the yield loads, the ultimate loads of the specimens are well known and were recorded during testing. The results of the failure loads are found in Table 7. The average failure load for 3-bolt, 5000 mm specimens, was 207 kN. For 3-bolt, 1000 mm specimens, the failure average was 214 kN. The specimens with 4-bolt, 5000 mm length, had a failure average of 227 kN. Finally, specimens with 4-bolt, 1000 mm, had an

average of 227 kN. Looking at the average failure values, the 3-bolt connection specimens failed at approximately the same load. The same can be said for the 4-bolt connection specimens.

5.3.5 Strains At Mid-Span

5.3.5.1 By Individual Gauge

The results of the strains at mid-span by gauge are shown in Appendix C, Figures C1 to C12. The figures are arranged so that the three angles that appear in each figure have the same dimensions. The angles that have dimensions of 5000 mm and connection size of 3-bolts had linear strain readings which suggest no yielding at mid-span. The maximum microstrains for gauge 1 was an average of 1403, gauge 2 an average of 1407 and gauge 3 an average of 1514. The 5000 mm 4-bolt angles had an average microstrain readings at gauge 1 of 1526, gauge 2 an average of 1522 and gauge 3 had an average of 1644. Angles of dimension 1000 mm, 3-bolts, had an average microstrain readings at gauge 1 of 1370, gauge 2 an average of 1732 and gauge 3 an average of 1680. Angles of dimension 1000 mm, 4-bolts, had microstrain readings at gauge 1 of 1552, gauge 2 an average of 1482 and gauge 3 an average of 1600. The 1000 mm angles all had gauge 1 start in compression and then turn into tension readings as load increased. Angles of length 1000 mm also had strain readings that were not linear all the way to failure as was the case for the 5000 mm angles.

5.3.5.2 By Angle

The results of the strains at mid-span for each angle are shown in Appendix C, Figures C13 to C24. As shown by the graphs of angles 1 to 6, all three gauges are linear

right up to failure. For these angles gauge 1 has the lowest strain value while gauge 3 has the highest strain and gauge 2 is in between the strains in gauges 1 and 3. When the failure load approached gauge 1 readings sometimes exceeded gauge 2 readings.

The graphs for angles 7 to 12 have different results compared to the first six angles tested. The results show that readings for gauges 2 and 3 are made up of two differently sloped lines. The intercept where the slope change happens at the approximate load that yielding starts at the first bolt hole. This explains why yielding at the mid-span was not observed during the test. In angles 7 and 9 gauge 2 did not work and strain results are not averages but instead are comprised of a single reading. It is interesting to note that gauge 1 starts in compression then moves to tension at approximately the same load that yielding starts at the first bolt hole.

5.3.6 Efficiency

Angle efficiency was calculated using two different equations. The first equation:

[7] $U_1 = P_u / (F_u * A_n)$

where P_u = the maximum load from testing.

The second equation is one that was proposed by Kulak and Wu (1997). The equation is:

[8] $U_2 = \{A_{cn} + \beta(F_y/F_u)A_o\} / \{A_n\}$

Results of the efficiency calculations can be found in Table 8. The 3-bolt average angle efficiency was: $U_1 = 0.740$ and $U_2 = 0.627$. The 4-bolt average angle efficiency was: $U_1 = 0.860$ and $U_2 = 0.841$. This shows that both equations predict the efficiency of the angle close to that of the Standard. The Standard uses efficiencies of 0.6 and 0.8 for 3-bolt and 4-bolt, respectively.

CHAPTER VI

DISCUSSION OF TEST RESULTS

6.1 General

This chapter will include a discussion of the test results by comparing the two parameters which were varied during the testing. These parameters are the length of the specimen and the size of the connection. Since net-section failure occurred in all of the tests conducted discussion of predicting failure modes is limited to theory and are discussed in a previous chapter as well as the next chapter. However, ultimate loads, strain distribution, yielding, elongation and efficiency of the test angles are discussed in the sections that follow.

6.2 Ultimate Loads

The average ultimate load for the angles with a length of 5000 mm was 217 kN. The range of loads for these angles was large since the lowest value was equal to 203 kN and the high loads was 236 kN. The angles with 1000 mm did not generate better results. The range of loads went from 180 kN to 250 kN, having an average ultimate load of 220 kN. Since these load ranges are so large it does not seem that the ultimate load of the angle is governed by it length. The averages seem to suggest that length has no effect.

When the connection size was looked at the ultimate load values made sense. The average ultimate load for the 3-bolt connection angles was 210 kN. From the six angles tested four failed with an average of 208 kN. The load range of this average was from 203 kN to 211 kN. The remaining two failed at 250 kN and 180 kN. Both of these angles had high yield and ultimate tensile stresses as determined by the tension coupon

tests. Therefore they should have had higher failure loads. The reason why the one failed at 180 kN is not clear. Perhaps the material around the connection was not as strong as the material of the coupon. The results of the 4-bolt connection were similar to those of the 3-bolt. The range of failure load was low, having lowest value equal to 220 kN and the highest being 237 kN. This generates an average ultimate load of 227 kN for the 4-bolt connection size.

The results of comparing length to connection size for the ultimate loads are clear. The length of the angle has no visible significance on the ultimate load. The connection size used has a direct influence on the load the angle can carry. These results are based on comparing 3-bolt and 4-bolt connections and length of 5000 mm and 1000 mm.

6.3 Strain Distribution

The discussion of strain distribution begins with the effects of the two different lengths and then proceeds to the two different connection sizes.

The graphs for the strain distribution of the 5000 mm length specimens are found in Appendix C, Figures C13 to C18. As shown in the graphs, all strain gauge values are linear up to failure. The gauge on the unconnected leg generally had the lowest strain while the gauge on the connected leg closest to the edge had the highest values. Near the failure loads for some of the angles, gauges 1 and 2 had similar readings. Gauge 3 on the connected leg always had highest strain reading.

The graphs of strain distribution for 1000 mm length angles are found in Appendix C, Figures C19 to C24. These angles had higher average strain values during the tests than those of the 5000 mm angles. Another difference was that gauge 1 on the unconnected leg started in compression then went to tension. This can be explained by

the shorter length of the angle. The movement of the center point as it tries to line up the centroid of the angle with the line of the load forces the unconnected leg into compression. This does not appear on the longer 5000 mm length because there is more angle between the connections that absorbed this compression load before it reached the mid-span. After enough load is applied the whole angle is in tension. Generally this occurred when the yield started at the first bolt. This shows up on the graphs when gauges 2 and 3 have the slope change in the linear lines. The slope change is not due to yielding at the mid-section but instead is due to the yielding at the first bolt.

Therefore, the effect of length on strain distribution is that longer lengths will have linear distribution up to failure and shorter lengths have compression at mid-span which turns to tension after connection yields.

The graphs for the strain distribution of the two connection sizes are found in Appendix C. The 3-bolt connection angles had lower average strain on gauges 1 and 3 compared to the 4-bolt connection angles. The average microstrain values for 3-bolt connection of gauges 1, 2 and 3 are 1386, 1569, 1597, respectively. The average microstrain values for 4-bolt connection of gauge 1, 2 and 3 are 1539, 1512 and 1622, respectively. The 4-bolt connection angles had higher failure loads; therefore it is reasonable to expect higher microstrain values. Gauge 2 of the 4-bolt connection has a lower value since two of the gauges did not function properly. This becomes important because the average is calculated using six values. The average here was calculated using four values. This should not matter if all gauges had similar readings. However, on the angles that gauge 2 did not function, the values for gauges 1 and 3 were high. The

average strain of gauge 1 is 1564 and for gauge 3 it is 1630. This would mean that the values for gauge 2 would also be high and would push the average value up as well.

The size of the connection governs the values of microstrain that are recorded. The longer the connection, 4-bolt greater than 3-bolt, the larger the strain that will be recorded. This is why 4-bolt connection angles had the ability to carry higher loads.

6.4 Yielding and Propagation

The starting point of yielding and its propagation through the specimen occurs the same way no matter what length or connection size. In all tests performed, yielding always began at the first bolt hole in the connection. Yielding then progressed to the second and on through the remaining bolt holes. While yielding progressed through the bolt holes it began on the unconnected leg. It started at the heel of the angle below the first bolt hole. It then proceeded towards the edge of the unconnected leg. After reaching the edge of the unconnected leg in front of the first bolt hole, yielding of the unconnected leg began in front of the second bolt hole. This pattern continued until the unconnected leg had yielded in front of all bolt holes in the connection. Once the yielding of the connection on both legs reached a certain point, the yielding of the angle towards the center began. The yielding on both legs started at the heel and progressed at approximately 45 degrees towards the edge of the legs. As the yielding proceeded towards mid-span the material above the first bolt hole began thinning. The material continued thinning at this point until failure occurred at this point. Figures 15 (a) to (d) show this process in diagram form. Figures 16, 17 and 18 show this yielding.

In the angles that were 5000 mm in length the yielding was localized to around the connection and did not proceed far towards the center. The angles with length of 1000 mm had yielding that went closer to the center of the angle before failure occurred. This is proven by the higher values of strain in the 1000 mm angles. The yielding in the 3 and 4-bolt angles differ only in the amount of yielding towards the mid-span. The 4-bolt angles had more yielding extending towards the mid-span. Therefore, it can be said that length and connection size has an effect on the amount of yielding which occurs but has no effect on the starting point. All specimens tested started to yield at the same point as described in the above paragraphs.

6.5 Elongation

As mentioned before, the total elongation was measured by a dial gauge located on the load cell face. When dealing with the 5000 mm length angles, the range of elongation was from 26.9 mm to 33.3 mm. The resulting elongation average was 29.7 mm. The angles with a length of 1000 mm had an elongation range of 24.4 mm to 38.8 mm. This gives an average elongation of 30.7 mm. When looking at the elongations of the 3 and 4 bolt connection the averages are 29.3 mm and 31.0 mm, respectively. Therefore, when elongations are compared on the basis of only angle length and only connection size, there does not seem to be any effect.

The 3-bolt, 5000 mm specimens, had an average elongation of 30.0 mm. The angles with a 3-bolt, 1000 mm specimens, had an average elongation of 28.6 mm. Angles with 4-bolt, 5000 mm the total elongation was 29.3 mm on average. Finally, the specimens of 4-bolt, 1000 mm had an average total elongation of 32.8 mm.

Therefore, connection size and angle length does not seem to have an effect on the total elongation of the specimen. All angles tested have similar average elongations.

6.6 Efficiency

The length of the angle has no effect on it efficiency. It is the size of the connection that has the effect on the efficiency value. Since the net cross-sectional area of the angle enters into the calculations, the size of the bolt enters into the equation. This is seen when the equations used in efficiency calculations are studied.

Results of the efficiency calculations are found in Table 8. The 3-bolt average angle efficiency was $U_1 = 0.740$ and $U_2 = 0.627$. The 4-bolt average angle efficiency was $U_1 = 0.860$ and $U_2 = 0.841$. This shows that both equations predict the efficiency of the angle close to that of the Standard. The Standard uses efficiencies of 0.6 and 0.8 for 3-bolt and 4-bolt respectively. Therefore the equation developed by Kulak and Wu (1997) provides better results compared with the Standard.

CHAPTER VII

CONCLUSIONS AND RECOMMENDATIONS

7.1 Conclusions

Based on the experimental and theoretical results obtained in this research the following conclusions can be drawn:

(a) The failure mode of all tests done was net-section failure. Looking at the equation that was proposed by Temple (1998), in Chapter IV, the result is net-section failure. Therefore, the equation accurately describes net-section failure.

(b) The ultimate load carrying capacity of the angle depends on the size of the connection and not the length of the member.

(c) The efficiency equation developed by Kulak and Wu (1997) provides excellent results compared with the Standard S16.1 Clause 12.3.3.2(b).

(d) The size of the connection governs the values of microstrain that are recorded. The larger the connection, 4-bolt as compared to 3-bolt, the larger the microstrains. Longer specimen lengths have linear distribution up to failure while the shorter lengths have compression at mid-span turning to tension after connection yields.

(e) The length and connection size effect the amount of yielding which occurs but have no effect on the starting point. All specimens tested start to yield at the same point.

(f) For the specimens tested in the research the connection size and angle length do not effect the amount of elongation. All specimens tested show similar elongations with no apparent pattern.

7.2 Recommendations for Further Research

Due to the limitations of the laboratory apparatus, the maximum tensile force applied to the specimens was 400 kN. This limiting force made it impossible to test many angles. The results of the gross cross-section failure calculations showed tensile forces greater than 400 kN. Further testing should be done with a stronger set-up design so that larger angles can be tested for gross cross-section failure. Different lengths as well as the connection sizes should be tested in order to determine if gross section failure has similar specimen efficiency to that of net-section failure specimens. The strain distribution, ultimate loads, the starting point of yielding and its propagation through the specimen should be studied.

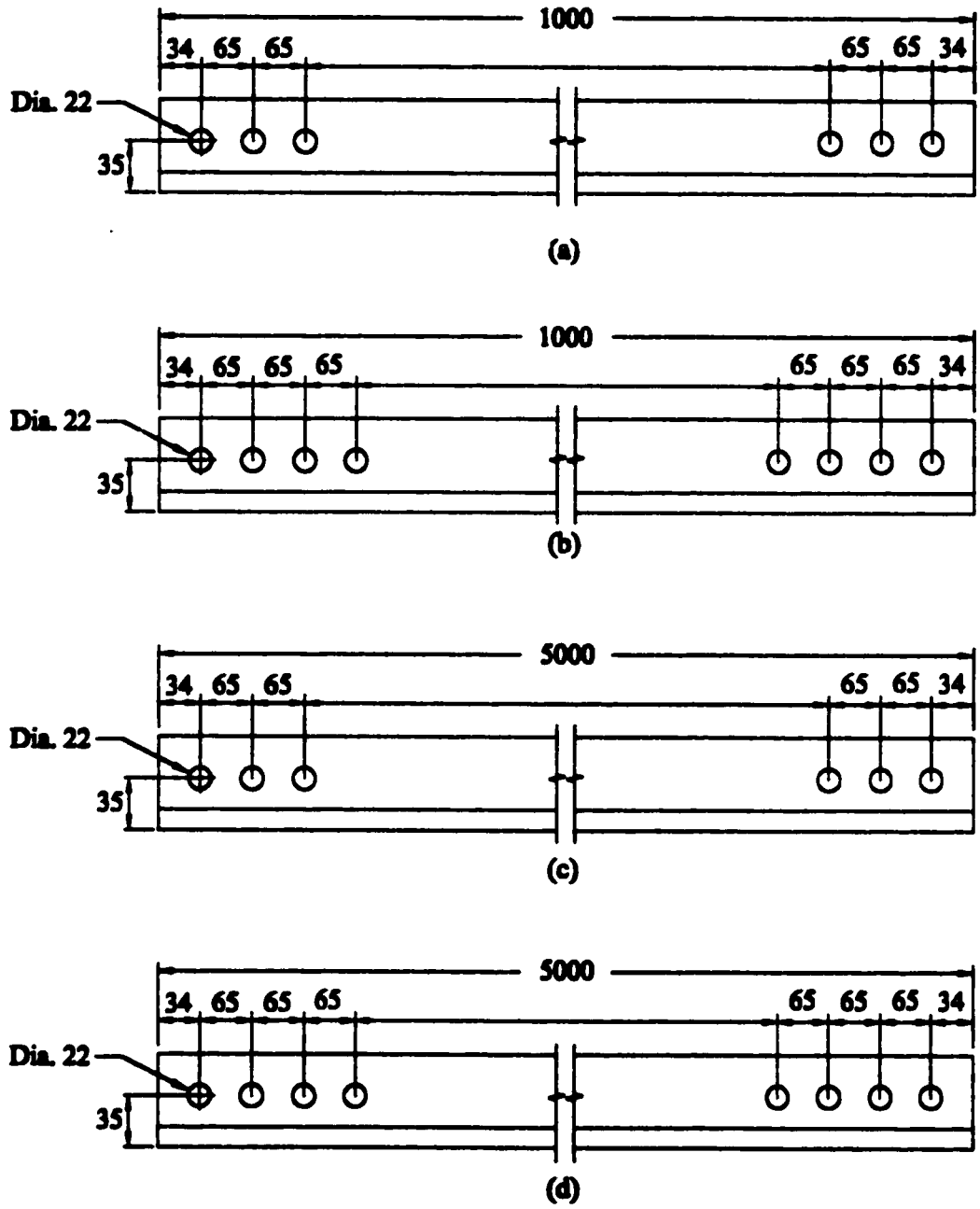

**Note: All Dimensions are in mm
Drawing not to scale

Figure 1: Specimen Dimensions
(a) 3-Bolt, 1000mm (b) 4-Bolt, 1000mm
(c) 3-Bolt, 5000mm (d) 4-Bolt, 5000mm

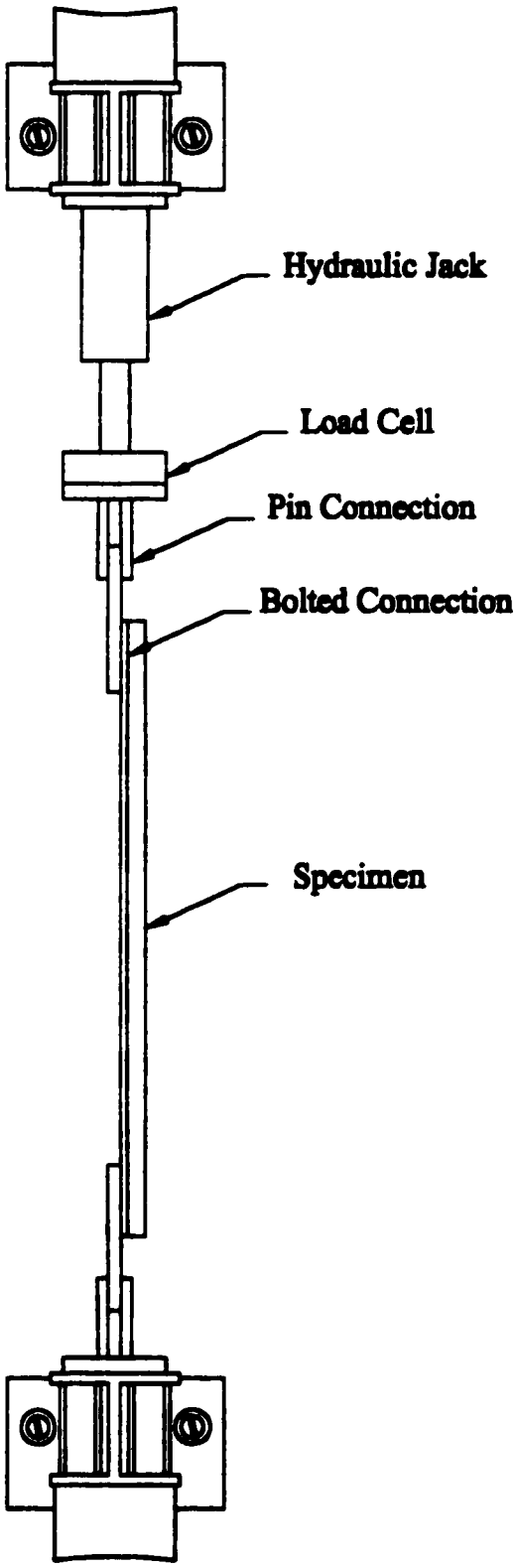

Figure 2: Top view of the Test set-up.

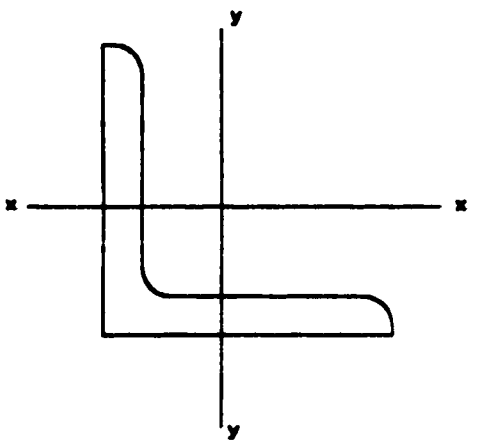

End View

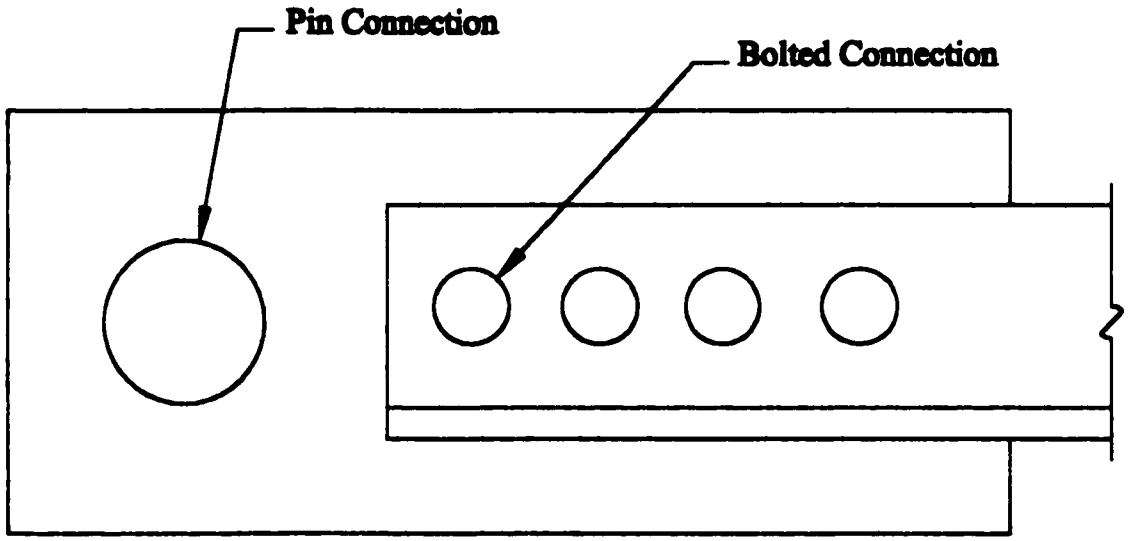

Side View

Figure 3: End Conditions of 64x64x6.4 Angle

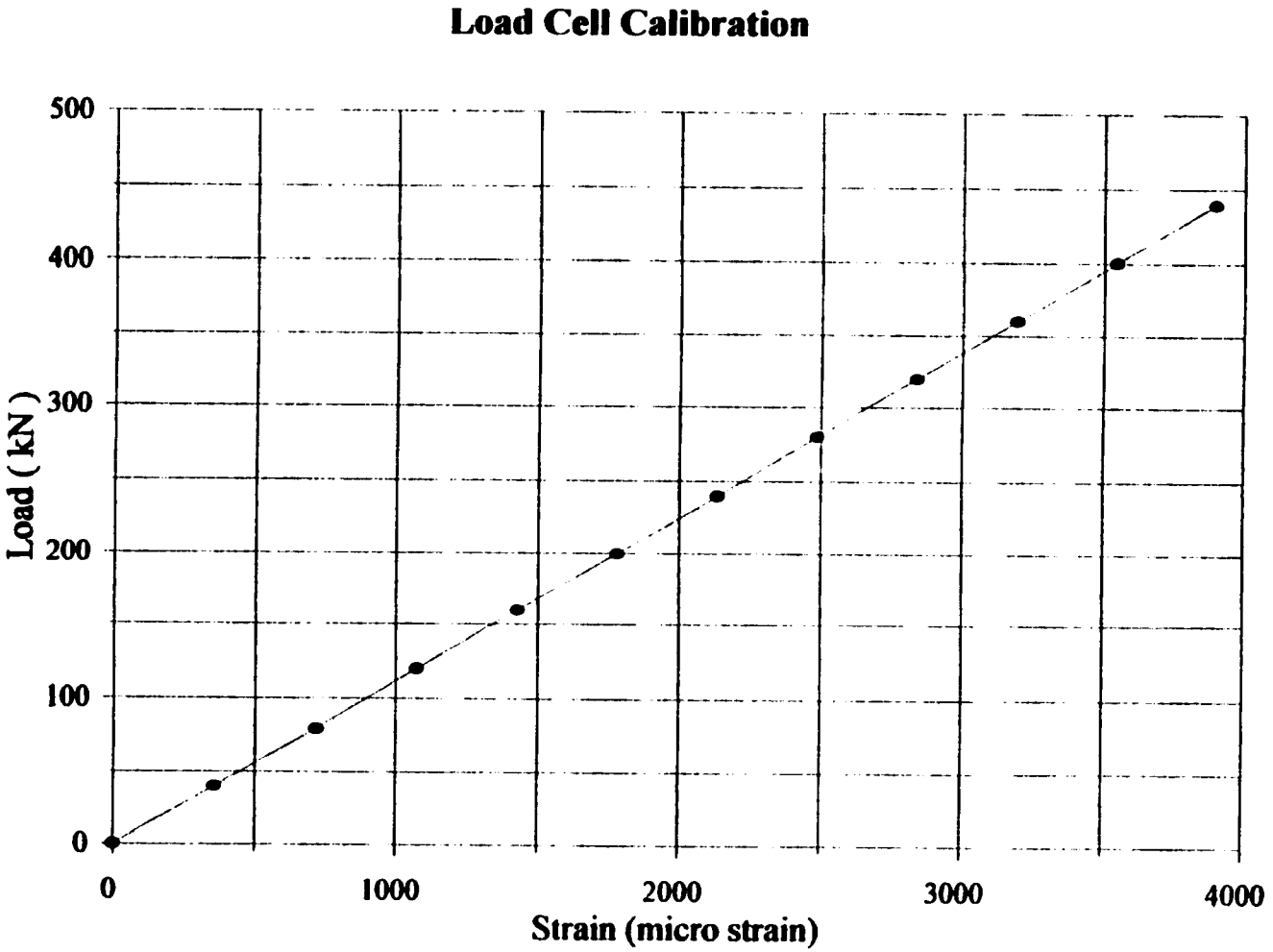

Figure 4: Load Cell Calibration

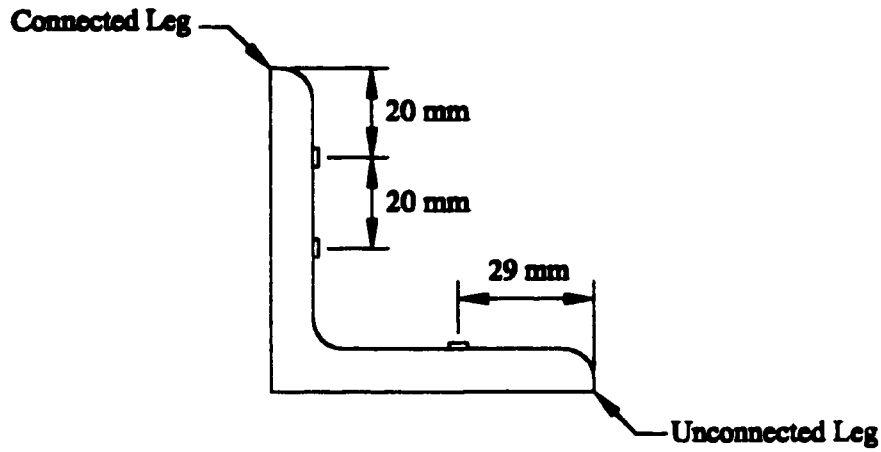

(a)

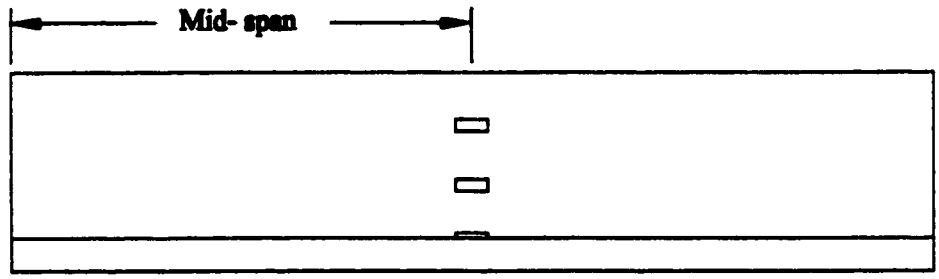

(b)

Figure 5: Strain Gauge Placement (a) End View (b) Front View

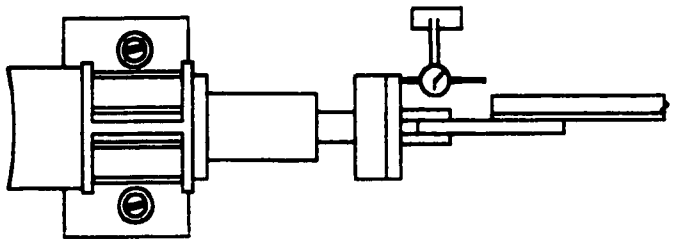

(a)

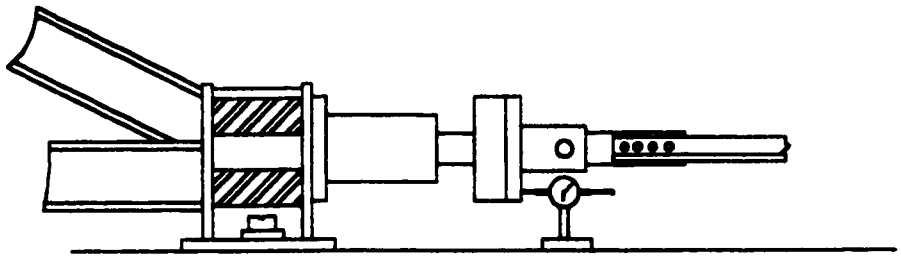

(b)

Figure 6: Elongation Dial Gauge Placement
(a) Top View, (b) Side View

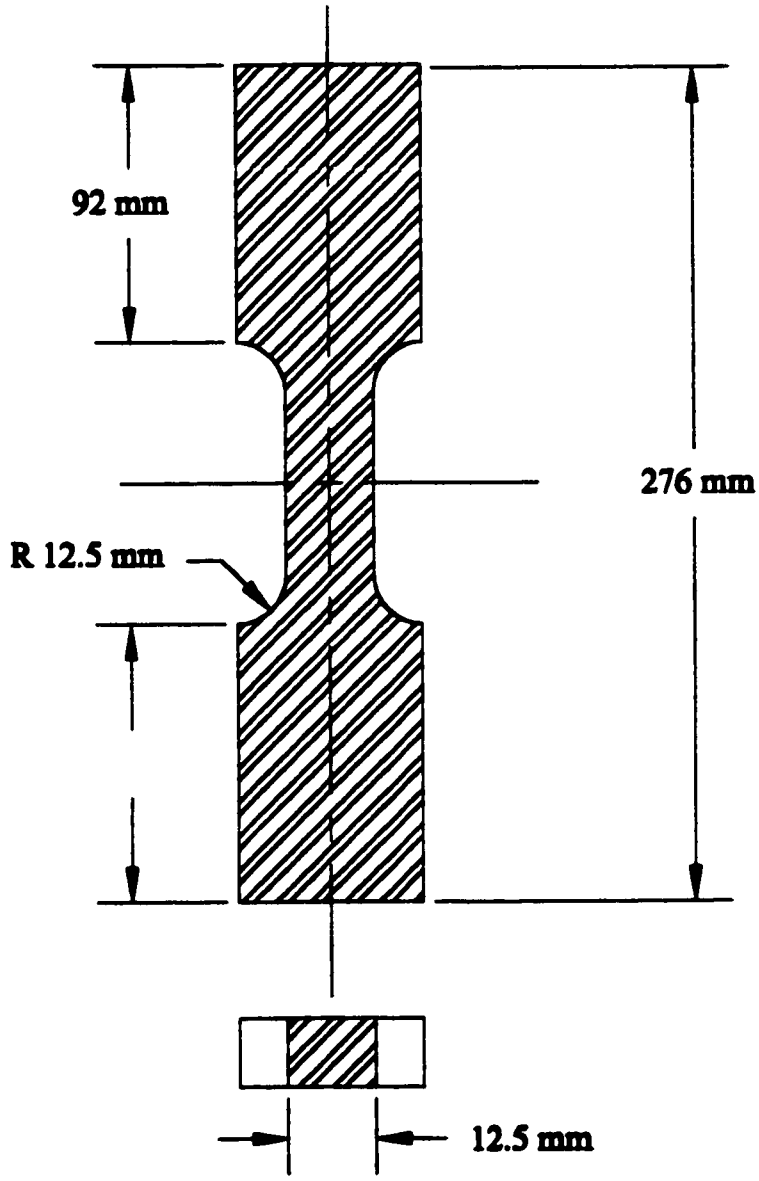

Figure 7: Tension Coupon

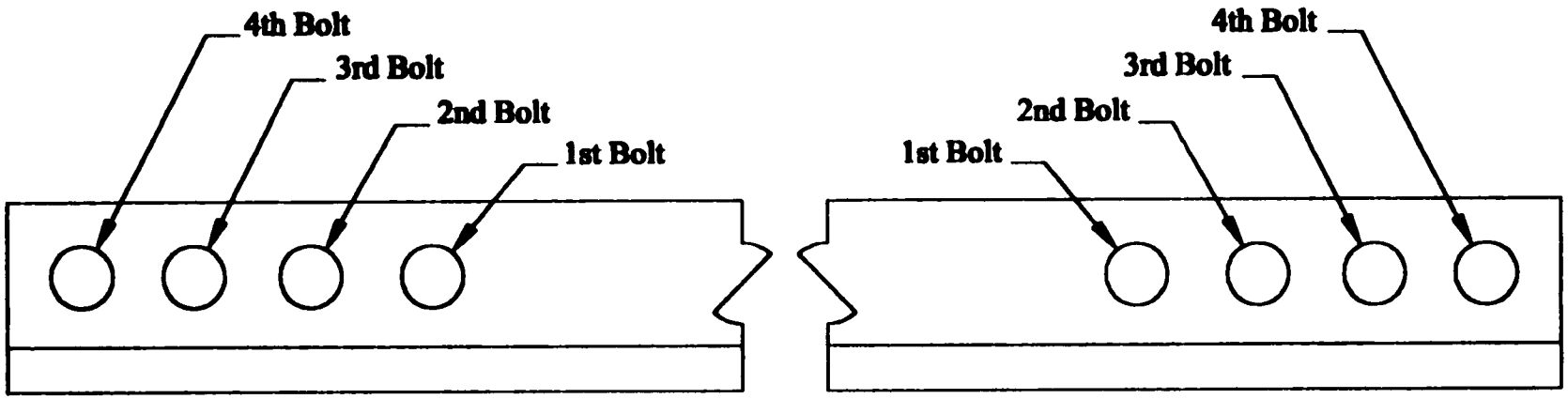

Figure 8: Location of Bolt Holes

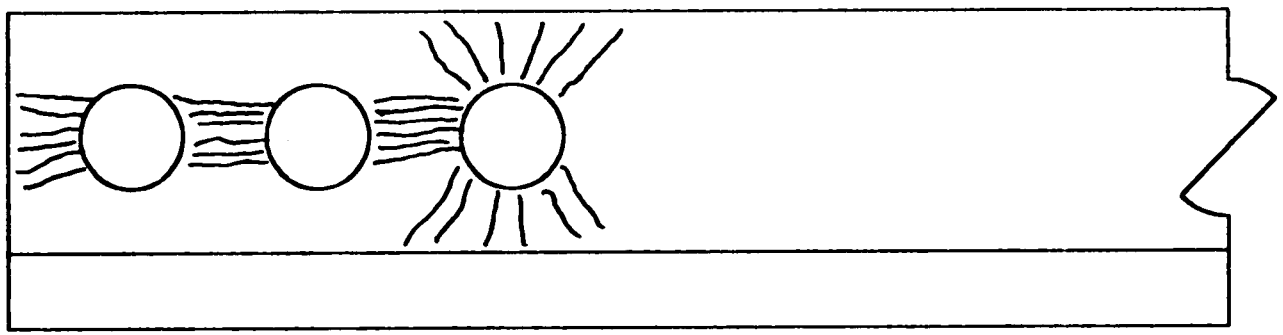

(a)

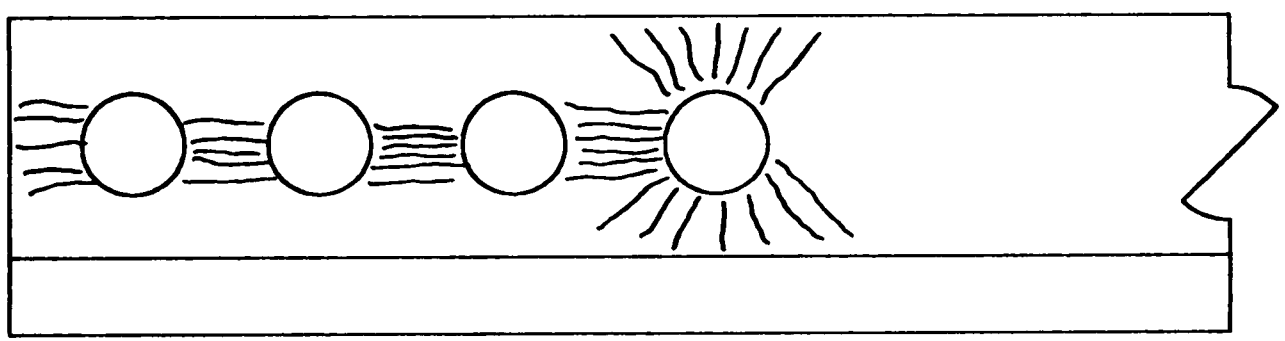

(b)

Figure 9: Yielding Pattern Through Connection (a) 3-Bolt, (b) 4-Bolt

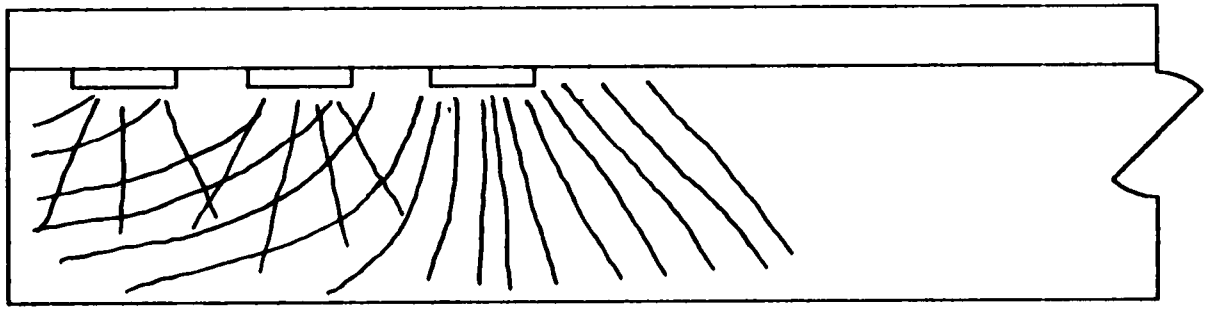

(a)

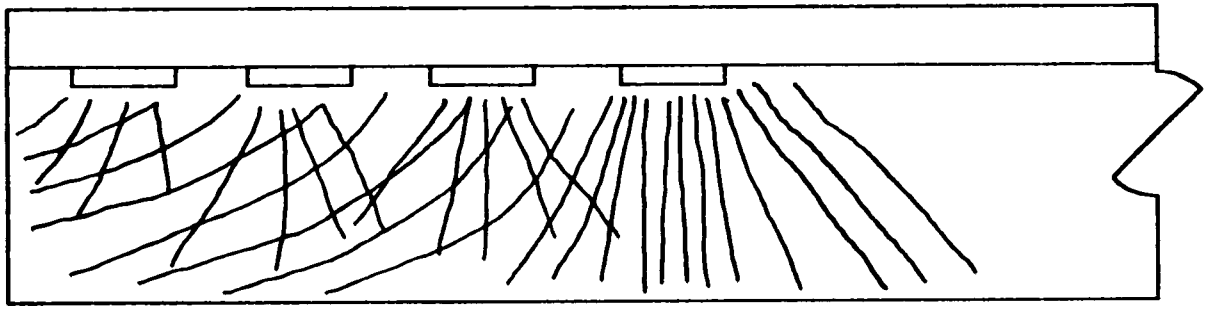

(b)

Figure 10: Yielding Pattern On Unconnected Leg (a) 3-Bolt (b) 4-Bolt

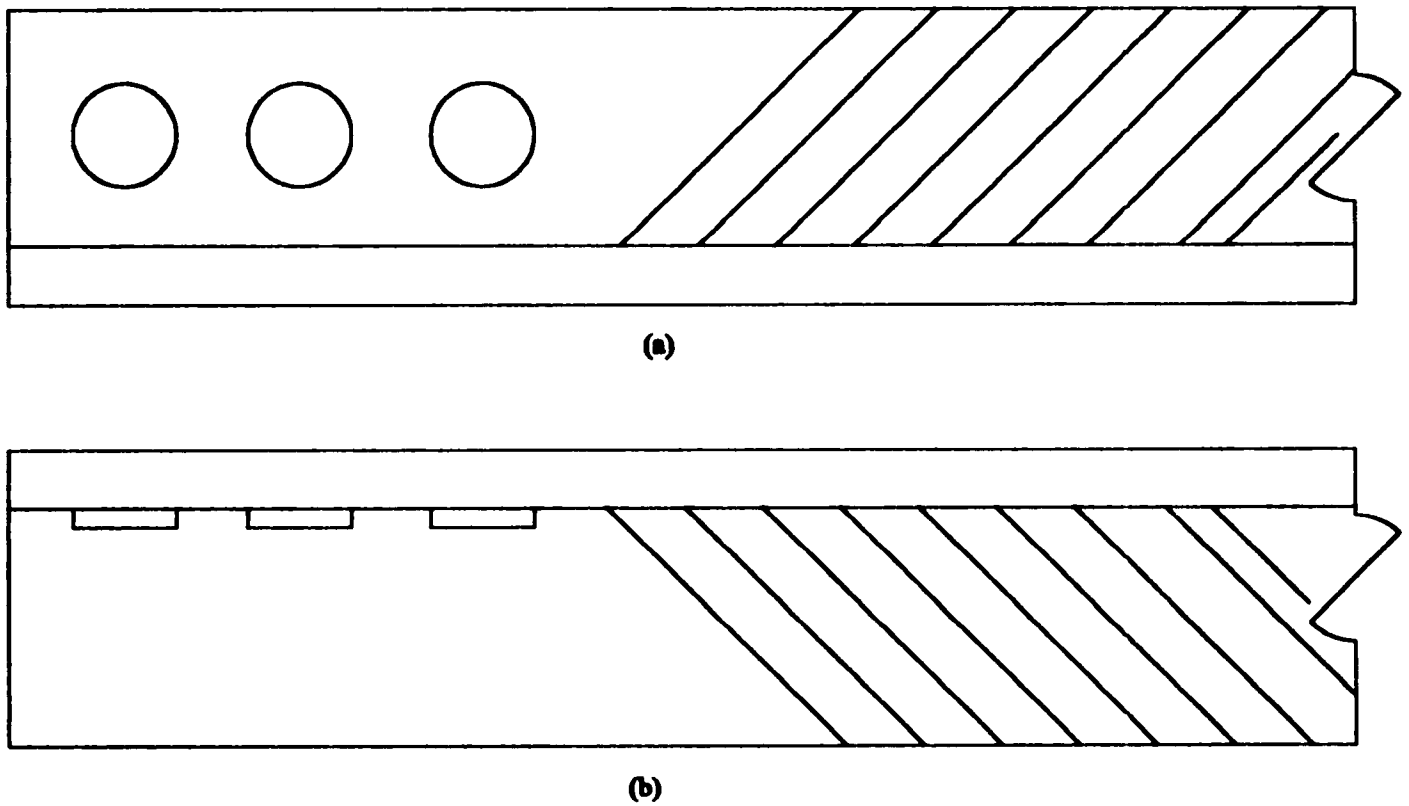

Figure 11: Yield Pattern Towards The Mid-Span (a) On Connected Leg (b) On Unconnected Leg

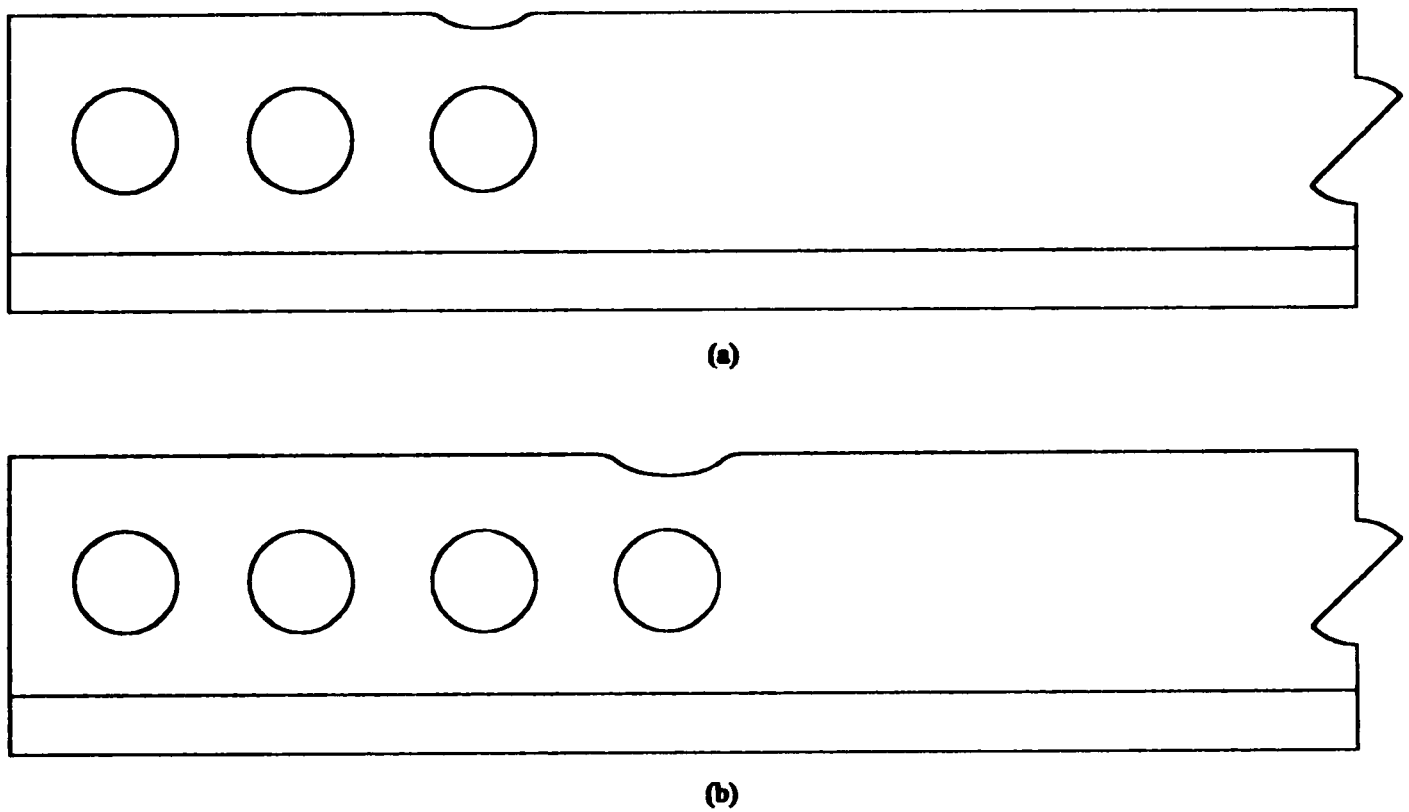

Figure 12: Thinning Of Material (a) 3-Bolt (b) 4-Bolt

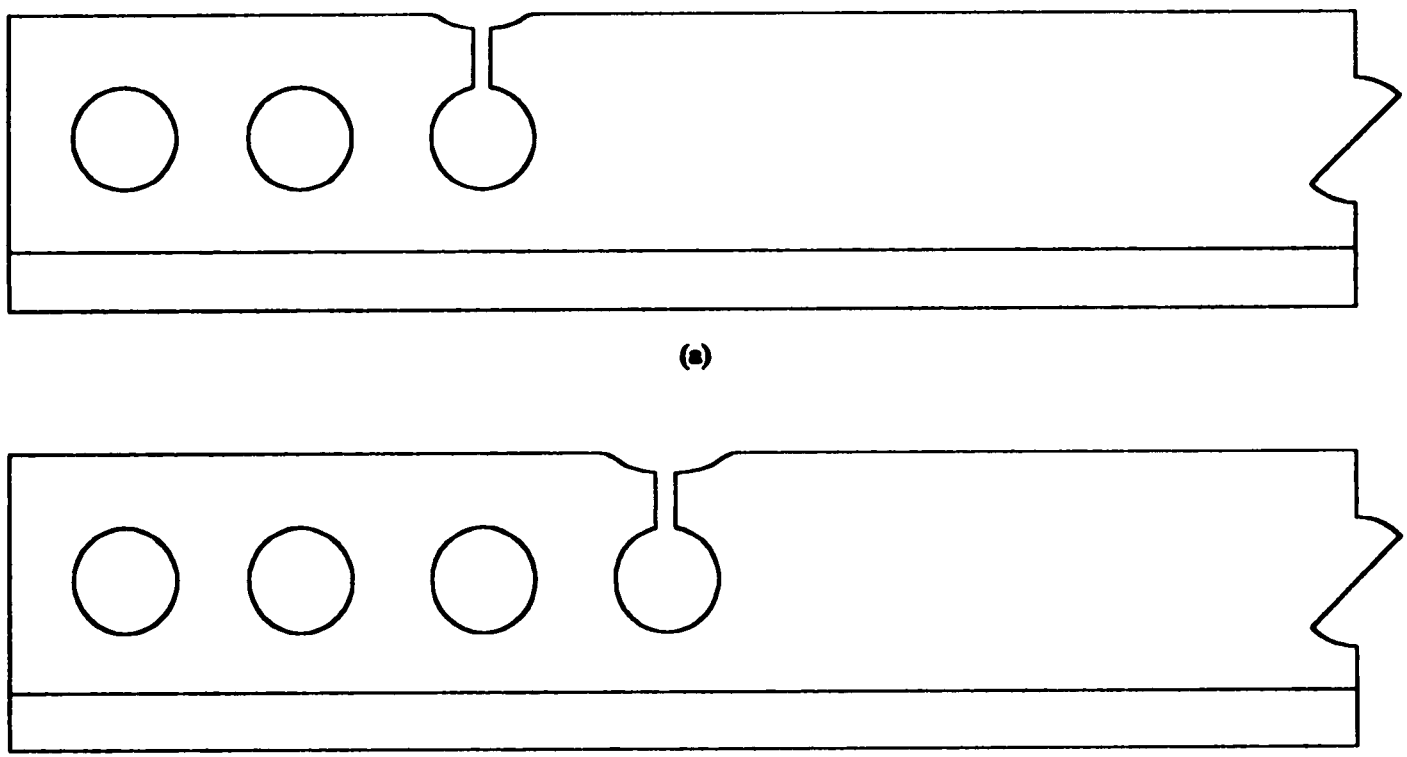

Figure 13: Net-Section Failure (a) 3-Bolt (b) 4-Bolt

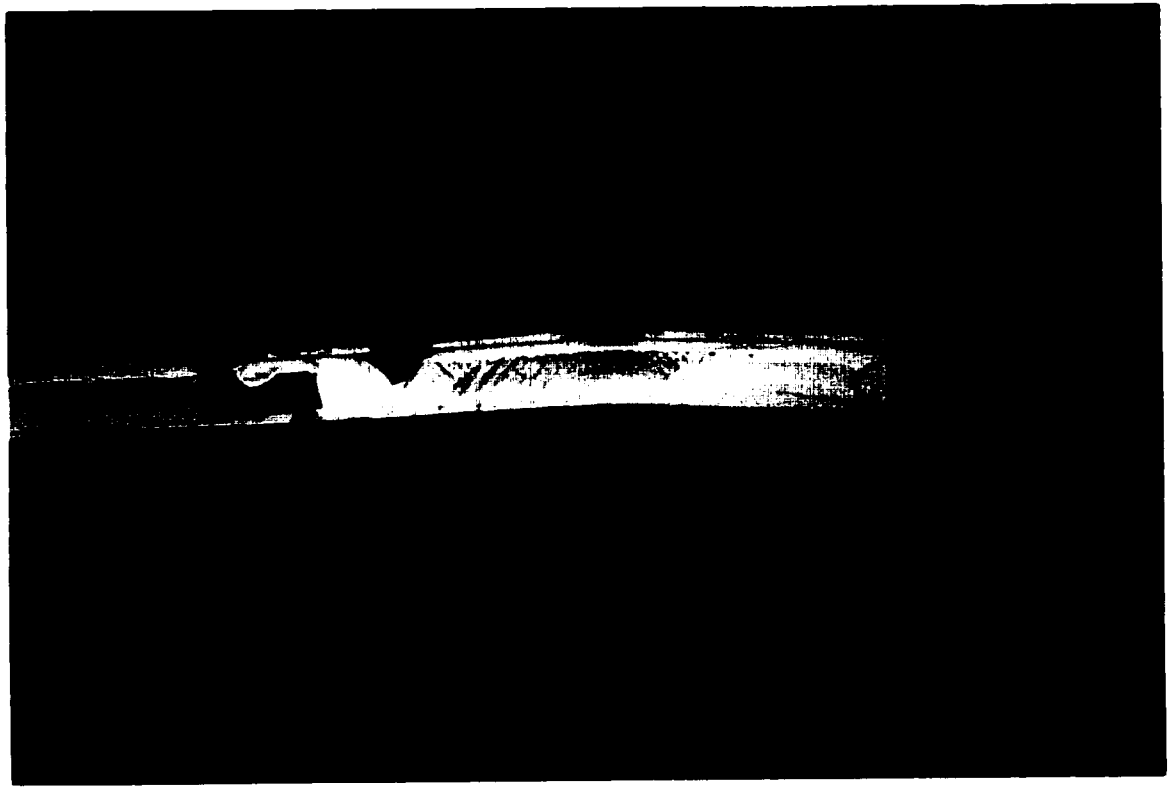

Figure 14(a): Permanent Deformation

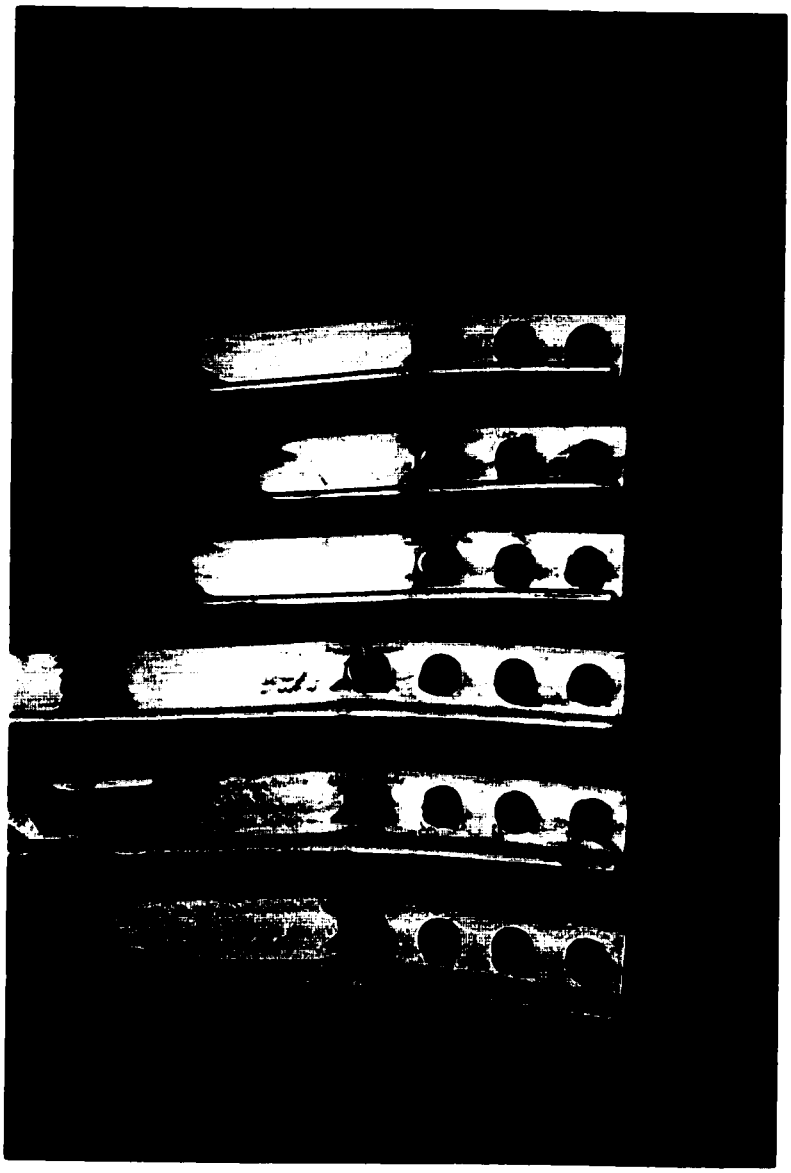

Figure 14(b): Permanent Deformation

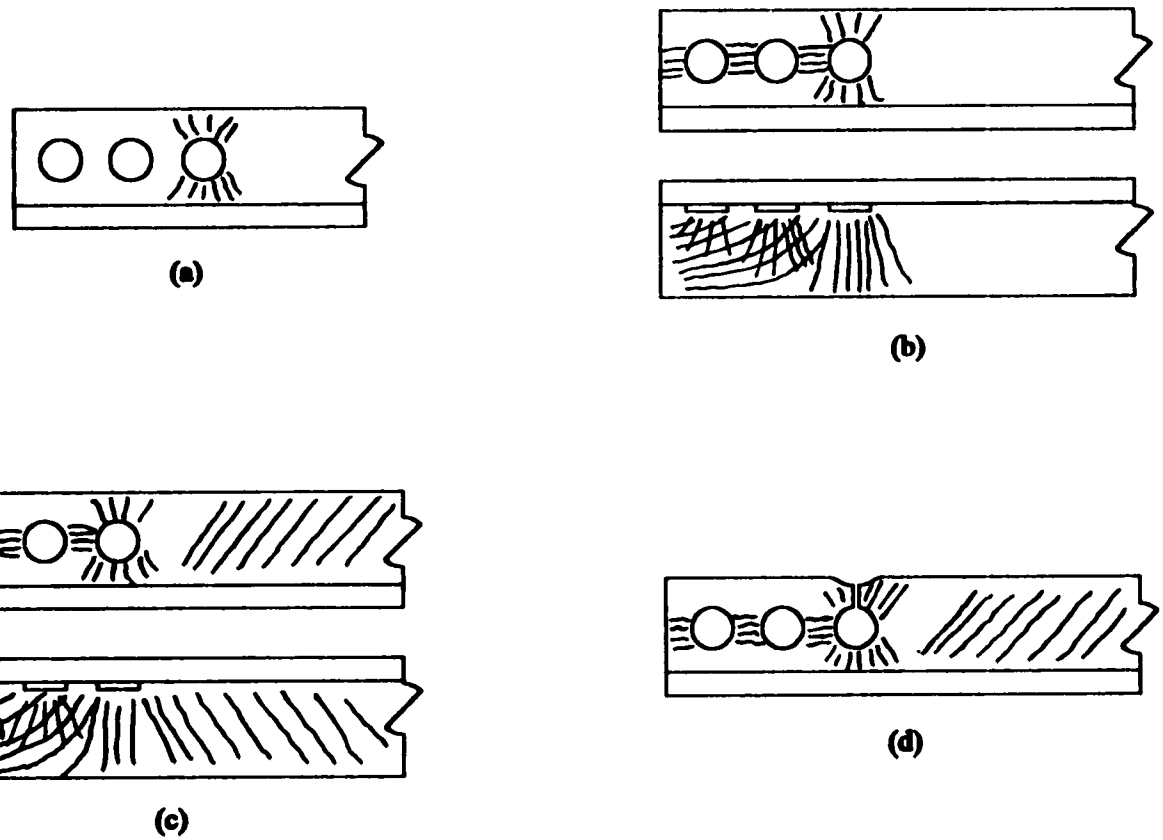

Figure 15: Yield Propagation (a) At 1st Bolt (b) Through connection (c) Towards Mid-Span (d) At Failure

Figure 16: Photograph #1 of Yielding

Figure 17: Photograph #2 of Yielding

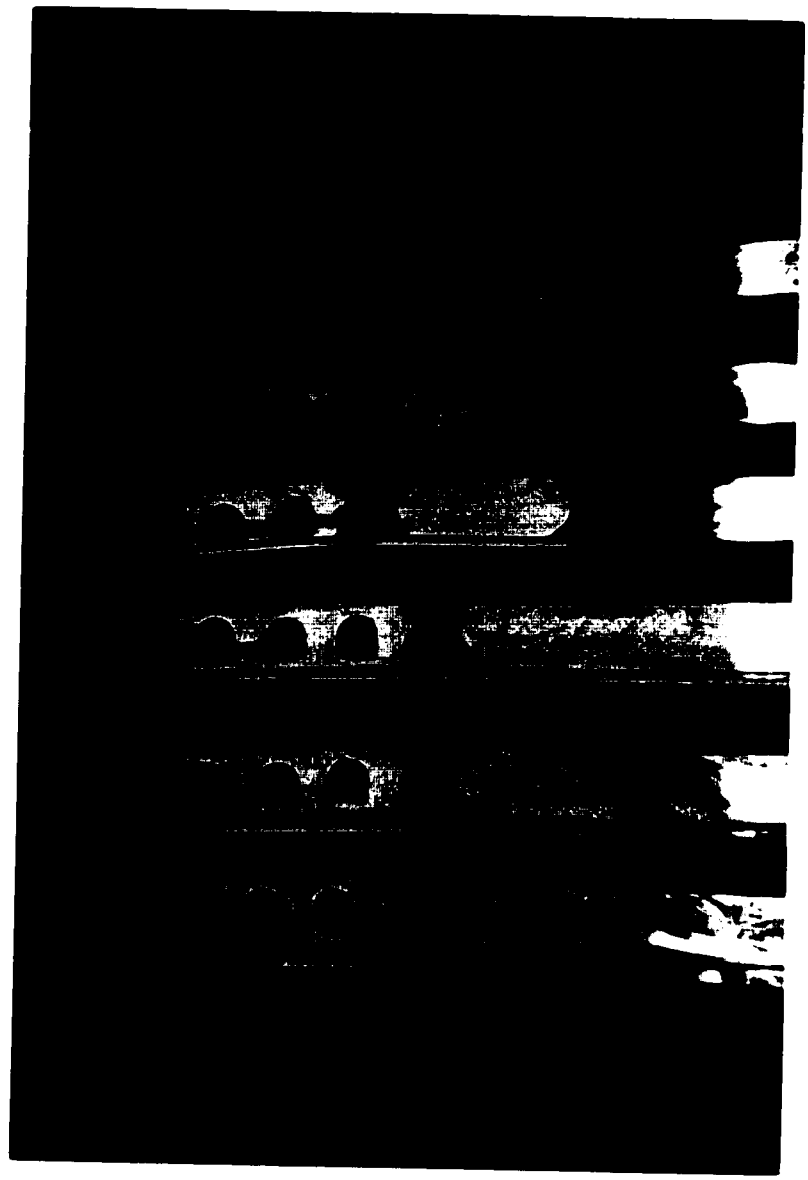

Figure 18: Photograph #3 of Yielding

Table 1: Specimen Dimensions

Angle Number	Size (All in mm's)	Length (mm)	Connection Size
1	64x64x6.4	5000	3-bolt
2	64x64x6.4	5000	3-bolt
3	64x64x6.4	5000	3-bolt
4	64x64x6.4	5000	4-bolt
5	64x64x6.4	5000	4-bolt
6	64x64x6.4	5000	4-bolt
7	64x64x6.4	1000	4-bolt
8	64x64x6.4	1000	3-bolt
9	64x64x6.4	1000	4-bolt
10	64x64x6.4	1000	4-bolt
11	64x64x6.4	1000	3-bolt
12	64x64x6.4	1000	3-bolt

Table 2: Calculations For Gross Cross Sectional Failure

Trial #	**1**				
Angle	L102x76x6.4				
A_g =	**1090**	mm^2			
A_h =	153.6	(24) X (thickness) mm^2			
A_{ne} =	936.4	mm^2			
(F_u/F_y)=	1.5				
A'_{ne1} =	561.8		T_R =	205.1	kN
A'_{ne2} =	**749.1**		T_R =	**273.4**	kN
$A'_{ne1}(F_u/F_y)$ =	842.8	$A_g > A'_{ne}(F_u/F_y)$			
$A'_{ne2}(F_u/F_y)$ =	**1124**	$A_g < A'_{ne}(F_u/F_y)$			
Trial #	**2**				
Angle	L127x76x6.4				
A_g =	**1250**	mm^2			
A_h =	154	(24) X (thickness) mm^2			
A_{ne} =	1096	mm^2			
(F_u/F_y)=	1.5				
A'_{ne1} =	658		T_R =	240	kN
A'_{ne2} =	**877**		T_R =	**320**	kN
$A'_{ne1}(F_u/F_y)$ =	987	$A_g > A'_{ne}(F_u/F_y)$			
$A'_{ne2}(F_u/F_y)$ =	**1316**	$A_g < A'_{ne}(F_u/F_y)$			

**Note:

A'_{ne1} = 3-Bolt (0.6) Using Steel Hankbook {12.3.3.2(b)}

A'_{ne2} = 4-Bolt (0.8) Using Steel Hankbook {12.3.3.2(b)}

$T_R = A'_{ne} * (F_Y)$

F_Y = 365 MPa

Table 3: Calculations For Net Cross Sectional Failure

Trial #	1				
Angle	L51x38x6.4				
A_g =	524.0	mm^2			
A_h =	153.6	(24) X (thickness) mm^2			
A_{ne} =	370.4	mm^2			
(F_u/F_y)=	1.5				
A'_{ne1} =	222.2		T_R =	81.1	kN
A'_{ne2} =	296.3		T_R =	108.2	kN
$A'_{ne1}(F_u/F_y)$ =	333.4	$A_g > A'_{ne}(F_u/F_y)$			
$A'_{ne2}(F_u/F_y)$ =	444.5	$A_g > A'_{ne}(F_u/F_y)$			
Trial #	2				
Angle	L64x51x6.4				
A_g =	685.0	mm^2			
A_h =	153.6	(24) X (thickness) mm^2			
A_{ne} =	531.4	mm^2			
(F_u/F_y)=	1.5				
A'_{ne1} =	318.8		T_R =	116.4	kN
A'_{ne2} =	425.1		T_R =	155.2	kN
$A'_{ne1}(F_u/F_y)$ =	478.3	$A_g > A'_{ne}(F_u/F_y)$			
$A'_{ne2}(F_u/F_y)$ =	637.7	$A_g > A'_{ne}(F_u/F_y)$			

**Note:

A'_{ne1} = 3-Bolt (0.6) Using Steel Hankbook {12.3.3.2(b)}

A'_{ne2} = 4-Bolt (0.8) Using Steel Hankbook {12.3.3.2(b)}

$T_R = A'_{ne} * (F_Y)$

F_Y = 365 MPa

Table 4: Tension Coupon Results

Angle Number	$P_{y\ (Avg.)}$ (newtons)	$P_{u\ (Avg.)}$ (newtons)	Elong./$_{50mm}$ (Avg)	Area (mm^2) (Avg)	Yield Stress MPa	Ult. Stress MPa
1	24800	34350	30.0%	79.23	313.0	433.6
2	24800	33895	31.0%	78.63	316.8	431.1
3	24050	34450	32.3%	79.22	303.7	434.8
4	25450	34550	33.5%	79.81	318.8	432.9
5	24300	34300	35.5%	79.44	306.0	431.8
6	25250	34400	34.0%	79.55	317.3	432.4
7	24550	34150	31.3%	78.99	310.8	432.3
8	25300	35700	32.0%	82.72	305.9	431.6
9	25500	35850	34.0%	83.03	307.1	431.8
10	24400	33630	35.0%	79.26	302.0	424.2
11	30900	44300	29.0%	83.52	369.9	530.4
12	31000	44400	55.5%	83.92	369.4	529.0

Table 5: Elonation Results

Angle Number	Size (All in mm's)	Length (mm)	Connection Size	Total Elongation (mm)
1	64x64x6.4	5000	3-bolt	33.32
2	64x64x6.4	5000	3-bolt	28.43
3	64x64x6.4	5000	3-bolt	28.26
4	64x64x6.4	5000	4-bolt	26.90
5	64x64x6.4	5000	4-bolt	33.02
6	64x64x6.4	5000	4-bolt	27.97
7	64x64x6.4	1000	4-bolt	38.75
8	64x64x6.4	1000	3-bolt	33.38
9	64x64x6.4	1000	4-bolt	28.23
10	64x64x6.4	1000	4-bolt	31.15
11	64x64x6.4	1000	3-bolt	27.94
12	64x64x6.4	1000	3-bolt	24.43

Table 6: Approximate Yield Loads

Angle Number	Size (All in mm's)	Length (mm)	Connection Size	Yield Loads Approximate (kN)
1	64x64x6.4	5000	3-bolt	90.0
2	64x64x6.4	5000	3-bolt	95.0
3	64x64x6.4	5000	3-bolt	85.0
4	64x64x6.4	5000	4-bolt	120
5	64x64x6.4	5000	4-bolt	100
6	64x64x6.4	5000	4-bolt	130
7	64x64x6.4	1000	4-bolt	80.0
8	64x64x6.4	1000	3-bolt	80.0
9	64x64x6.4	1000	4-bolt	95.0
10	64x64x6.4	1000	4-bolt	100
11	64x64x6.4	1000	3-bolt	100
12	64x64x6.4	1000	3-bolt	100

Table 7: Failure Loads and Failure Mode

Angle Number	Size (All in mm's)	Length (mm)	Connection Size	Max. Load (kN) (Experiments)	Failure Mode
1	64x64x6.4	5000	3-bolt	208.0	Net- Section
2	64x64x6.4	5000	3-bolt	203.3	Net- Section
3	64x64x6.4	5000	3-bolt	209.7	Net- Section
4	64x64x6.4	5000	4-bolt	220.3	Net- Section
5	64x64x6.4	5000	4-bolt	225.8	Net- Section
6	64x64x6.4	5000	4-bolt	236.0	Net- Section
7	64x64x6.4	1000	4-bolt	230.5	Net- Section
8	64x64x6.4	1000	3-bolt	210.7	Net- Section
9	64x64x6.4	1000	4-bolt	225.0	Net- Section
10	64x64x6.4	1000	4-bolt	224.0	Net- Section
11	64x64x6.4	1000	3-bolt	250.7	Net- Section
12	64x64x6.4	1000	3-bolt	180.0	Net- Section

Table 8: Efficiency

Angle Number	Connection Size	Efficiency U_1	Efficiency U_2
1	3-bolt	0.783	0.631
2	3-bolt	0.770	0.634
3	3-bolt	0.787	0.624
8	3-bolt	0.797	0.627
11	3-bolt	0.772	0.624
12	3-bolt	0.556	0.624
4	4-bolt	0.831	0.849
5	4-bolt	0.854	0.833
6	4-bolt	0.891	0.848
7	4-bolt	0.871	0.839
9	4-bolt	0.851	0.834
10	4-bolt	0.862	0.843

APPENDIX A:

TENSION COUPON RESULTS

Table A1: Tension Coupon For Angle 1

Tension Coupon # 1A

F_y = 25100 kN

F_u = 34900 kN

	1	2	3	Avg.
Thickness	6.48	6.48	6.48	6.48
Width	12.40	12.40	12.39	12.40

Area = 80.33 mm^2

Yield Stress = 312.5 MPa

Ult. Stress = 434.5 MPa

Elong./$_{50mm}$ = 30%

Tension Coupon # 1B

F_y = 24500 kN

F_u = 33800 kN

	1	2	3	Avg.
Thickness	6.28	6.27	6.27	6.27
Width	12.41	12.41	12.54	12.45

Area = 78.12 mm^2

Yield Stress = 313.6 MPa

Ult. Stress = 432.6 MPa

Elong./$_{50mm}$ = 30%

Average Yield Stress = 313.0 MPa

Average Ult. Stress = 433.6 MPa

Table A2:Tension Coupon For Angle 2

Tension Coupon # 2A

F_y = 24800 kN

F_u = 33800 kN

	1	2	3	Avg.
Thickness	6.25	6.24	6.24	6.24
Width	12.54	12.54	12.54	12.54

Area = 78.29 mm^2

Yield Stress = 316.8 MPa

Ult. Stress = 431.7 MPa

Elong./$_{50mm}$ = 31%

Tension Coupon # 2B Strain Gauged

F_y = N/A kN

F_u = 33990 kN

	1	2	3	Avg.
Thickness	6.25	6.28	6.27	6.27
Width	12.60	12.60	12.60	12.60

Area = 78.96 mm^2

Yield Stress = N/A MPa

Ult. Stress = 430.5 MPa

Elong./$_{50mm}$ = N/A

Average Yield Stress = 316.8 MPa

Average Ult. Stress = 431.1 MPa

Table A3: Tension Coupon For Angle 3

Tension Coupon # 3A

F_y = 24100 kN

F_u = 35100 kN

	1	2	3	Avg.
Thickness	6.41	6.42	6.42	6.42
Width	12.64	12.52	12.53	12.56

Area = 80.61 mm^2

Yield Stress = 299.0 MPa

Ult. Stress = 435.4 MPa

Elong./$_{50mm}$ = 34%

Tension Coupon # 3B

F_y = 24000 kN

F_u = 33800 kN

	1	2	3	Avg.
Thickness	6.24	6.26	6.26	6.25
Width	12.45	12.43	12.46	12.45

Area = 77.83 mm^2

Yield Stress = 308.4 MPa

Ult. Stress = 434.3 MPa

Elong./$_{50mm}$ = 32.50%

Average Yield Stress = 303.7 MPa

Average Ult. Stress = 434.8 MPa

Table A4:Tension Coupon For Angle 4

Tension Coupon # 4A

F_y = 26300 kN

F_u = 35100 kN

	1	2	3	Avg.
Thickness	6.51	6.51	6.51	6.51
Width	12.46	12.45	12.46	12.46

Area = 81.09 mm^2

Yield Stress = 324.3 MPa

Ult. Stress = 432.8 MPa

Elong./$_{50mm}$ = 35%

Tension Coupon # 4B

F_y = 24600 kN

F_u = 34000 kN

	1	2	3	Avg.
Thickness	6.25	6.23	6.23	6.24
Width	12.55	12.61	12.61	12.59

Area = 78.52 mm^2

Yield Stress = 313.3 MPa

Ult. Stress = 433.0 MPa

Elong./$_{50mm}$ = 32%

Average Yield Stress = 318.8 MPa

Average Ult. Stress = 432.9 MPa

Table A5:Tension Coupon For Angle 5

Tension Coupon # 5A

F_y = 24500 kN

F_u = 35000 kN

	1	2	3	Avg.
Thickness	6.50	6.51	6.52	6.51
Width	12.50	12.46	12.48	12.48

Area = 81.24 mm^2

Yield Stress = 301.6 MPa

Ult. Stress = 430.8 MPa

Elong./$_{50mm}$ = 35%

Tension Coupon # 5B

F_y = 24100 kN

F_u = 33600 kN

	1	2	3	Avg.
Thickness	6.24	6.22	6.23	6.23
Width	12.46	12.43	12.49	12.46

Area = 77.63 mm^2

Yield Stress = 310.5 MPa

Ult. Stress = 432.8 MPa

Elong./$_{50mm}$ = 36%

Average Yield Stress = 306.0 MPa

Average Ult. Stress = 431.8 MPa

Table A6:Tension Coupon For Angle 6

Tension Coupon # 6A

F_y = 26000 kN

F_u = 35100 kN

	1	2	3	Avg.
Thickness	6.48	6.49	6.48	6.48
Width	12.49	12.48	12.55	12.51

Area = 81.08 mm^2

Yield Stress = 320.7 MPa

Ult. Stress = 432.9 MPa

Elong./$_{50mm}$ = 34%

Tension Coupon # 6B

F_y = 24500 kN

F_u = 33700 kN

	1	2	3	Avg.
Thickness	6.22	6.22	6.22	6.22
Width	12.51	12.52	12.60	12.54

Area = 78.02 mm^2

Yield Stress = 314.0 MPa

Ult. Stress = 431.9 MPa

Elong./$_{50mm}$ = N/A

Average Yield Stress = 317.3 MPa

Average Ult. Stress = 432.4 MPa

Table A7:Tension Coupon For Angle 7

Tension Coupon # 7A

F_y = 24000 kN

F_u = 33600 kN

	1	2	3	Avg.
Thickness	6.23	6.25	6.23	6.24
Width	12.45	12.46	12.48	12.46

Area = 77.73 mm^2

Yield Stress = 308.8 MPa

Ult. Stress = 432.3 MPa

Elong./$_{50mm}$ = 31.5%

Tension Coupon # 7B

F_y = 25100 kN

F_u = 34700 kN

	1	2	3	Avg.
Thickness	6.46	6.46	6.46	6.46
Width	12.45	12.40	12.42	12.42

Area = 80.25 mm^2

Yield Stress = 312.8 MPa

Ult. Stress = 432.4 MPa

Elong./$_{50mm}$ = 31%

Average Yield Stress = 310.8 MPa

Average Ult. Stress = 432.3 MPa

Table A8:Tension Coupon For Angle 8

Tension Coupon # 8A

F_y = 25200 kN

F_u = 35100 kN

	1	2	3	Avg.
Thickness	6.23	6.22	6.23	6.23
Width	12.96	13.05	13.08	13.03

Area = 81.13 mm^2

Yield Stress = 310.6 MPa

Ult. Stress = 432.6 MPa

Elong./$_{50mm}$ = 32%

Tension Coupon # 8B

F_y = 25400 kN

F_u = 36300 kN

	1	2	3	Avg.
Thickness	6.47	6.48	6.48	6.48
Width	12.96	13.03	13.06	13.02

Area = 84.30 mm^2

Yield Stress = 301.3 MPa

Ult. Stress = 430.6 MPa

Elong./$_{50mm}$ = 32%

Average Yield Stress = 305.9 MPa

Average Ult. Stress = 431.6 MPa

Table A9:Tension Coupon For Angle 9

Tension Coupon # 9A

F_y = 25900 kN

F_u = 36500 kN

	1	2	3	Avg.
Thickness	6.46	6.46	6.47	6.46
Width	13.11	13.08	13.03	13.07

Area = 84.50 mm^2

Yield Stress = 306.5 MPa

Ult. Stress = 432.0 MPa

Elong./$_{50mm}$ = 34%

Tension Coupon # 9B

F_y = 25100 kN

F_u = 35200 kN

	1	2	3	Avg.
Thickness	6.23	6.23	6.22	6.23
Width	13.05	13.10	13.15	13.10

Area = 81.57 mm^2

Yield Stress = 307.7 MPa

Ult. Stress = 431.5 MPa

Elong./$_{50mm}$ = 34%

Average Yield Stress = 307.1 MPa

Average Ult. Stress = 431.8 MPa

Table A10:Tension Coupon For Angle 10

Tension Coupon # 10A

F_y = 24400 kN

F_u = 34800 kN

	1	2	3	Avg.
Thickness	6.49	6.48	6.47	6.48
Width	12.47	12.47	12.47	12.47

Area = 80.81 mm^2

Yield Stress = 302.0 MPa

Ult. Stress = 430.7 MPa

Elong./$_{50mm}$ = 35%

Tension Coupon # 10B Strain Guaged

F_y = N/A kN

F_u = 32460 kN

	1	2	3	Avg.
Thickness	6.05	6.02	6.60	6.22
Width	12.49	12.48	12.49	12.49

Area = 77.71 mm^2

Yield Stress = N/A MPa

Ult. Stress = 417.7 MPa

Elong./$_{50mm}$ = N/A

Average Yield Stress = 302.0 MPa

Average Ult. Stress = 424.2 MPa

Table A11:Tension Coupon For Angle 11

Tension Coupon # 11A

F_y = 31800 kN

F_u = 44700 kN

	1	2	3	Avg.
Thickness	6.48	6.49	6.49	6.49
Width	12.93	12.98	13.05	12.99

Area = 84.24 mm^2

Yield Stress = 377.5 MPa

Ult. Stress = 530.6 MPa

Elong./$_{50mm}$ = 30%

Tension Coupon # 11B

F_y = 30000 kN

F_u = 43900 kN

	1	2	3	Avg.
Thickness	6.38	6.38	6.34	6.37
Width	12.95	13.00	13.07	13.01

Area = 82.81 mm^2

Yield Stress = 362.3 MPa

Ult. Stress = 530.1 MPa

Elong./$_{50mm}$ = 28%

Average Yield Stress = 369.9 MPa

Average Ult. Stress = 530.4 MPa

Table A12:Tension Coupon For Angle 12

Tension Coupon # 12A

F_y = 31000 kN

F_u = 44900 kN

	1	2	3	Avg.
Thickness	6.50	6.49	6.50	6.50
Width	13.06	13.05	12.99	13.03

Area = 84.67 mm^2

Yield Stress = 366.1 MPa

Ult. Stress = 530.3 MPa

Elong./$_{50mm}$ = 28.50%

Tension Coupon # 12B

F_y = 31000 kN

F_u = 43900 kN

	1	2	3	Avg.
Thickness	6.38	6.37	6.37	6.37
Width	12.98	13.05	13.12	13.05

Area = 83.17 mm^2

Yield Stress = 372.7 MPa

Ult. Stress = 527.8 MPa

Elong./$_{50mm}$ = 27%

Average Yield Stress = 369.4 MPa

Average Ult. Stress = 529.0 MPa

APPENDIX B:

ELONGATION CURVES

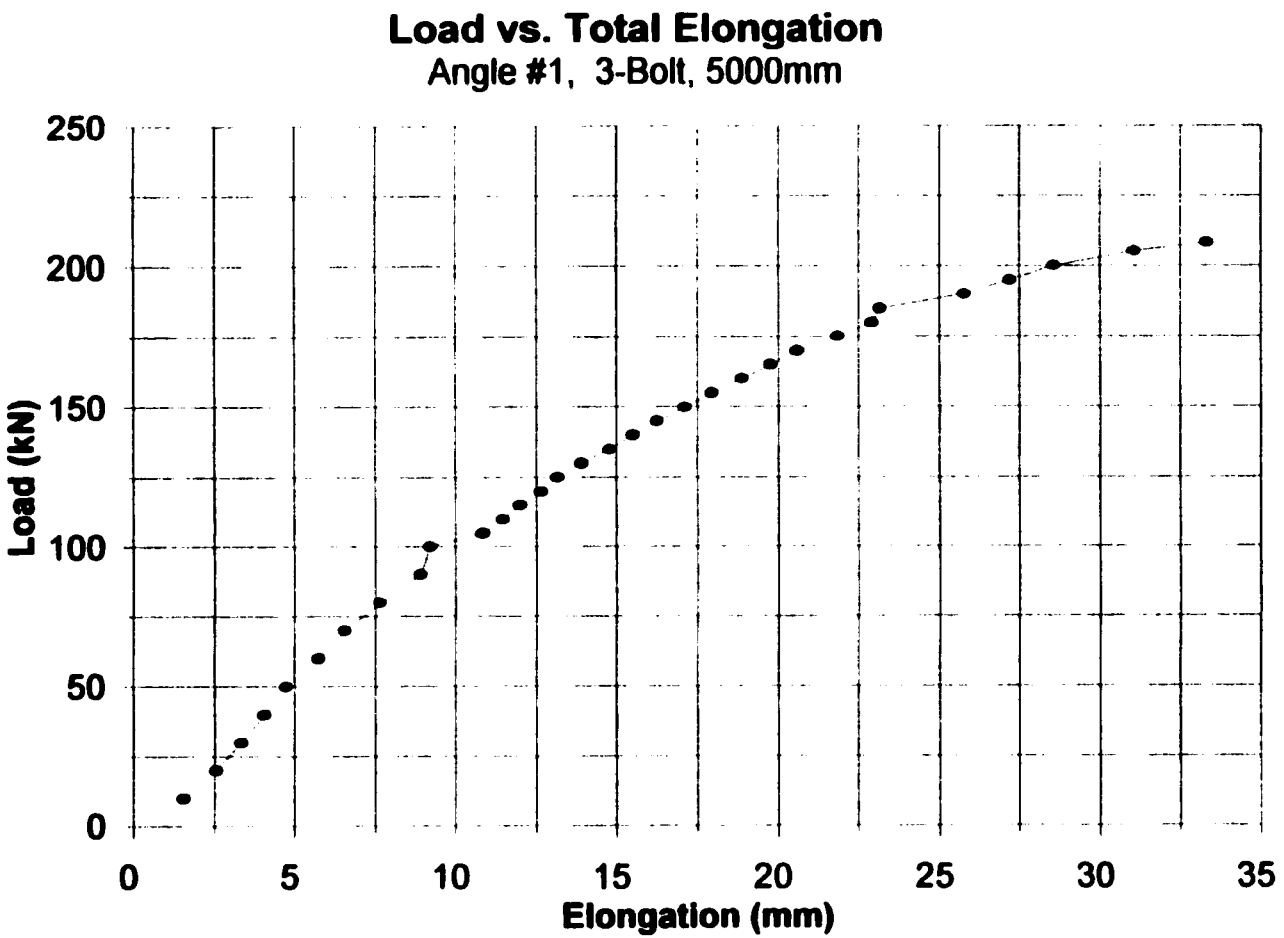

Figure B1: Total Elongation

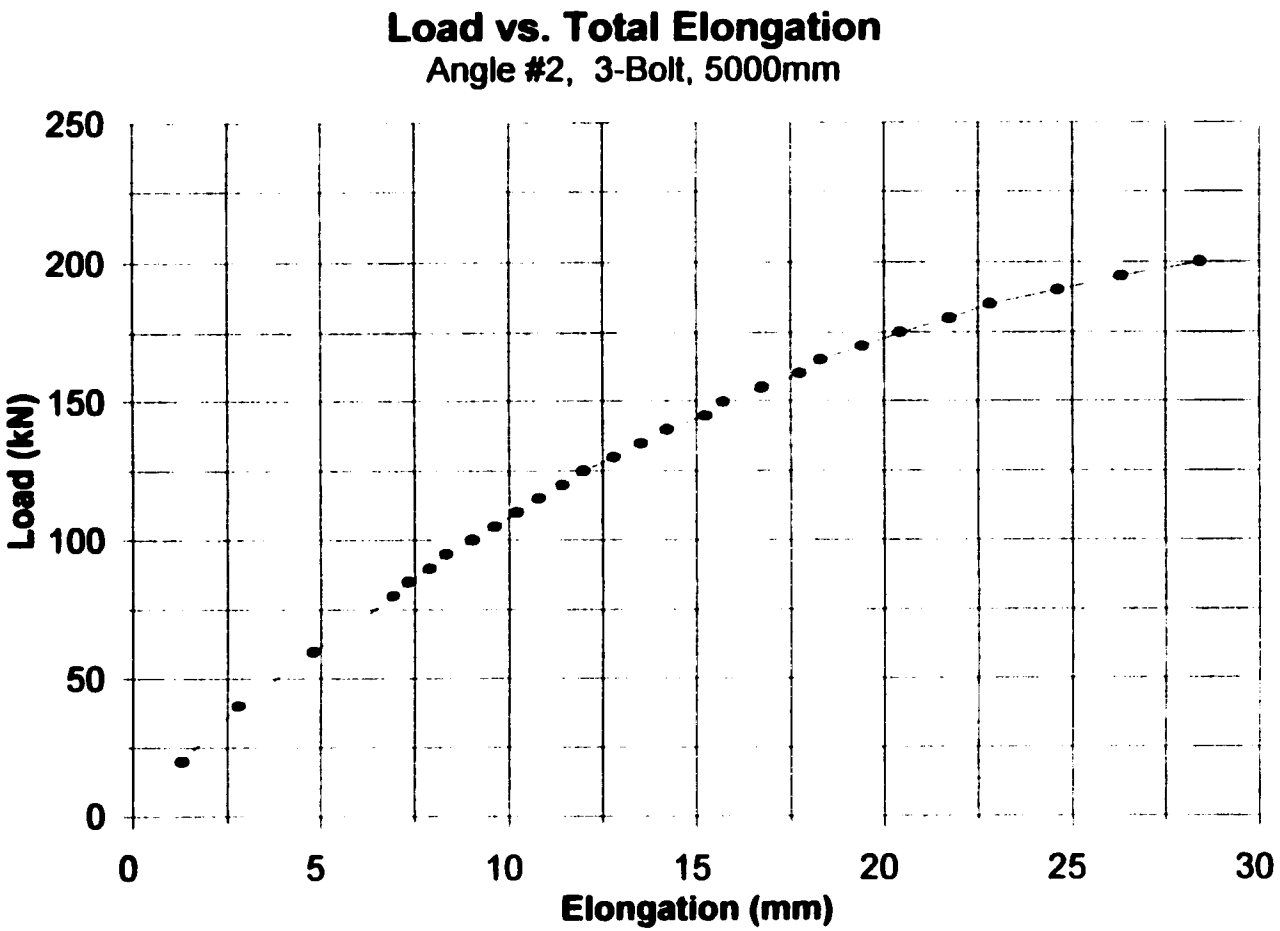

Figure B2: Total Elongation

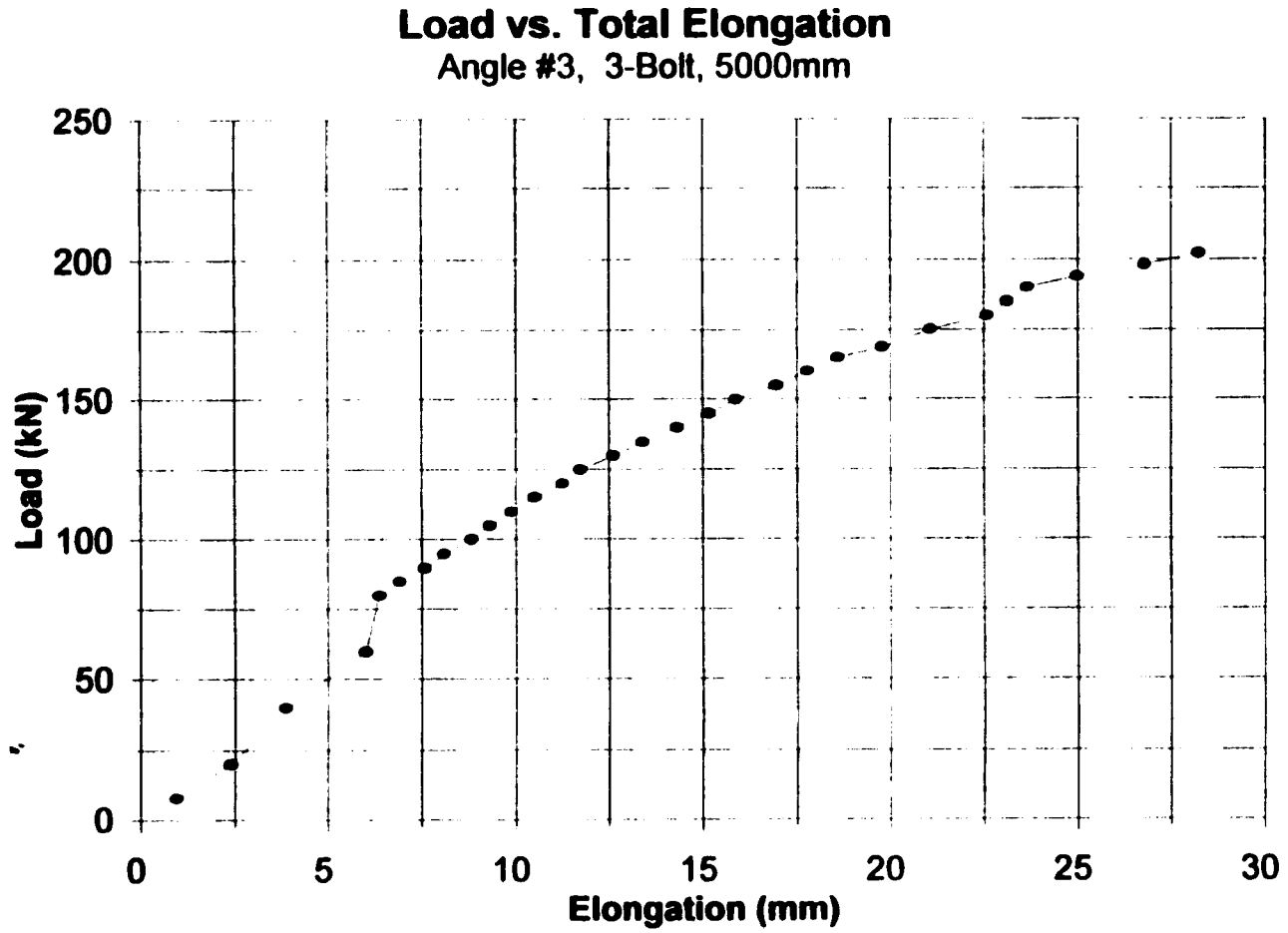

Figure B3: Total Elongation

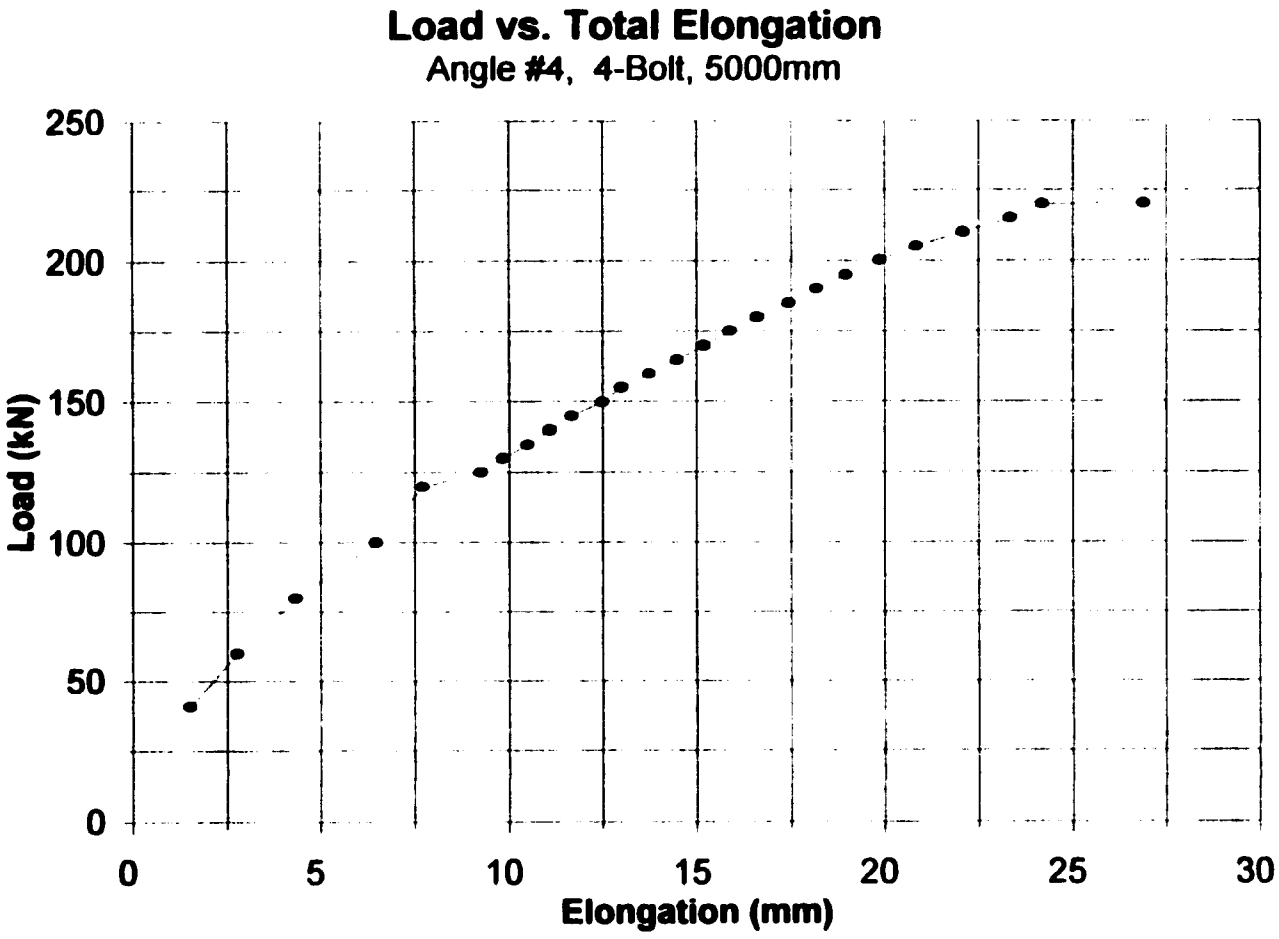

Figure B4: Total Elongation

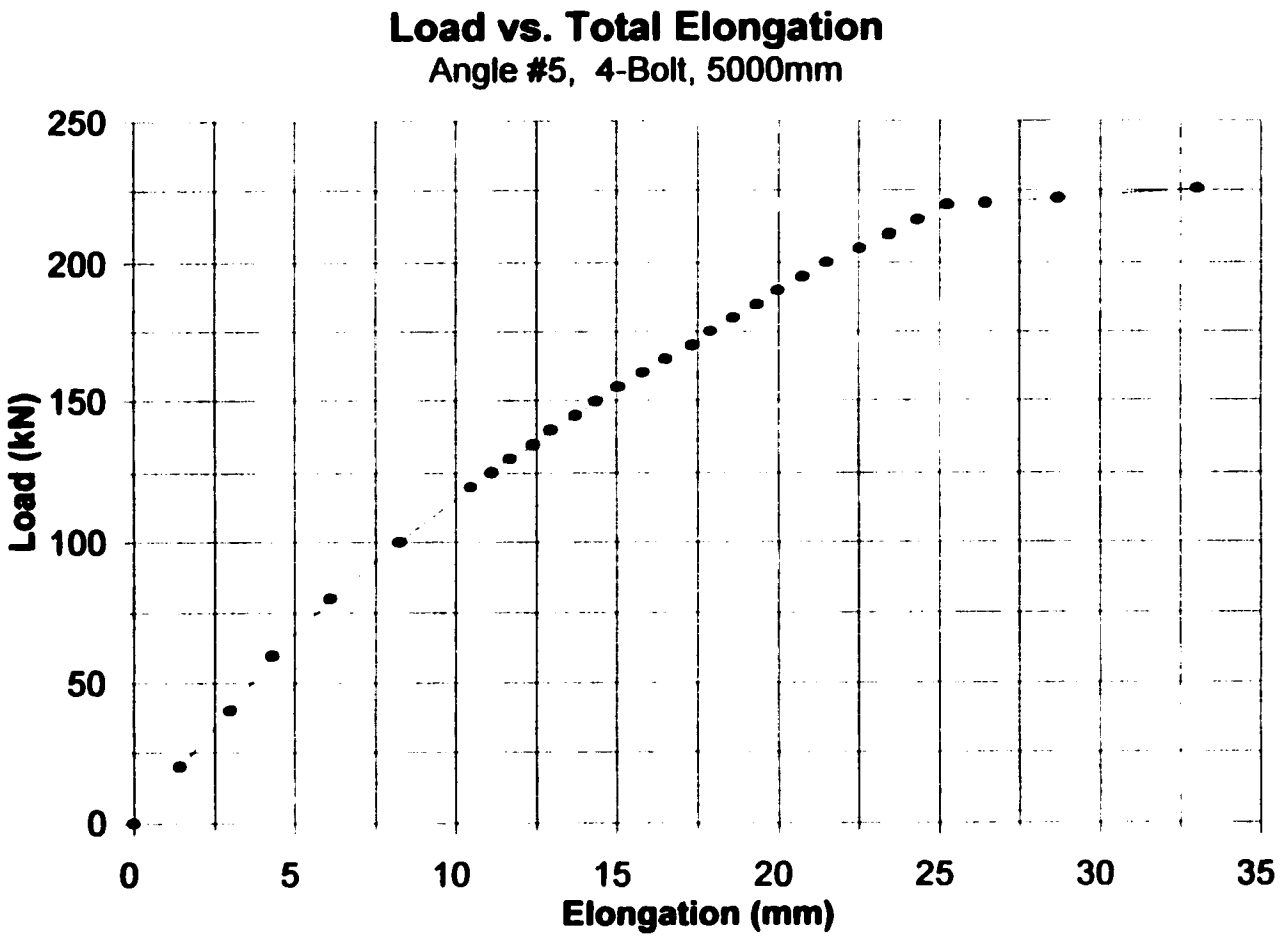

Figure B5: Total Elongation

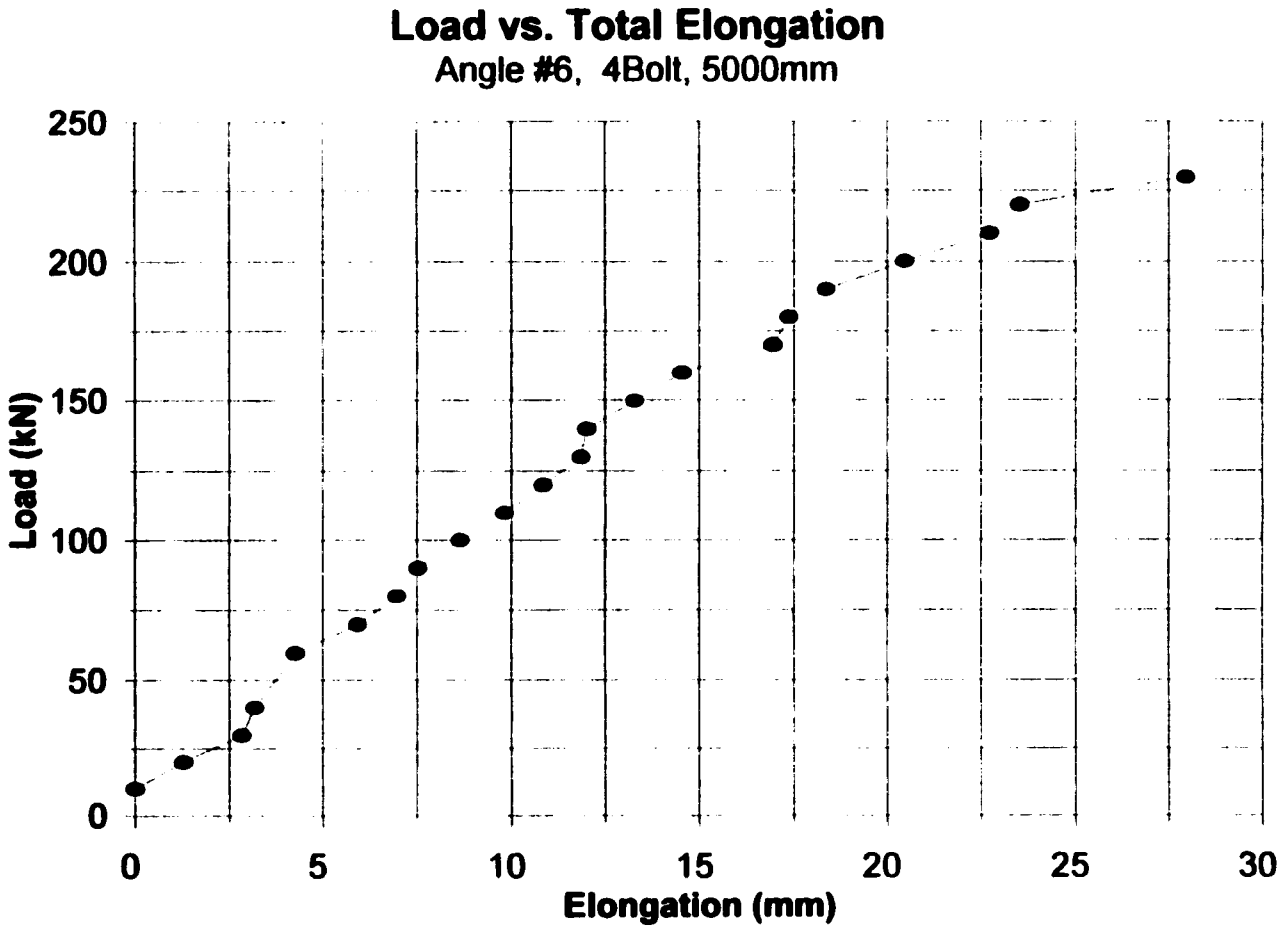

Figure B6: Total Elongation

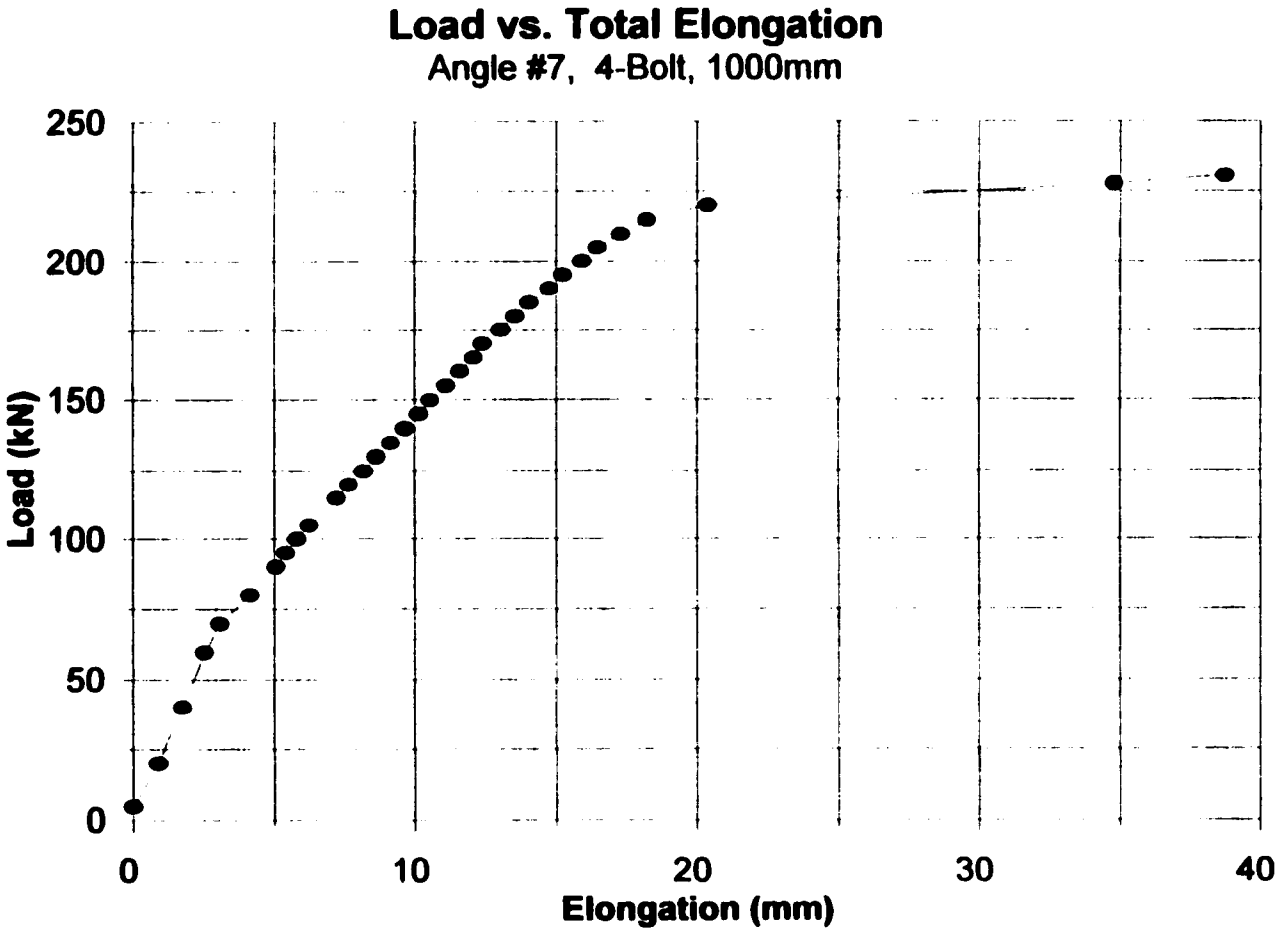

Figure B7: Total Elongation

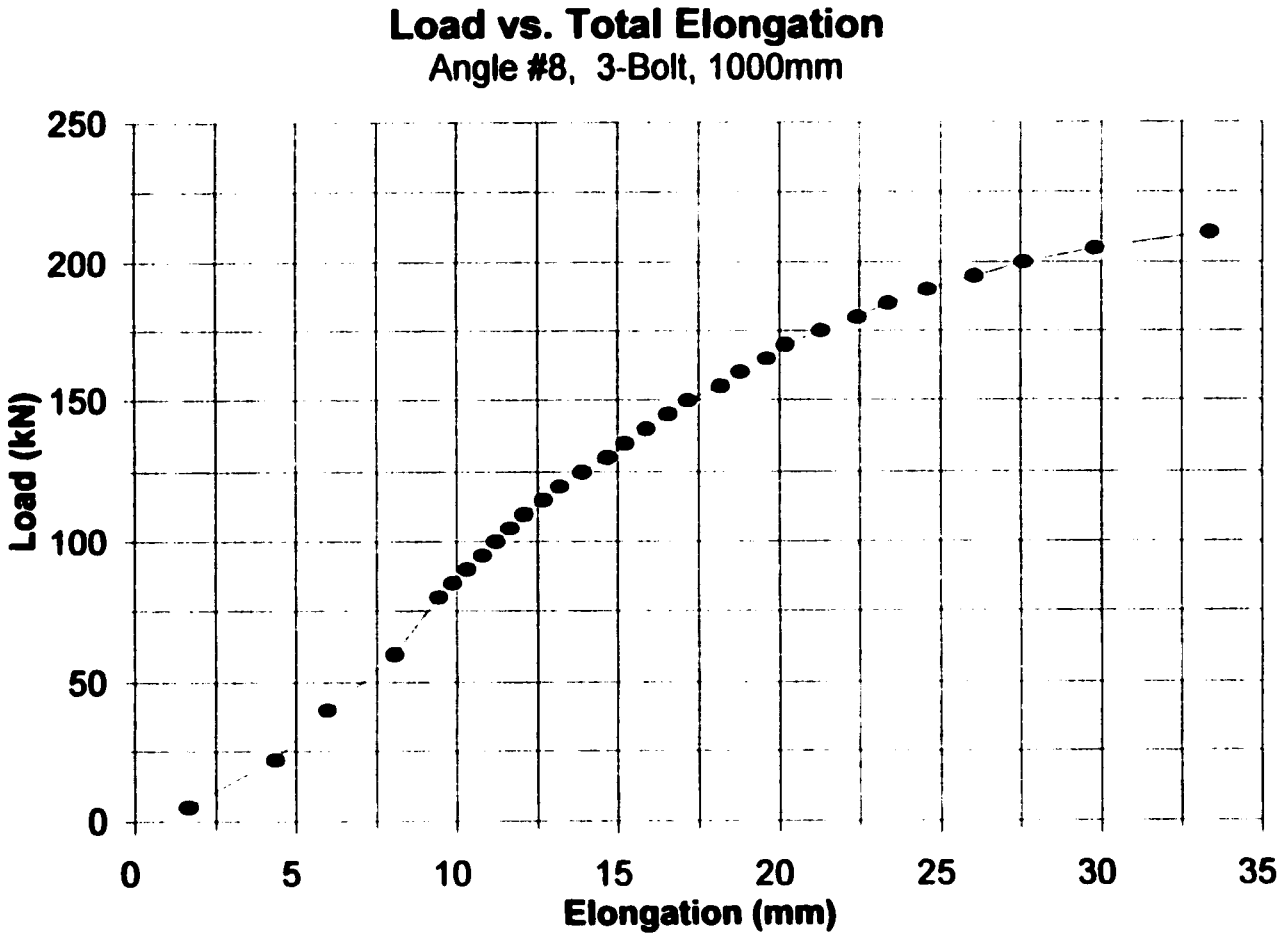

Figure B8: Total Elongation

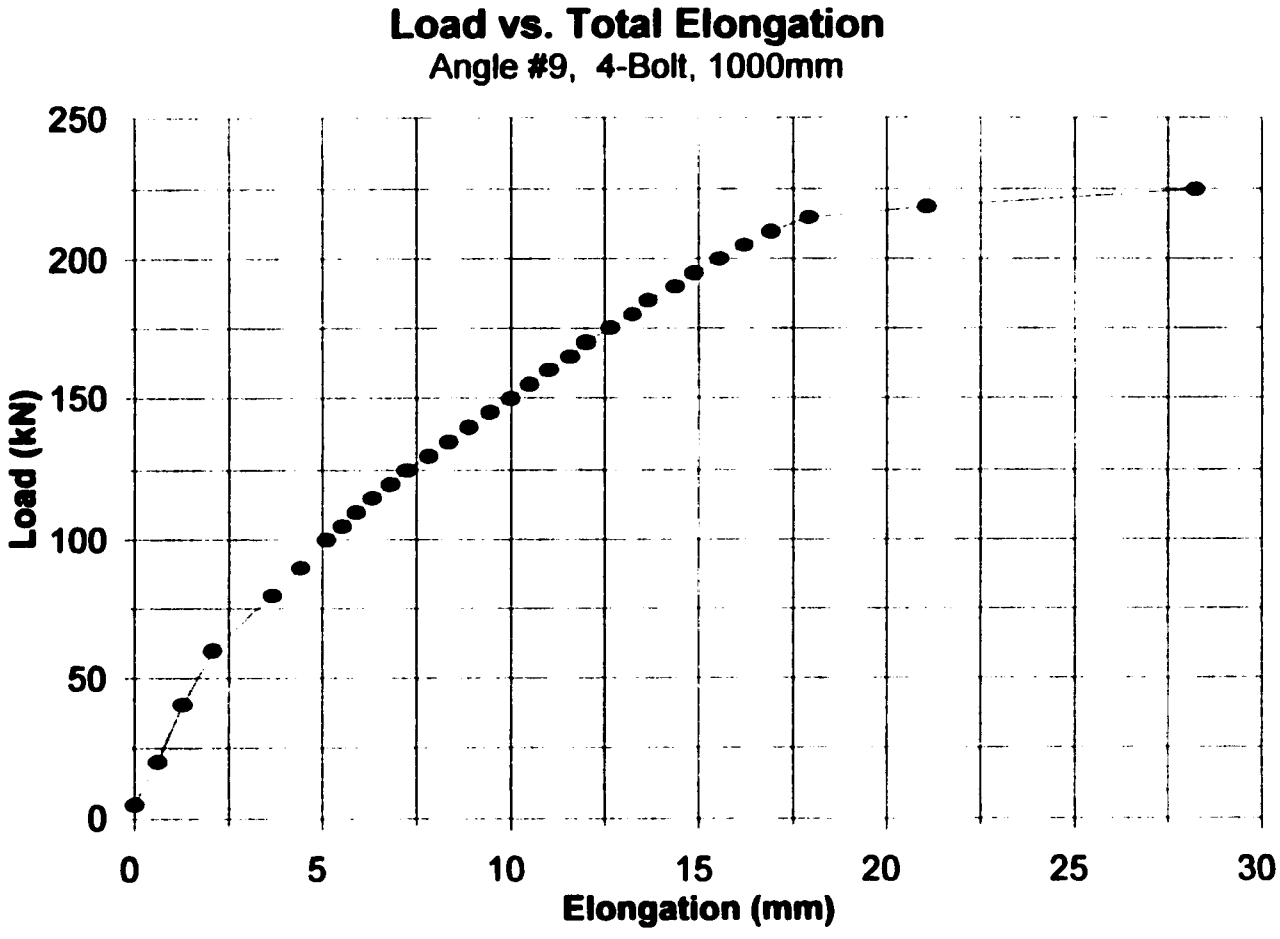

Figure B9: Total Elongation

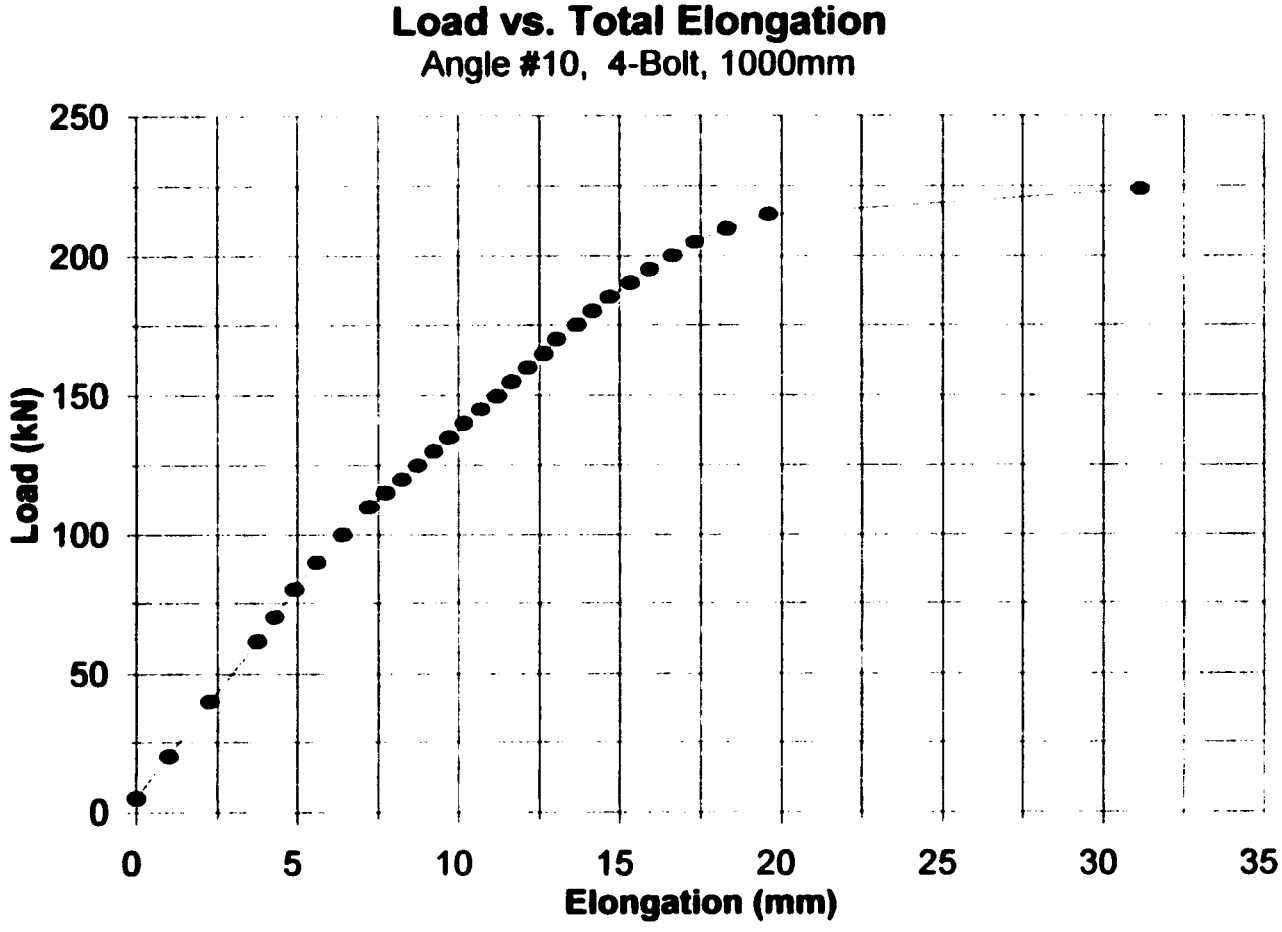

Figure B10: Total Elongation

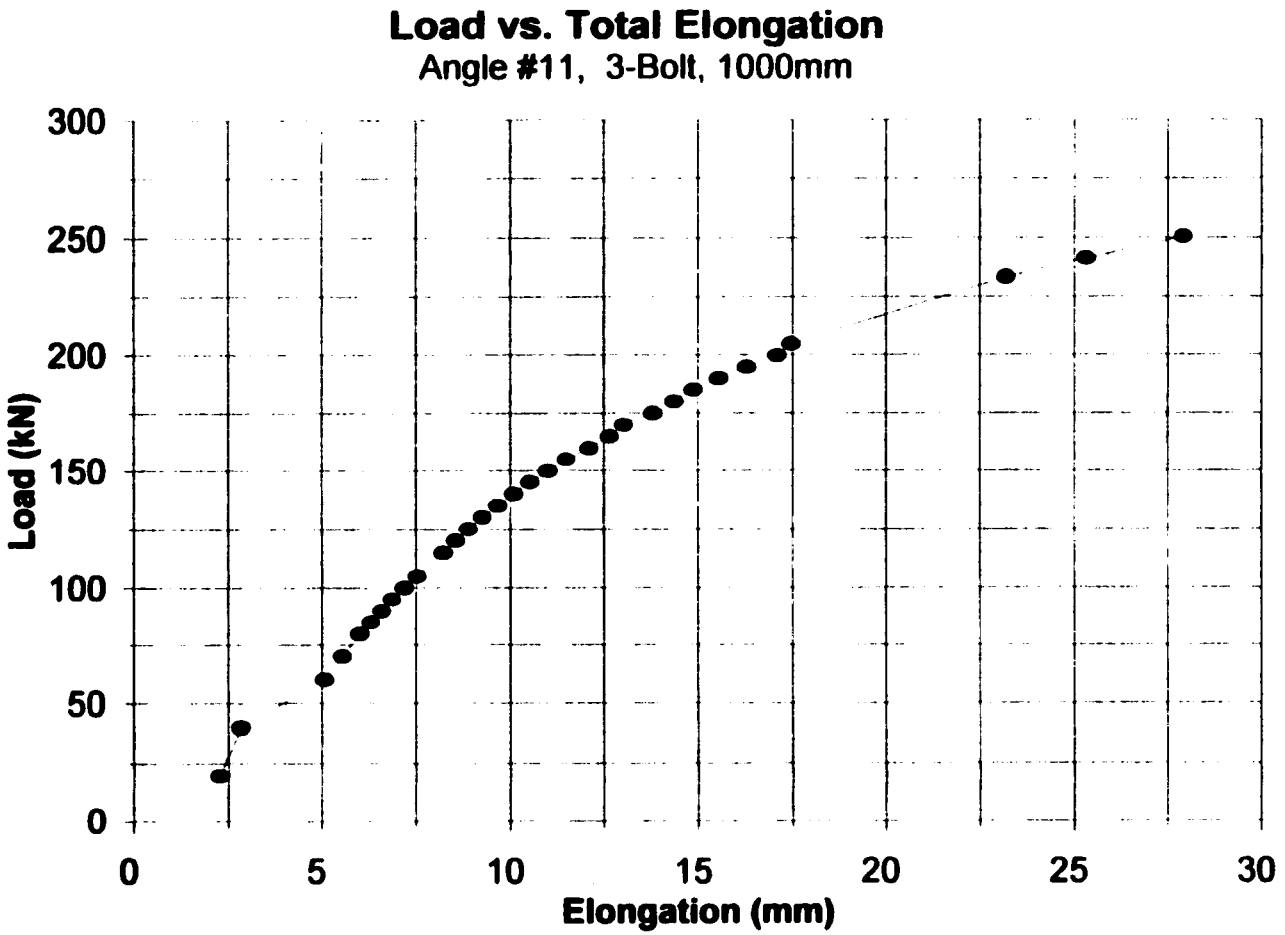

Figure B11: Total Elongation

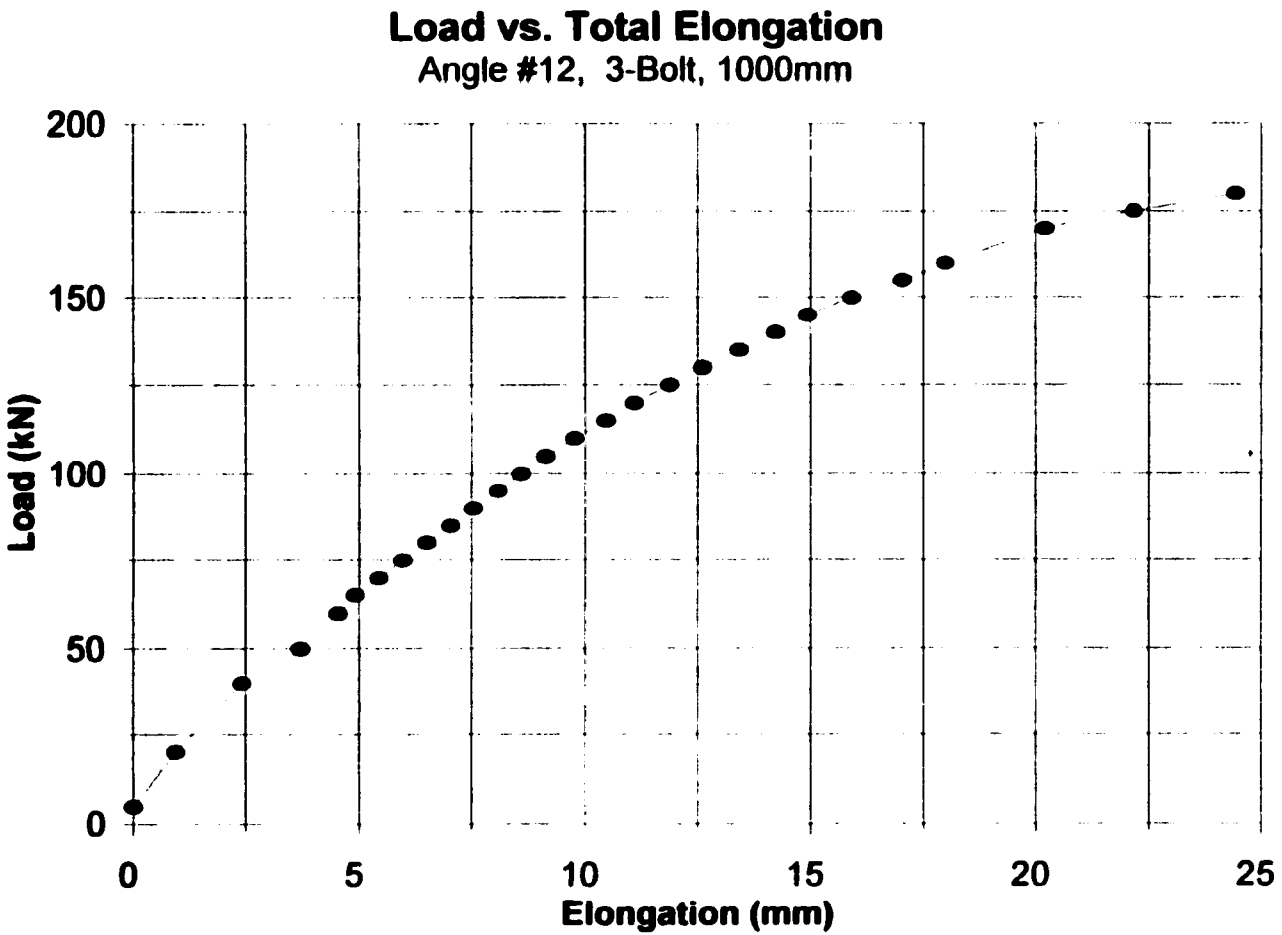

Figure B12: Total Elongation

APPENDIX C:

STRAIN DISTRIBUTION CURVES

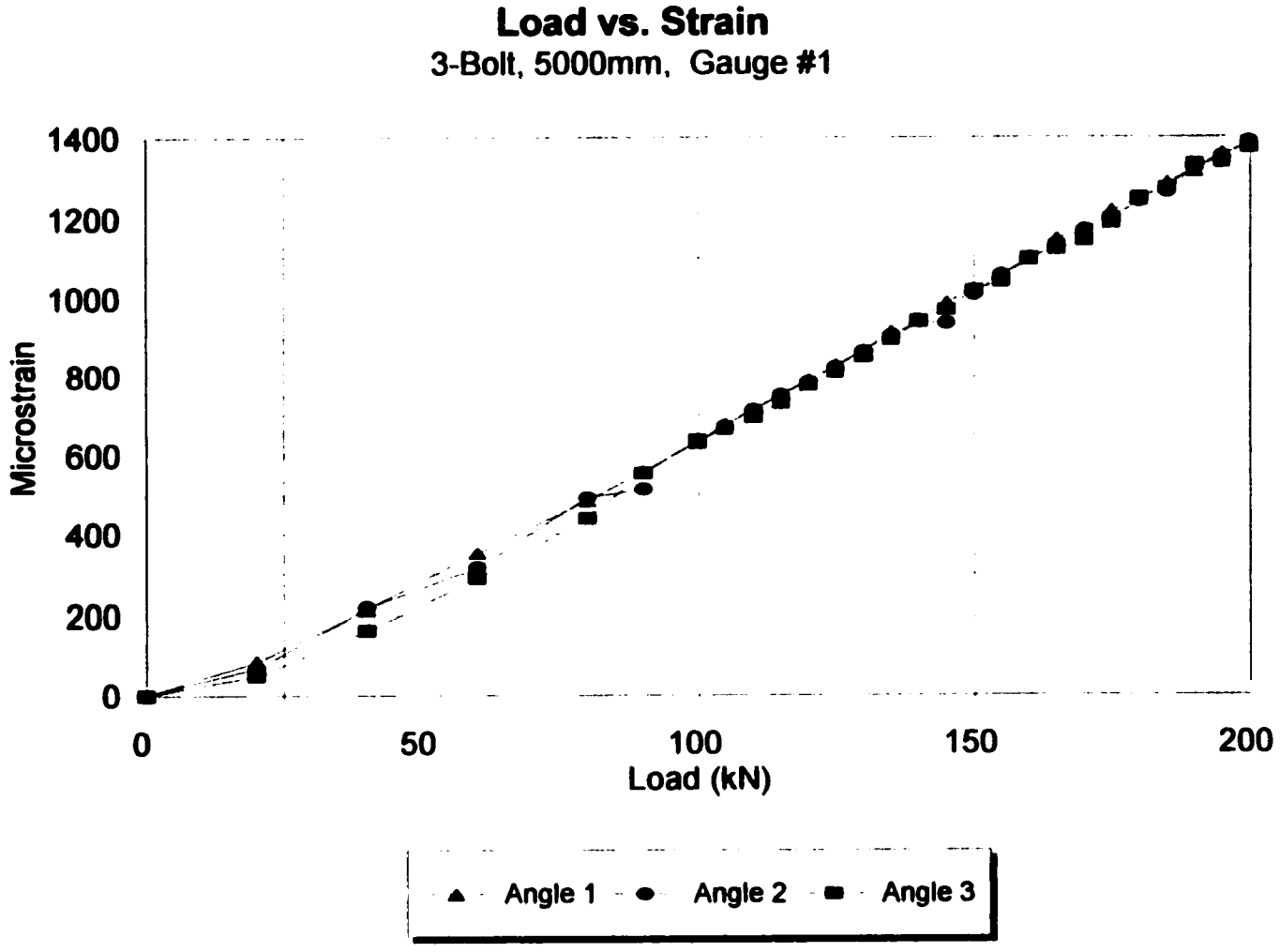

Figure C1: Load vs. Strain

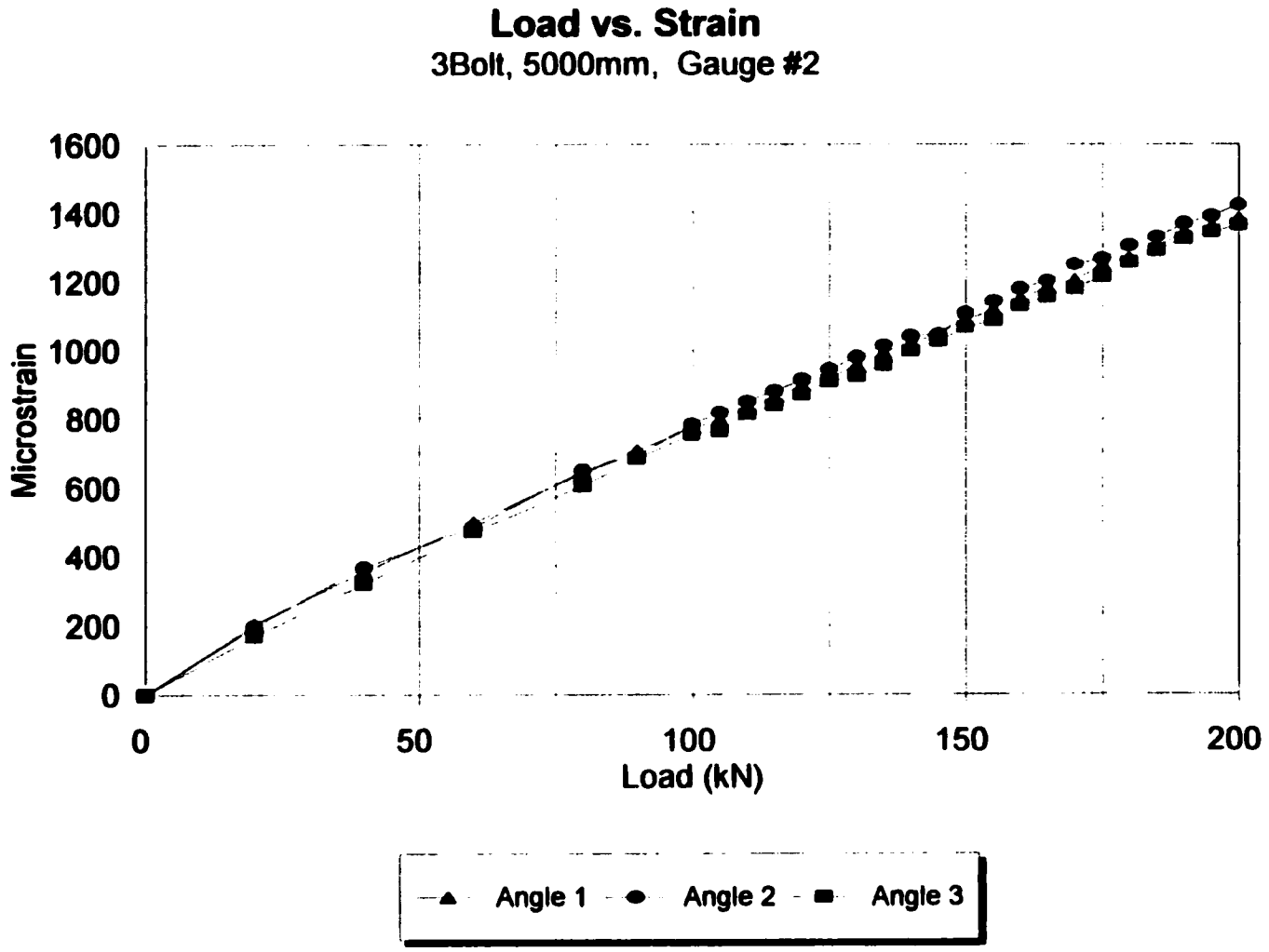

Figure C2: Load vs. Strain

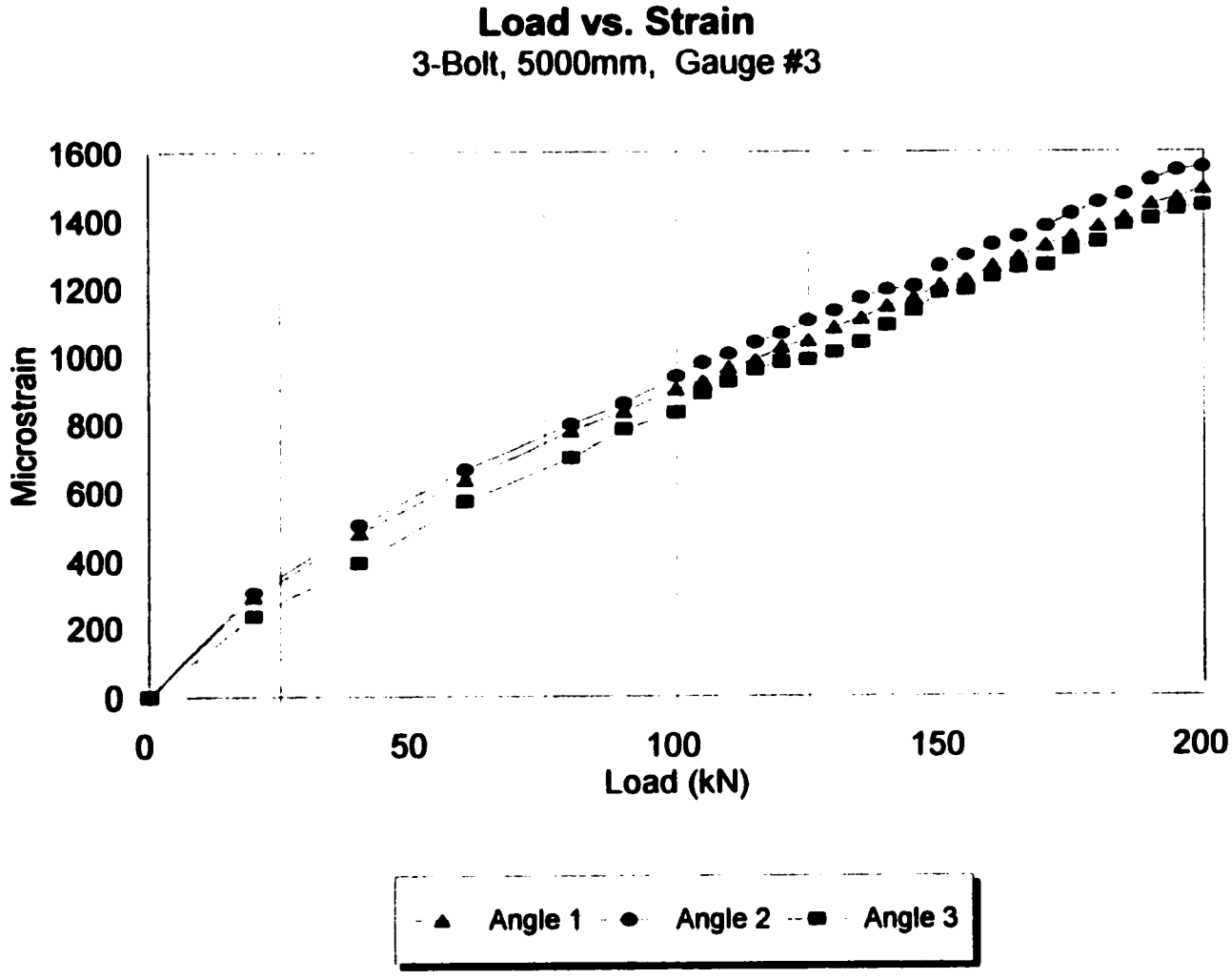

Figure C3: Load vs. Strain

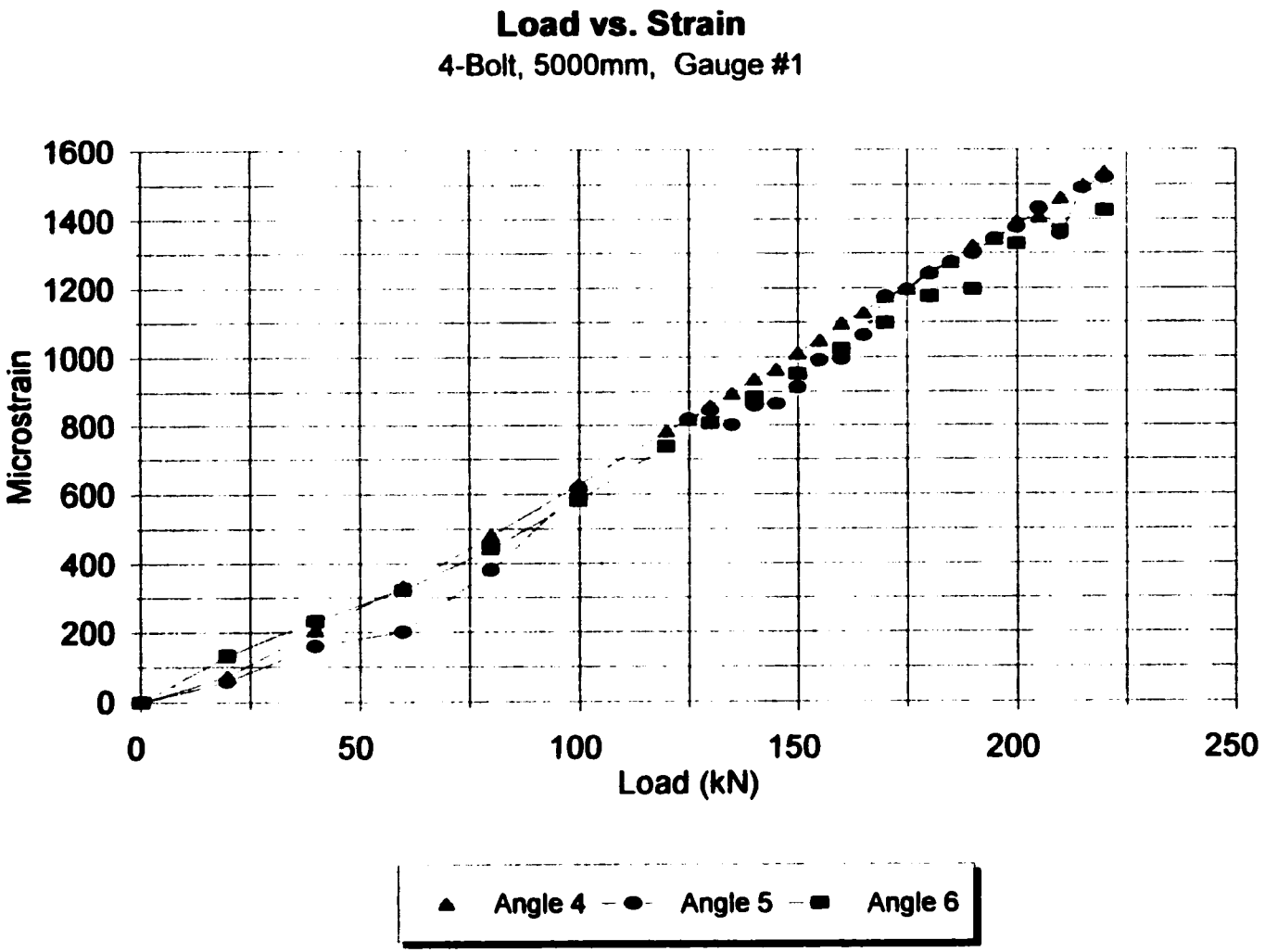

Figure C4: Load vs. Strain

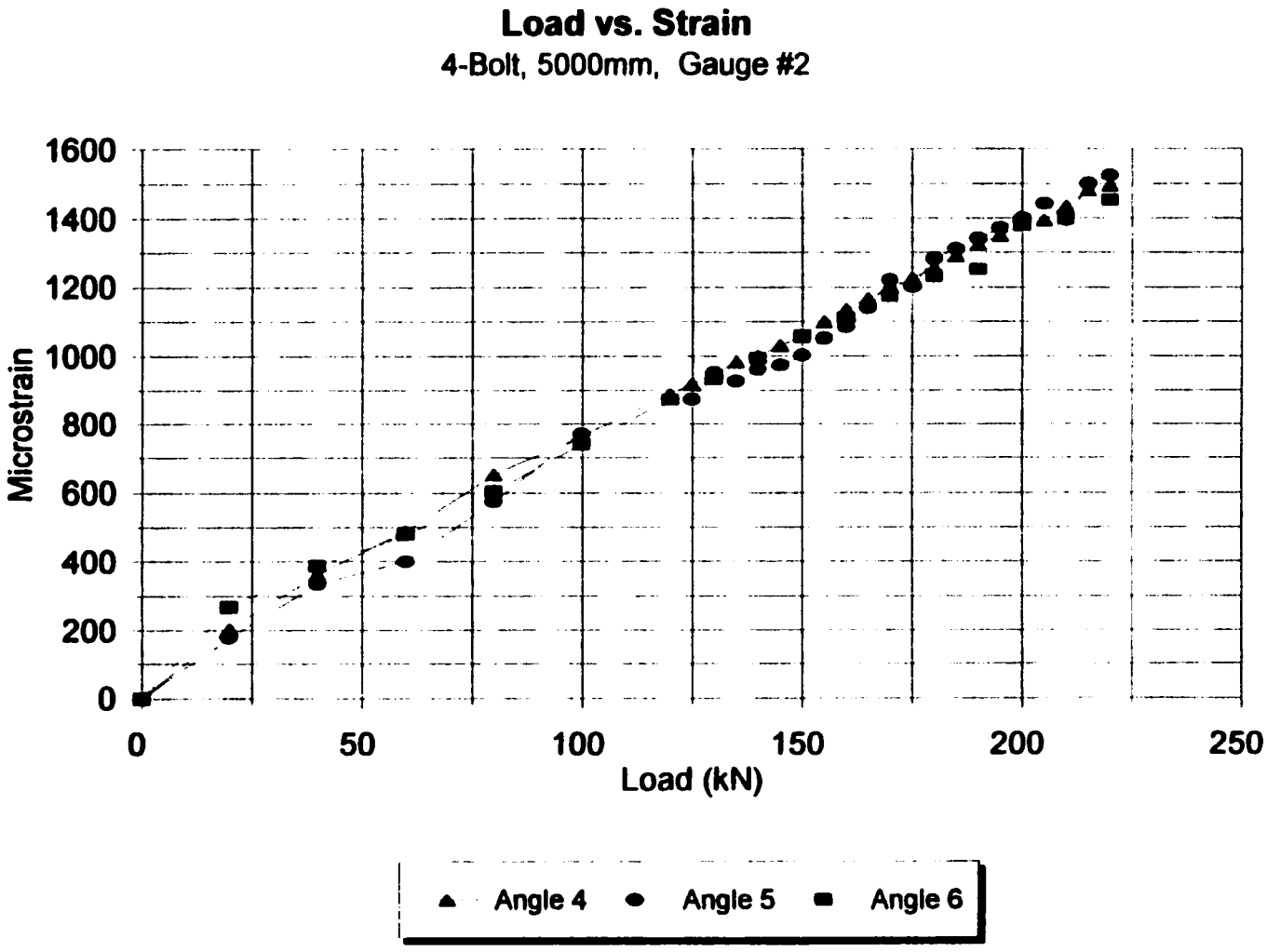

Figure C5: Load vs. Strain

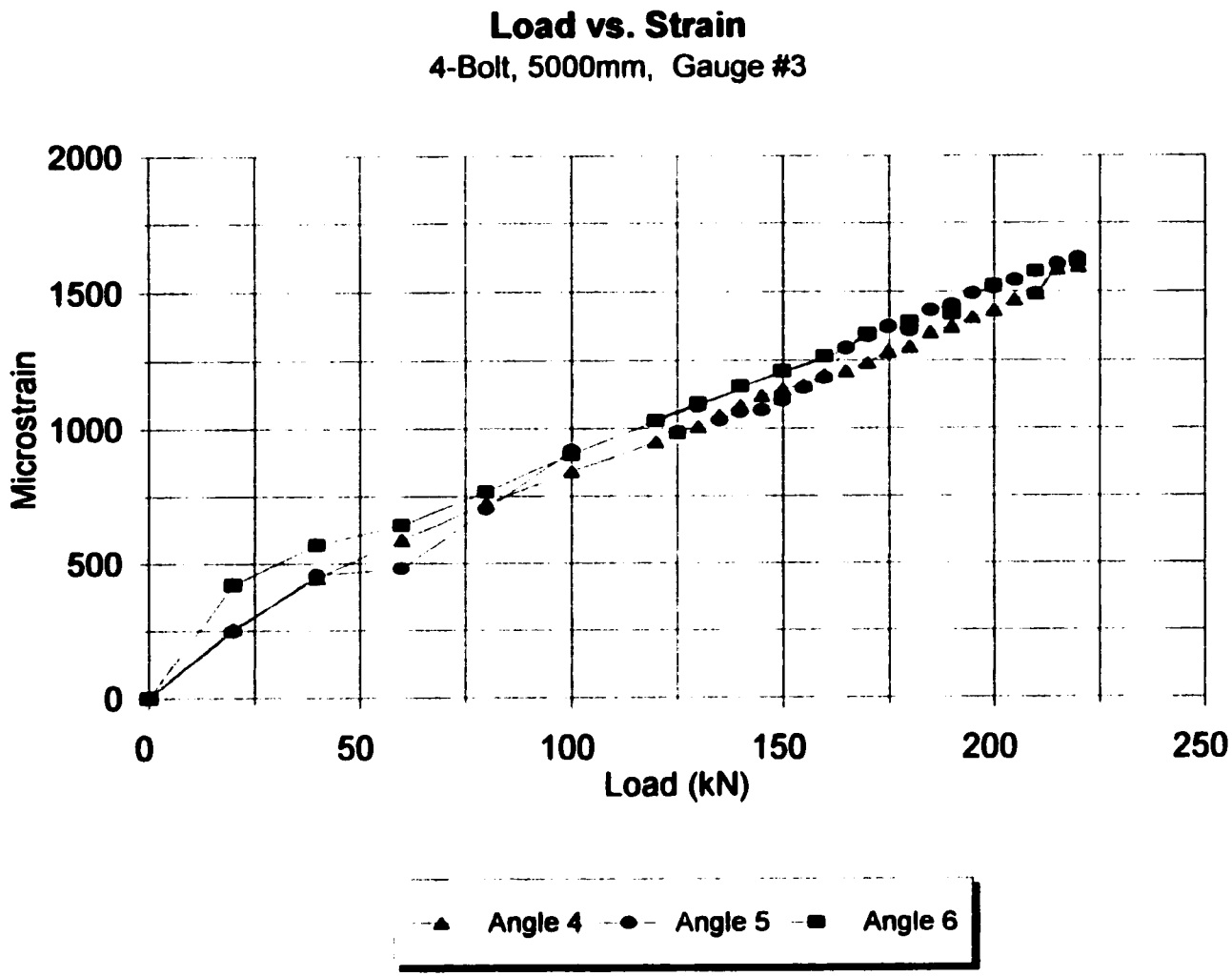

Figure C6: Load vs. Strain

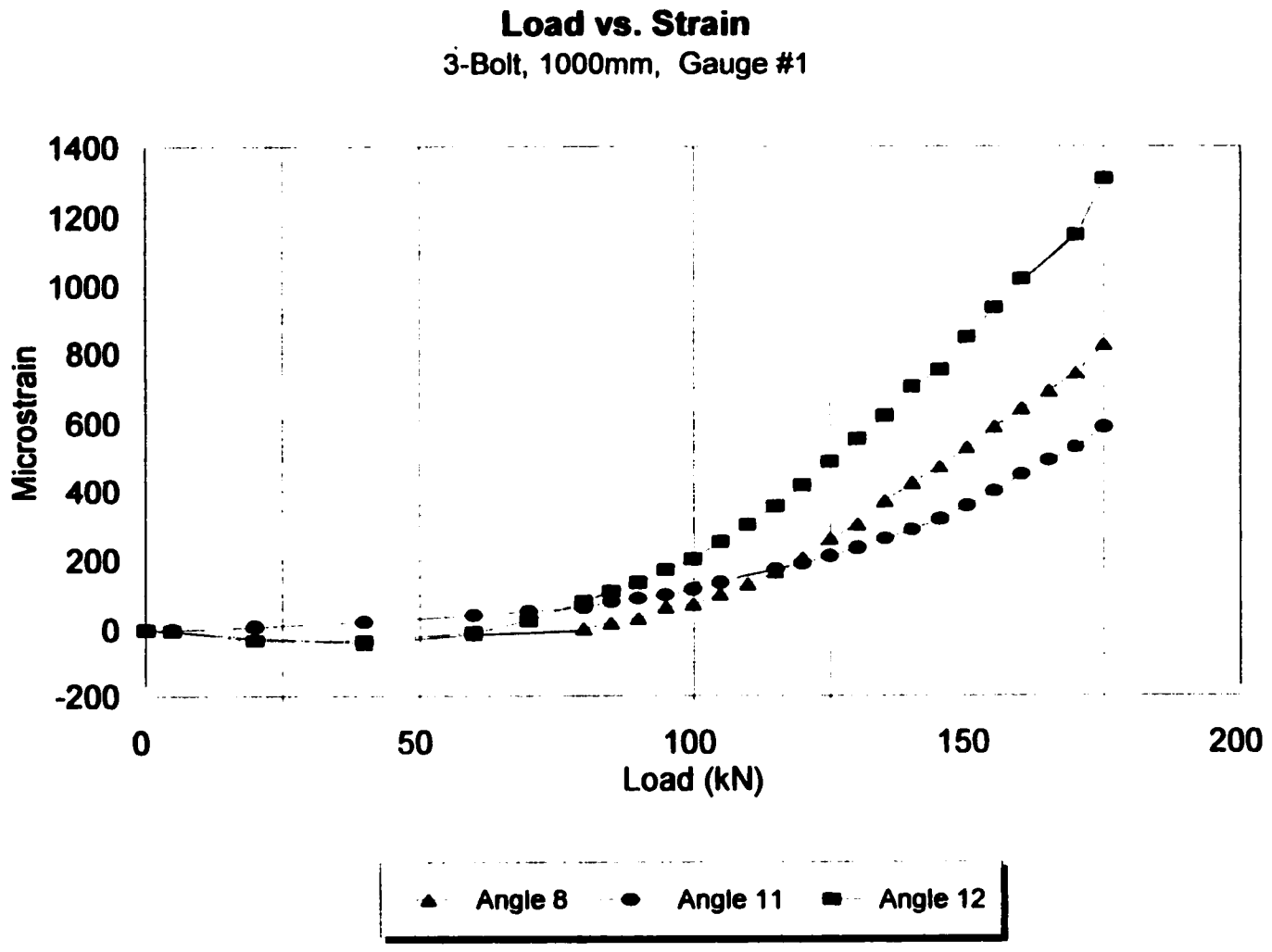

Figure C7: Load vs. Strain

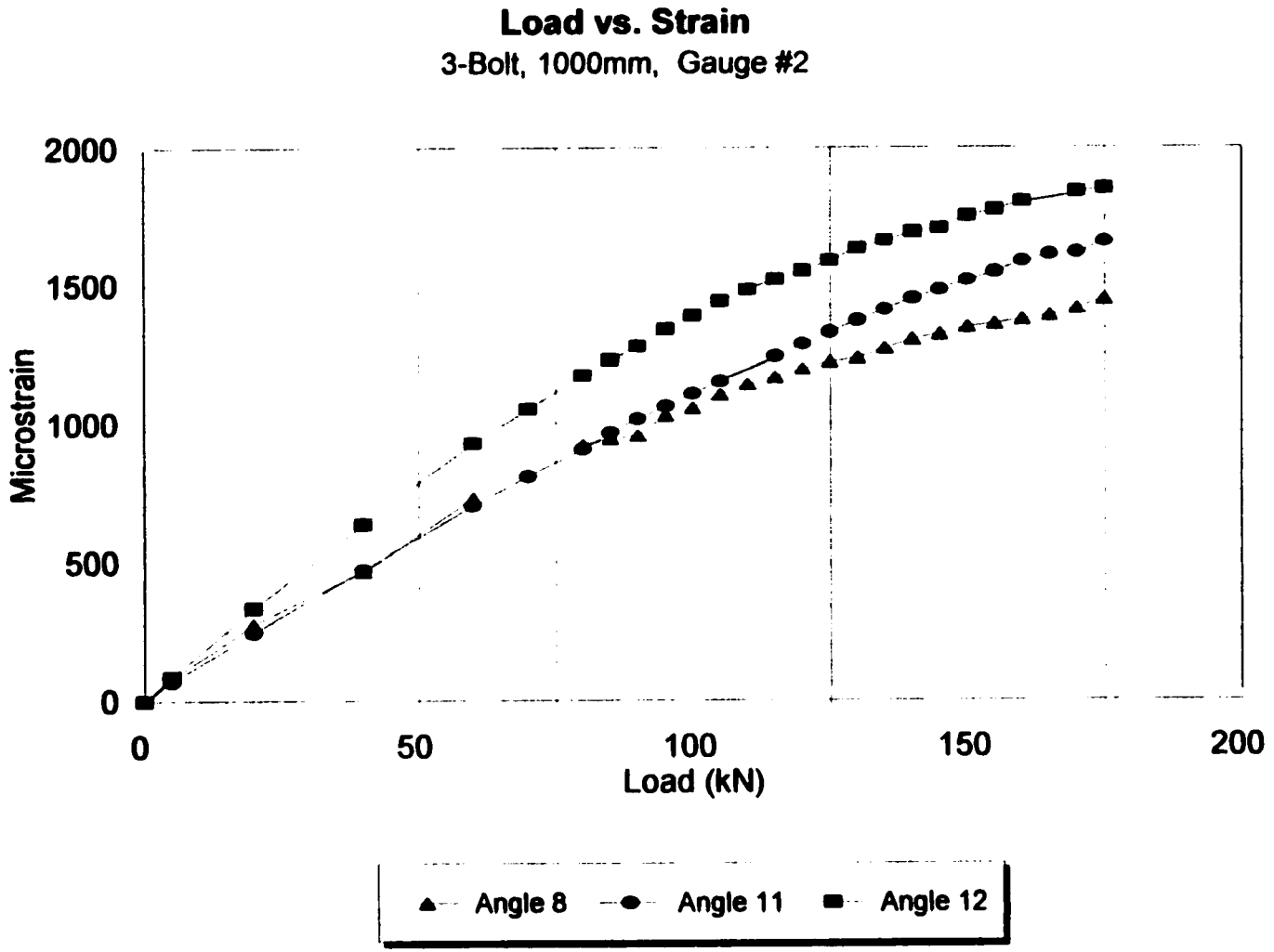

Figure C8: Load vs. Strain

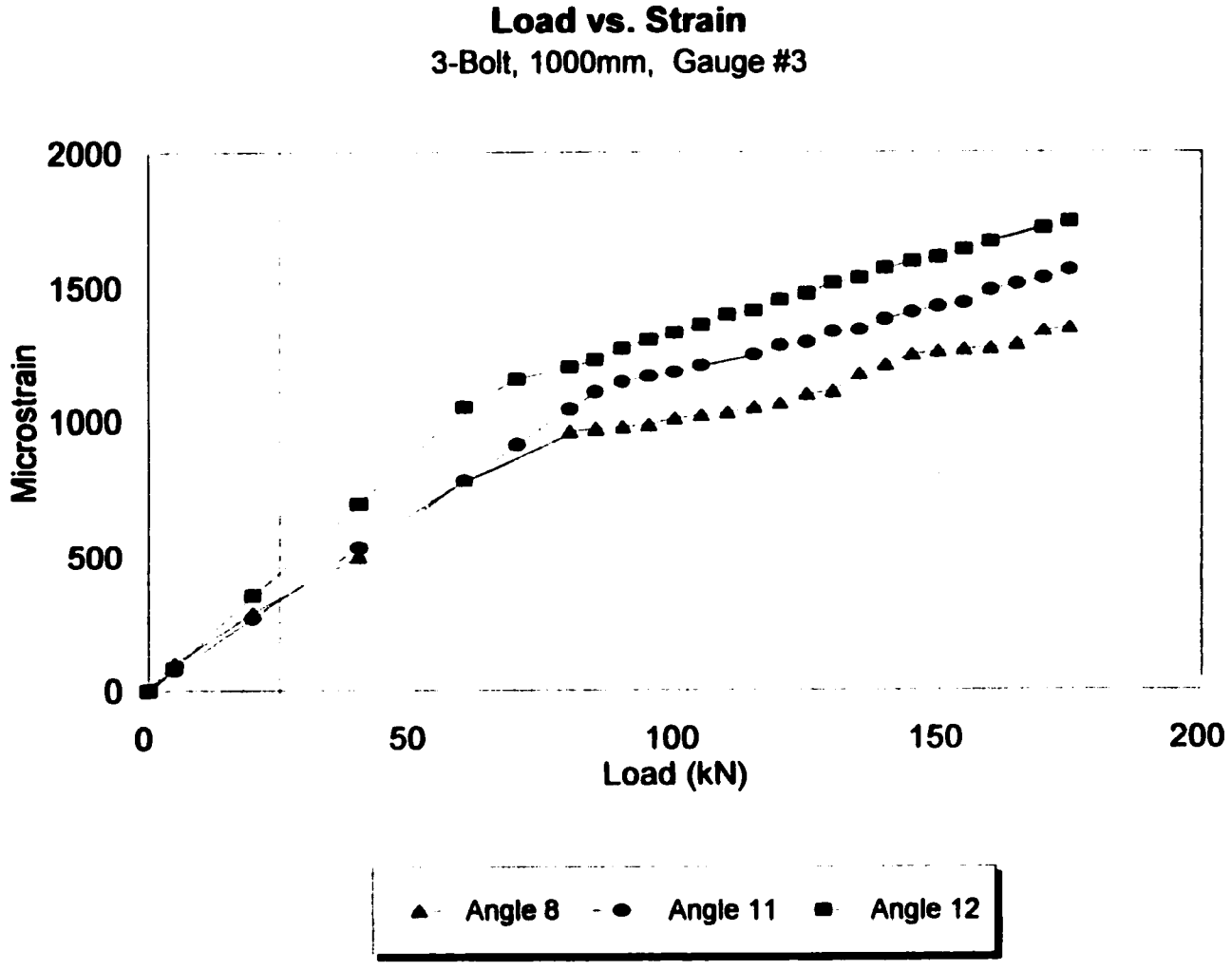

Figure C9: Load vs. Strain

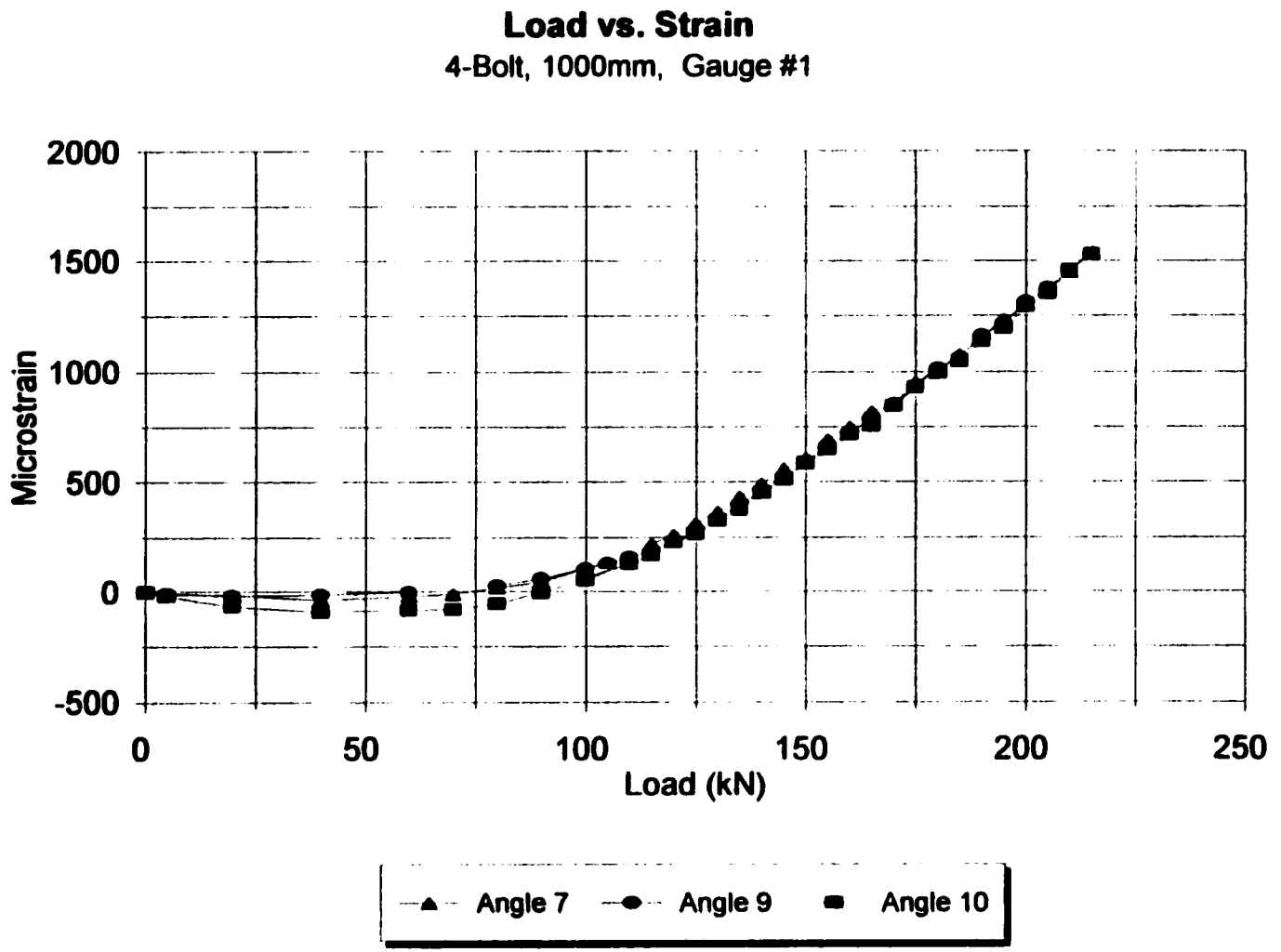

Figure C10: Load vs. Strain

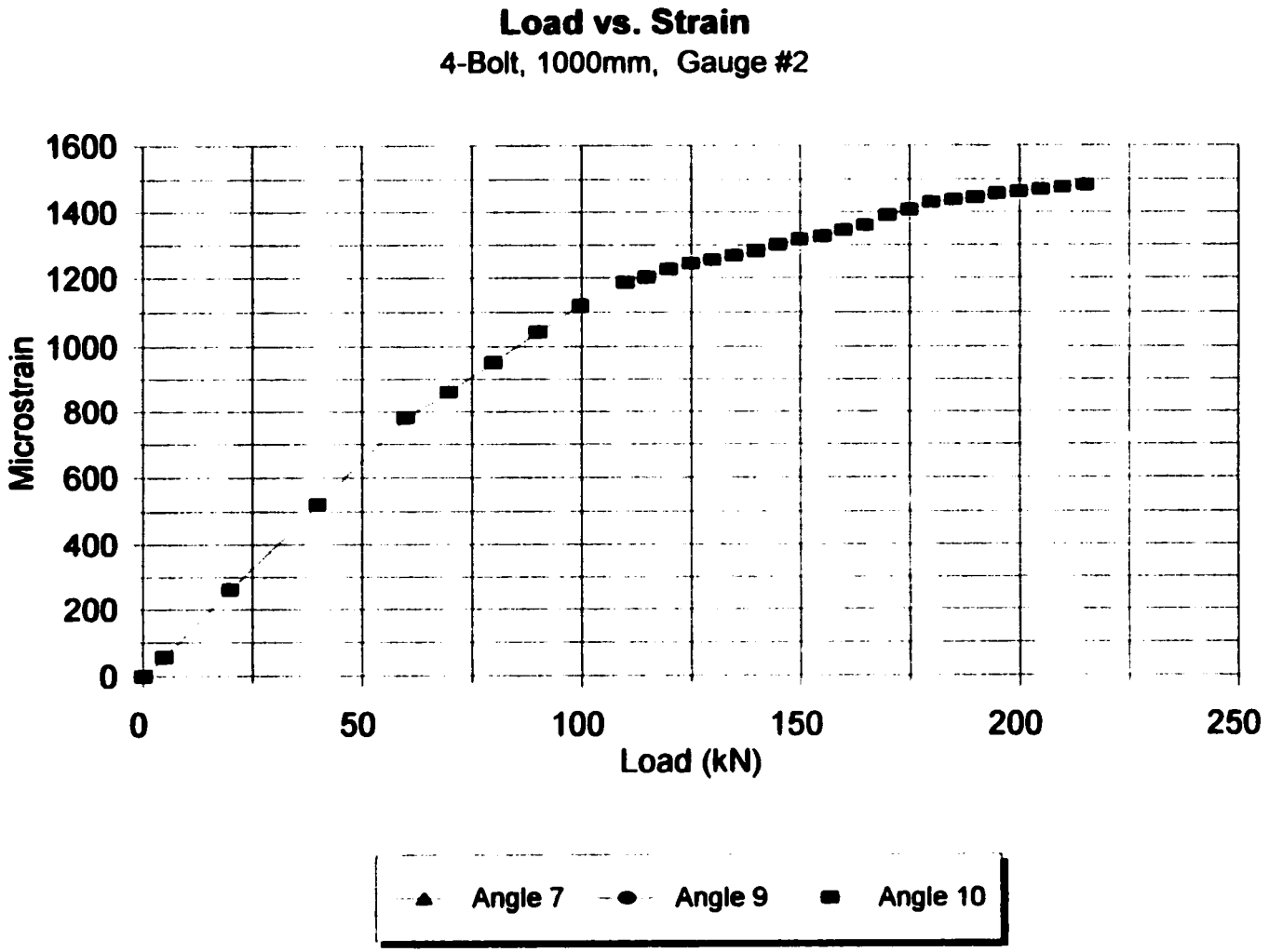

Figure C11: Load vs. Strain

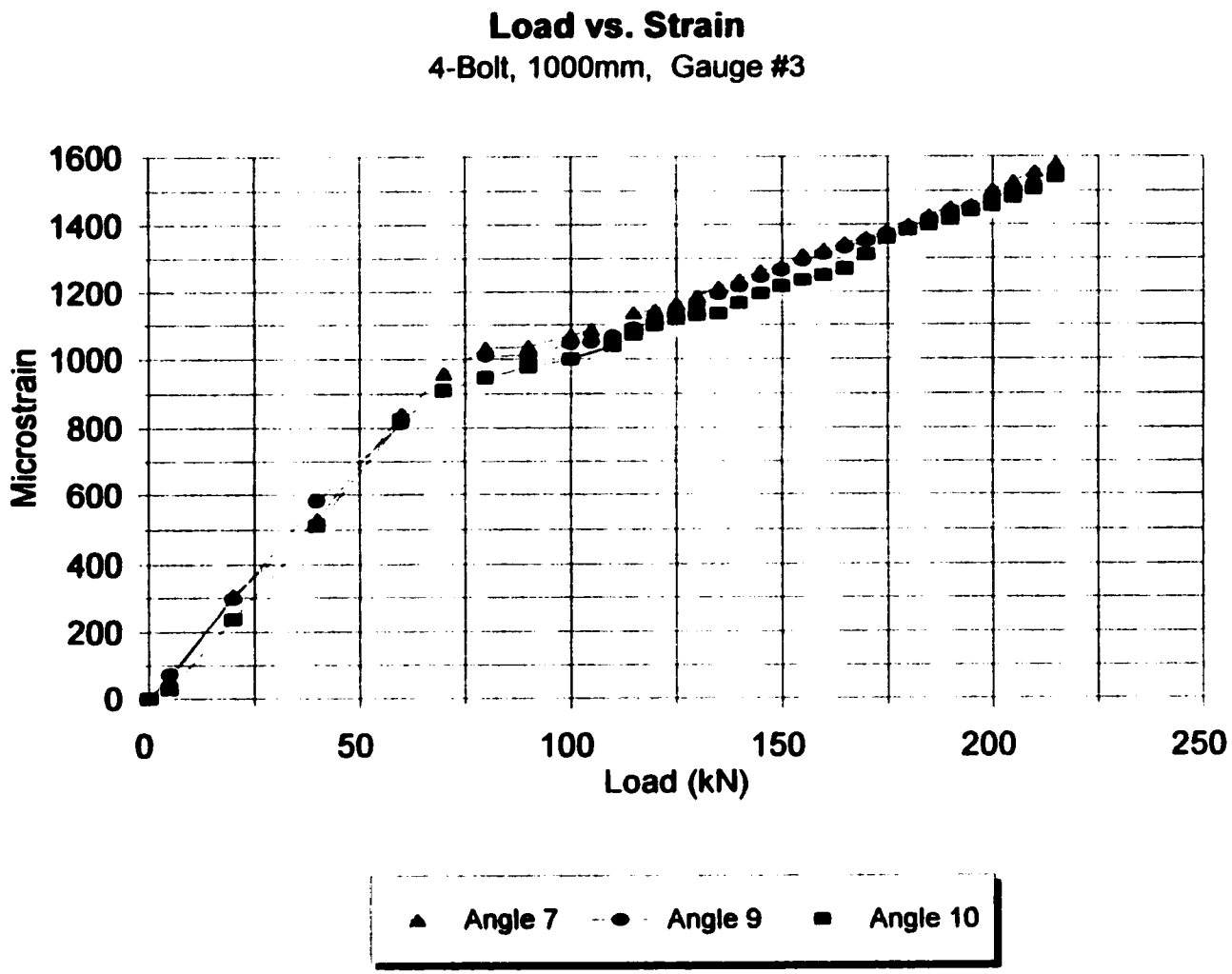

Figure C12: Load vs. Strain

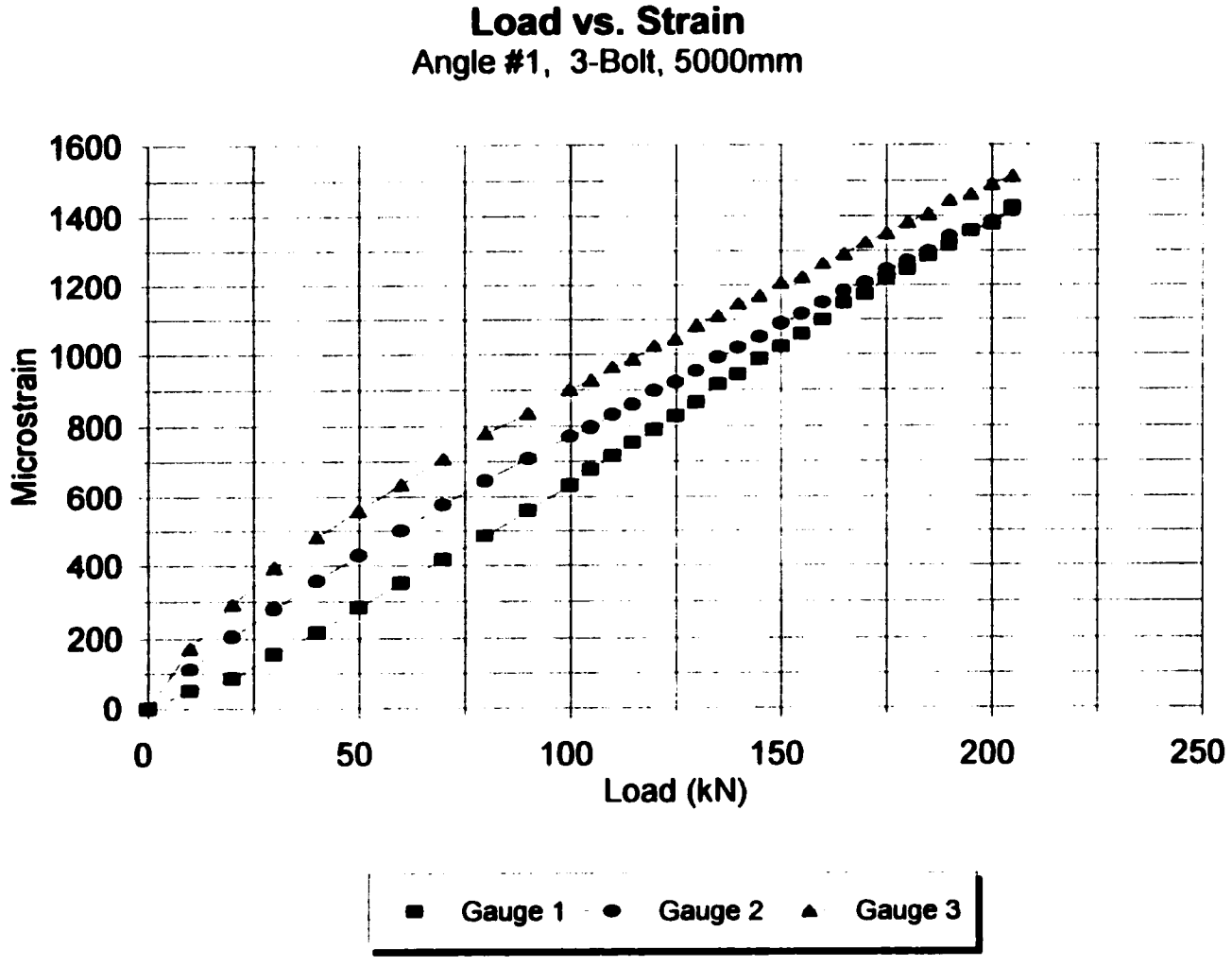

Figure C13: Load vs. Strain

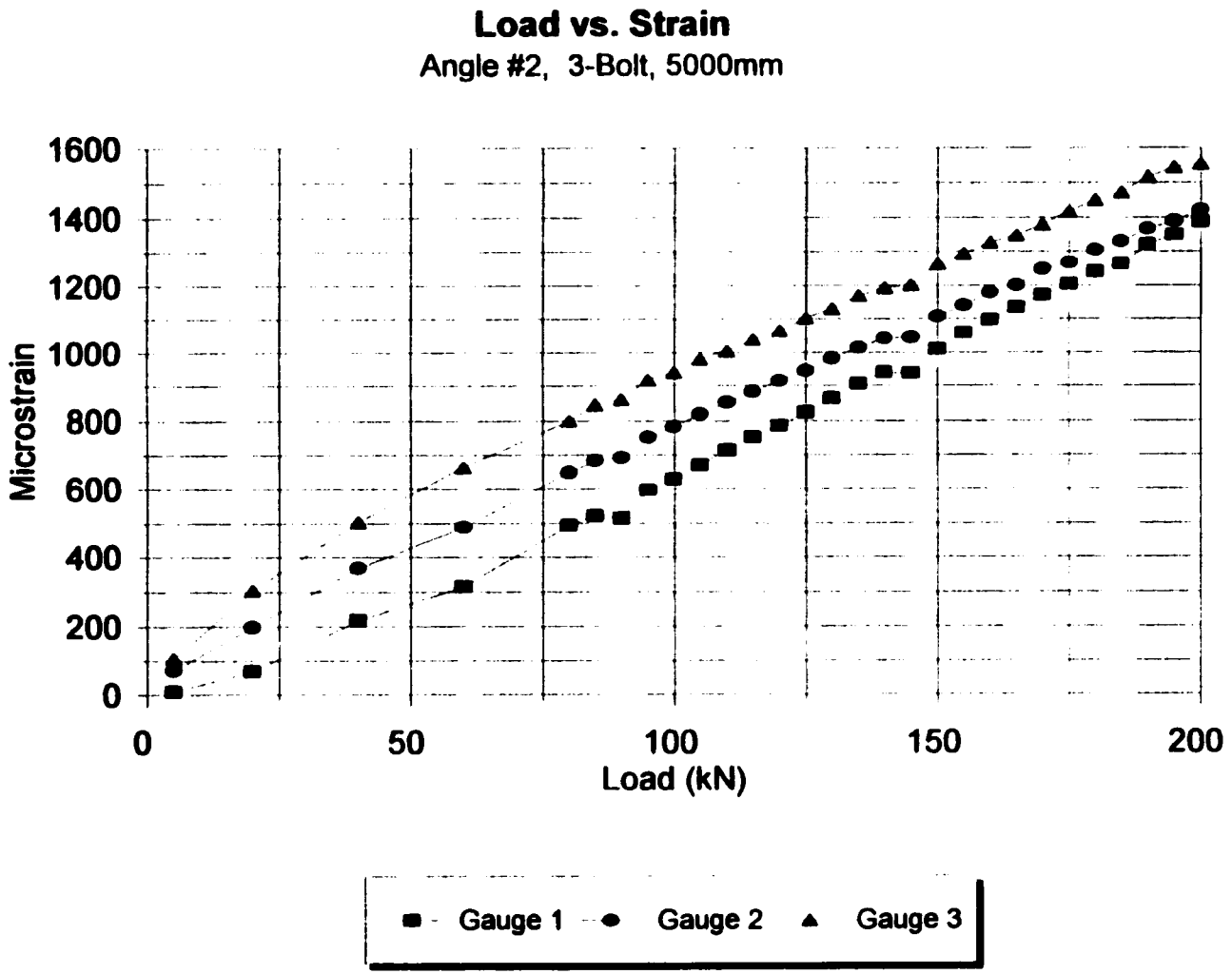

Figure C14: Load vs. Strain

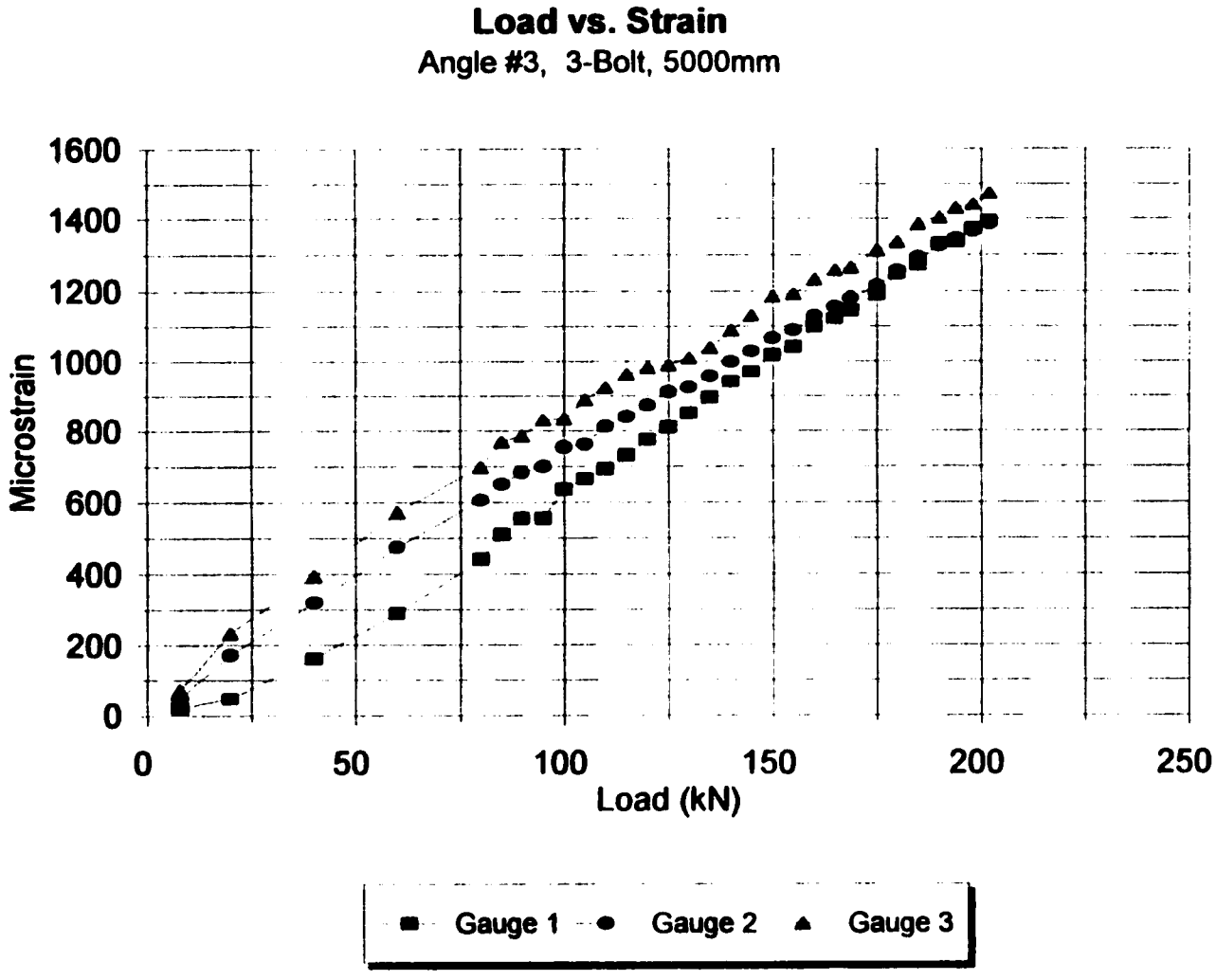

Figure C15: Load vs. Strain

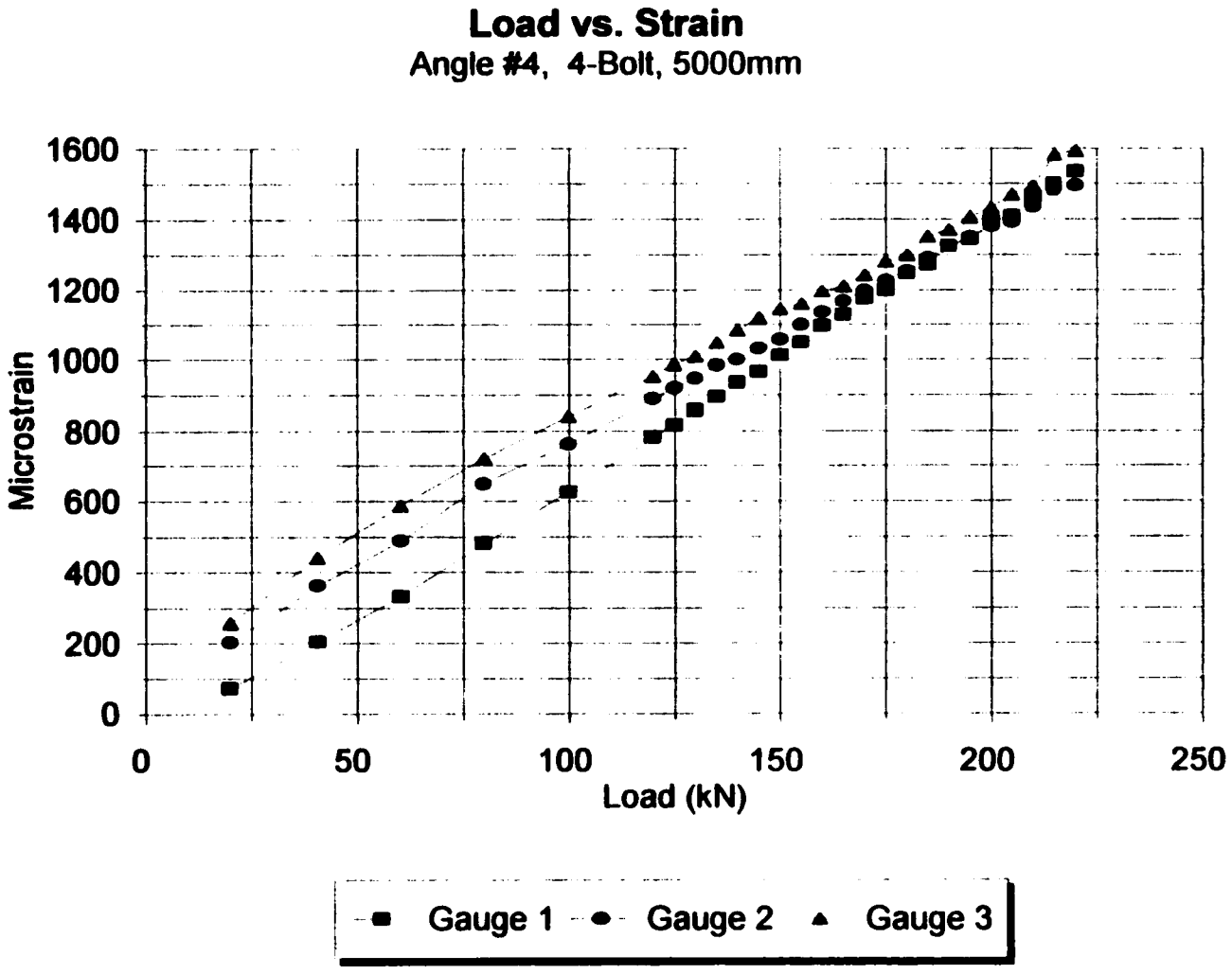

Figure C16: Load vs. Strain

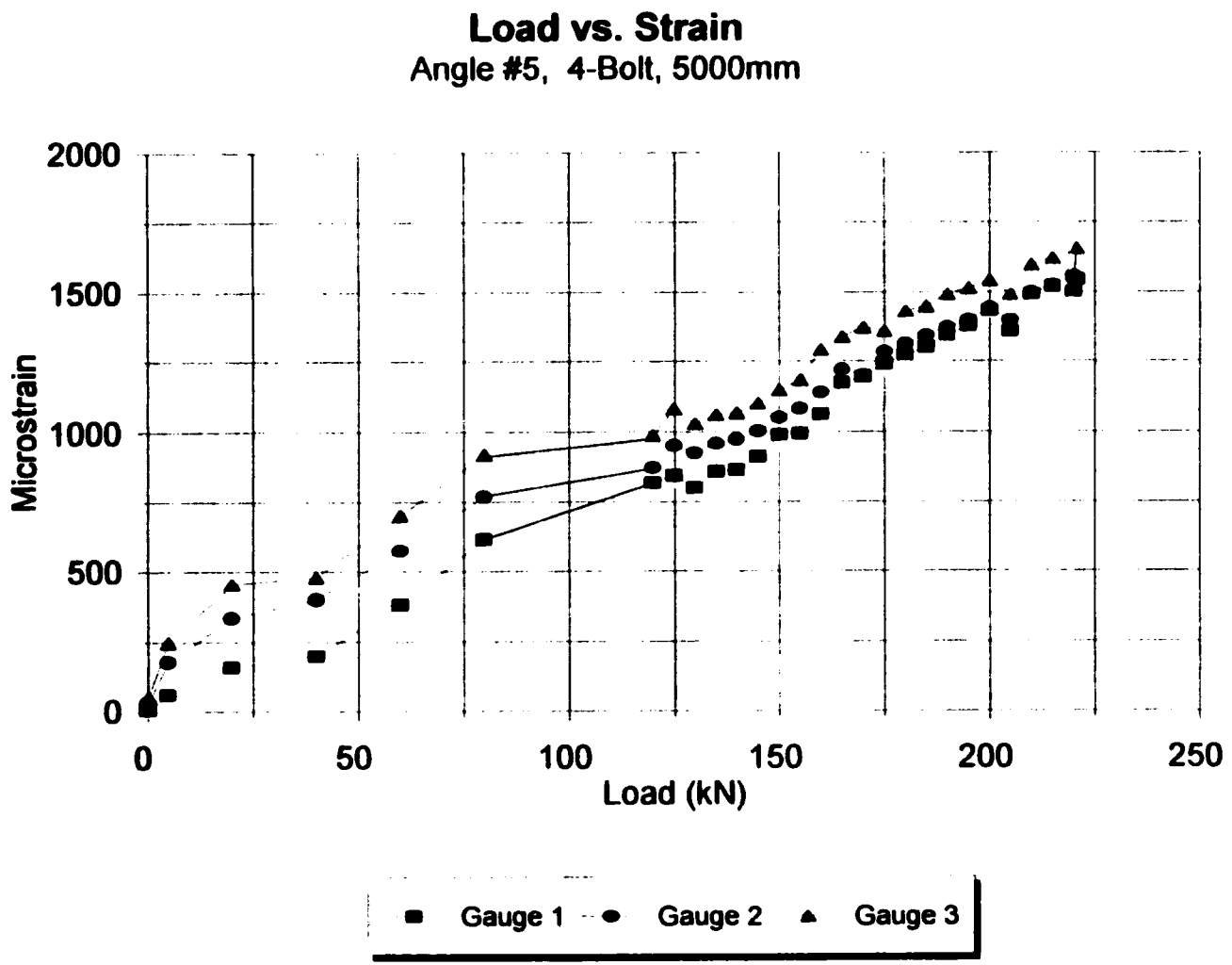

Figure C17: Load vs. Strain

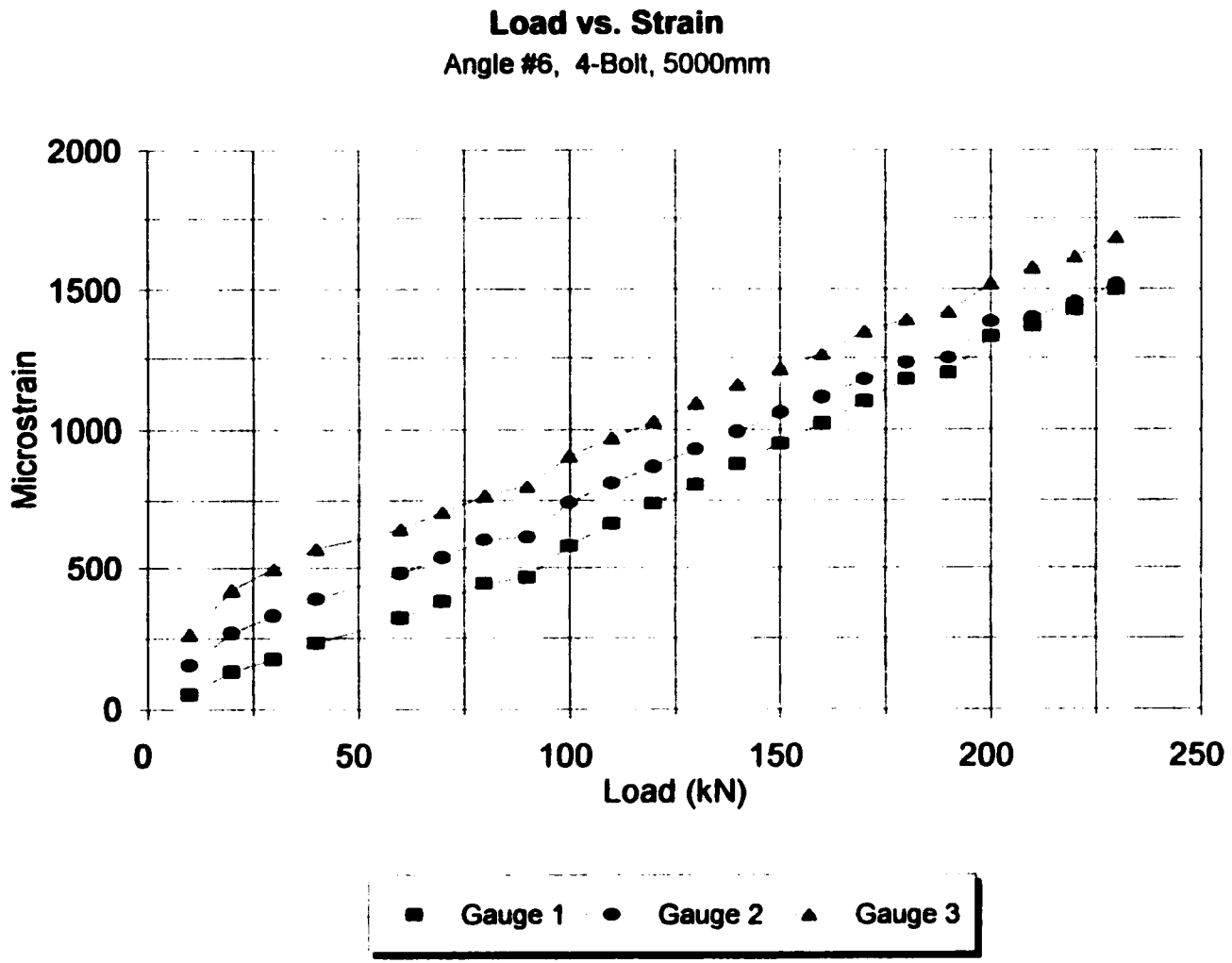

Figure C18: Load vs. Strain

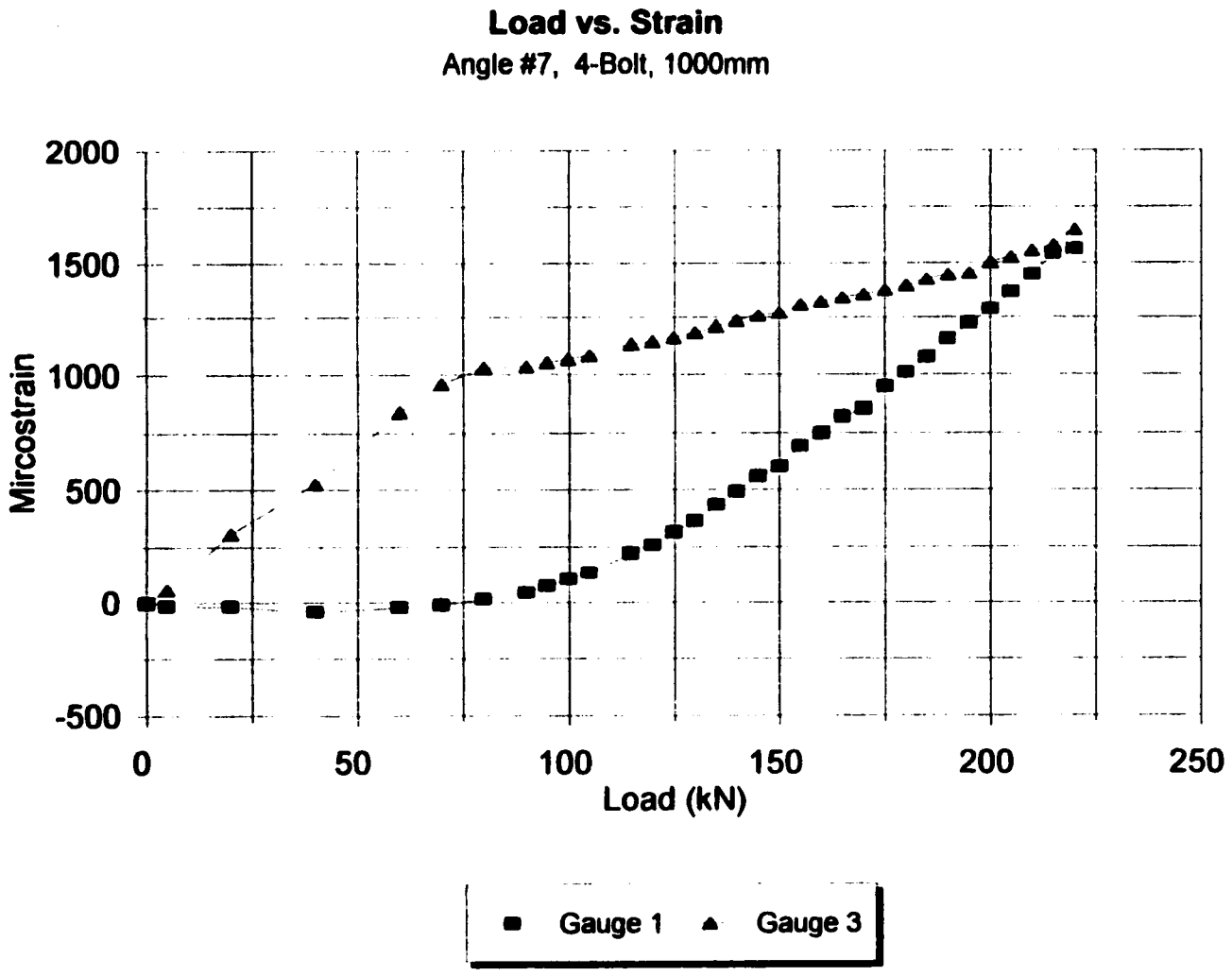

Figure C19: Load vs. Strain

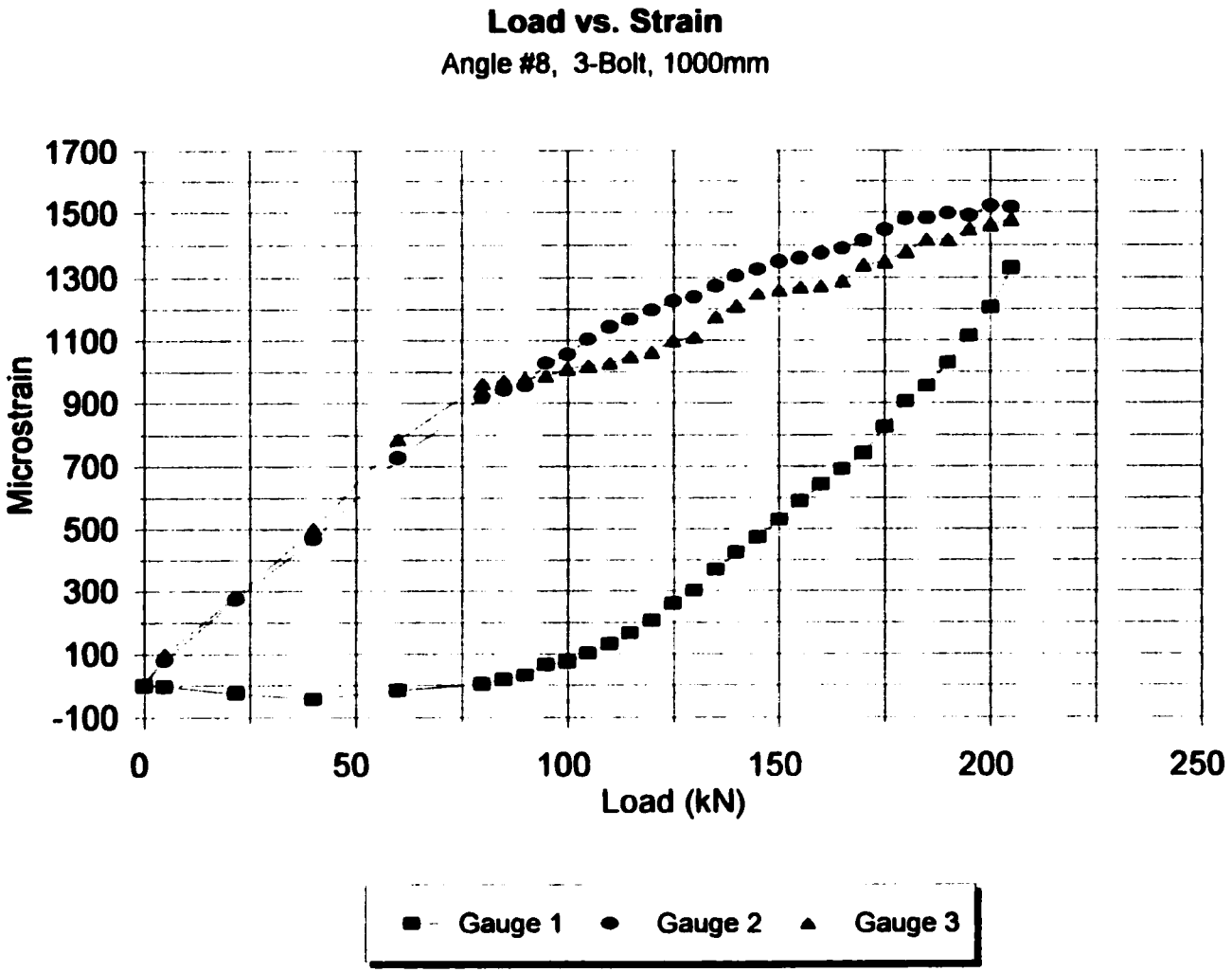

Figure C20: Load vs. Strain

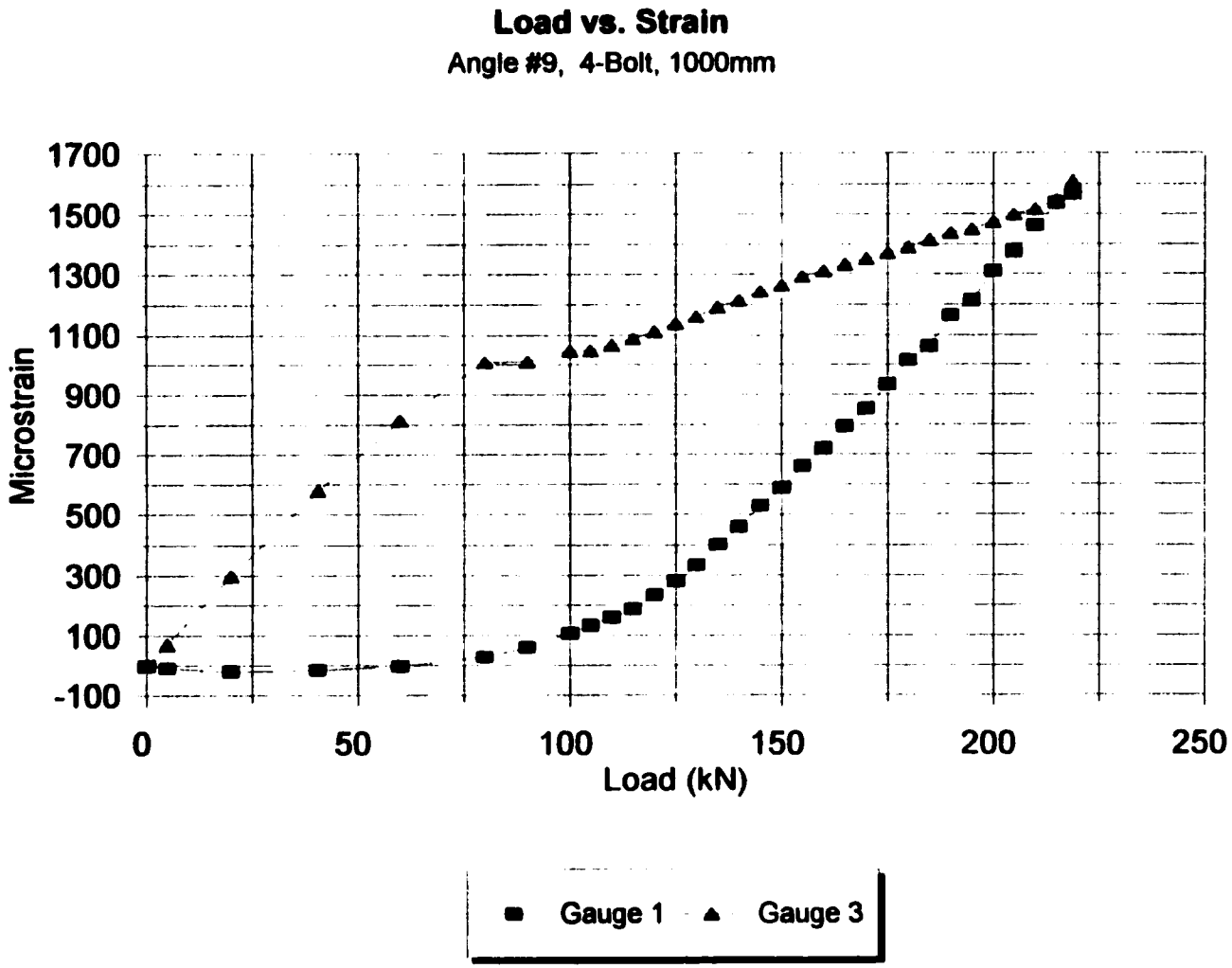

Figure C21: Load vs. Strain

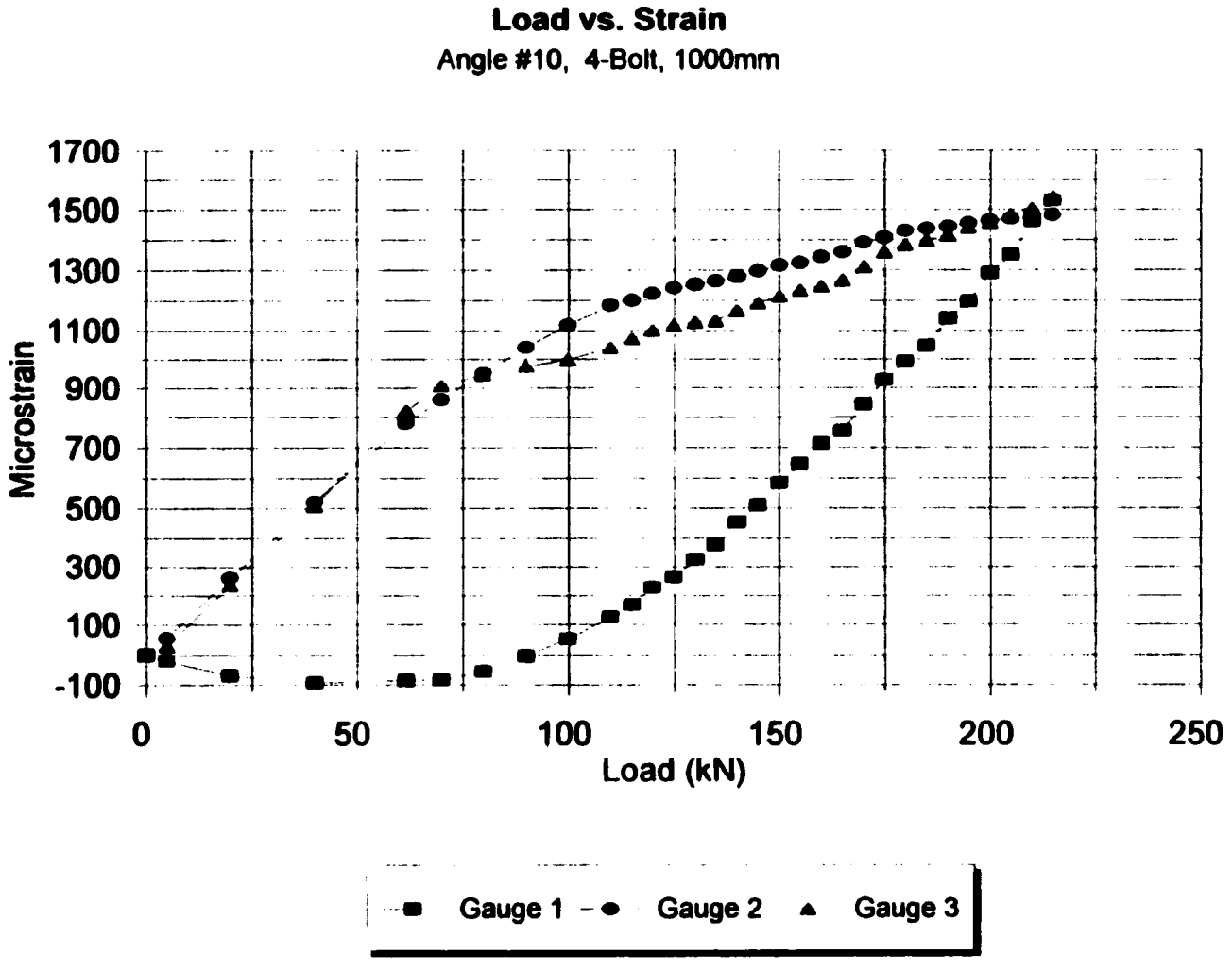

Figure C22: Load vs. Strain

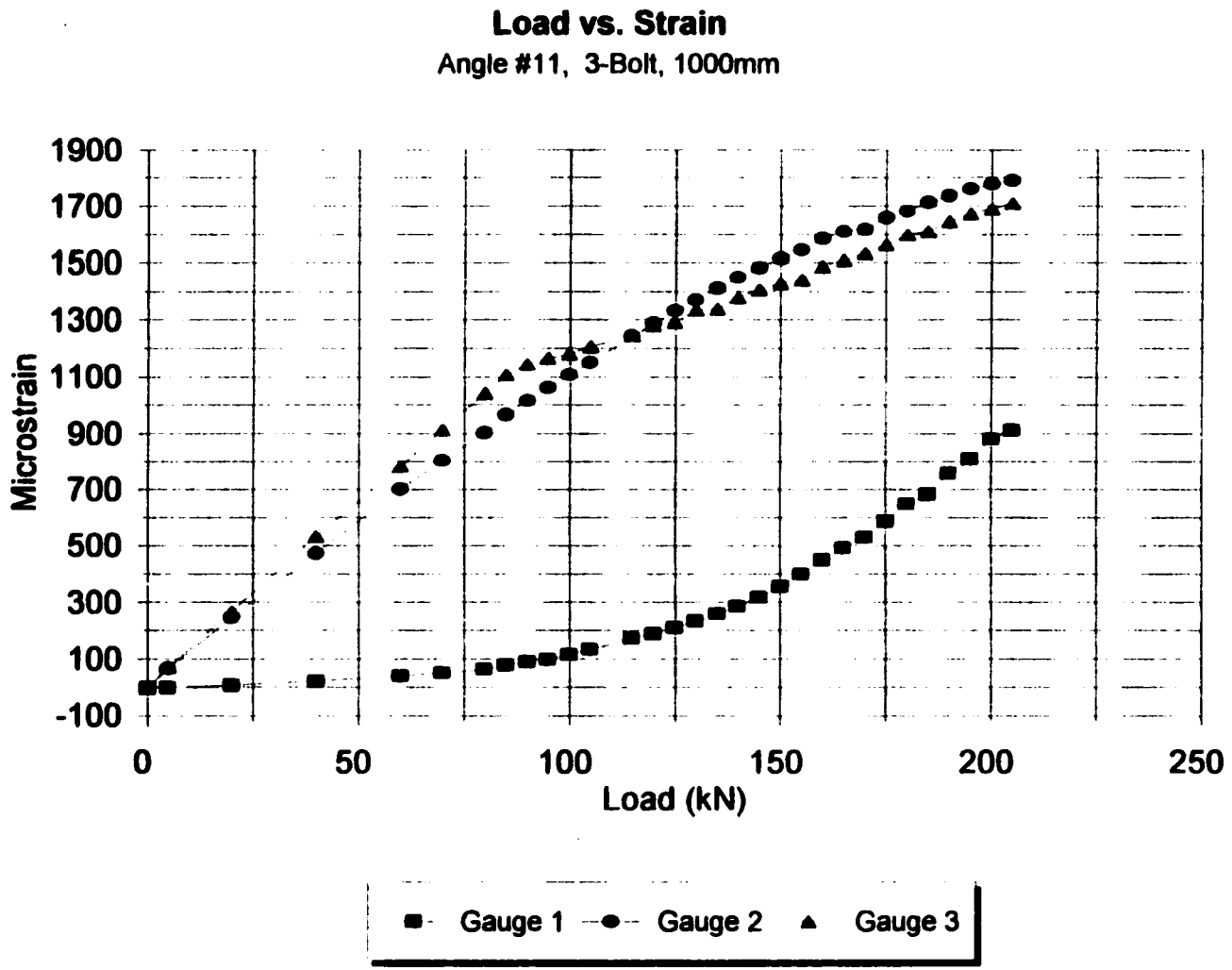

Figure C23: Load vs. Strain

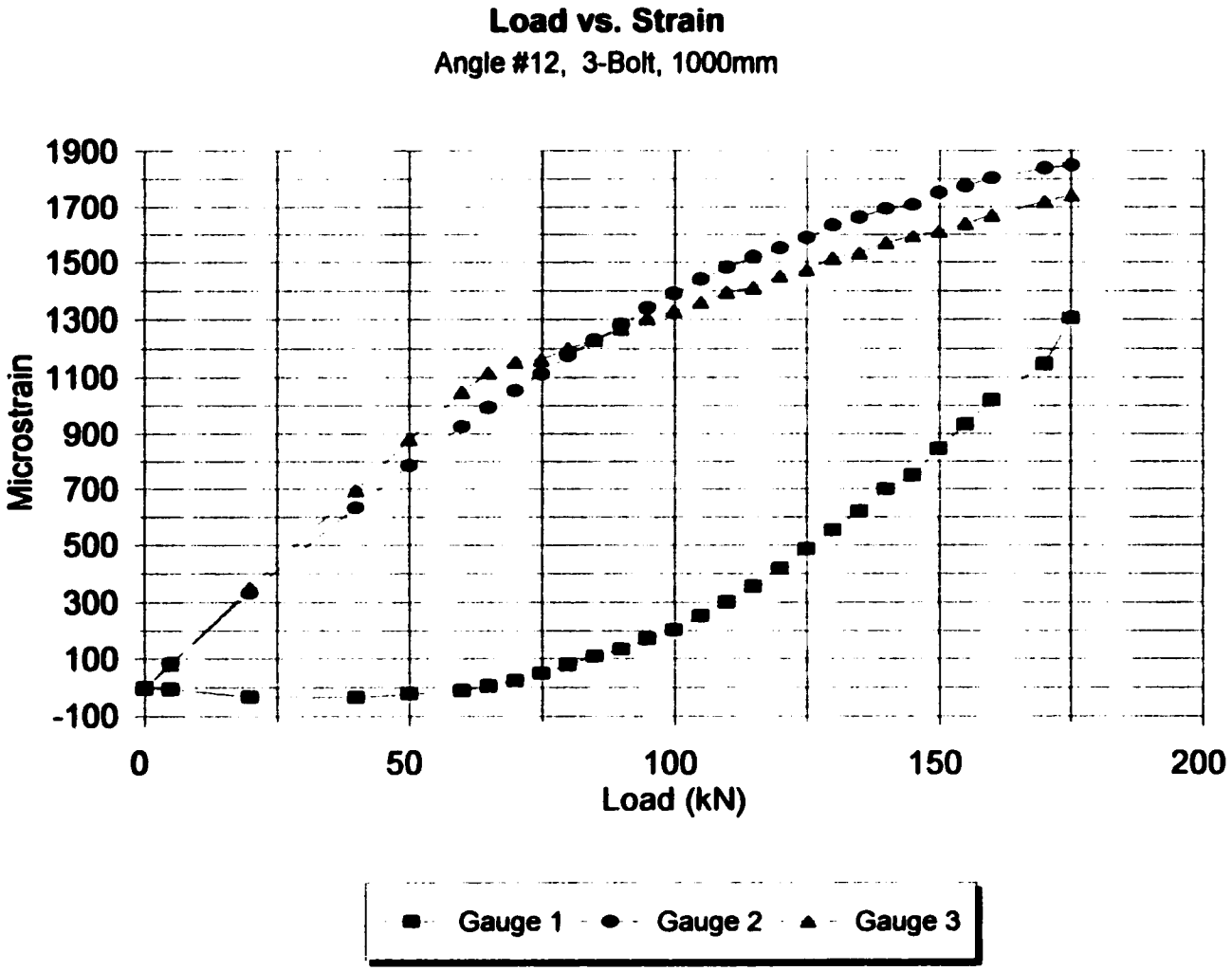

Figure C24: Load vs. Strain

REFERENCES

American Society for Testing and Materials. 1989. Section 3, Metals Test Methods and Analytical Procedures, Volume 03.01, Philadelphia, PA.

CSA. 1992. Structural Quality Steels. Standard CAN/CSA-G40.21-M92, Canadian Standard Association, Rexdale, Ont.

CSA. 1994. Limit States Design of Steel Structures. Standard CAN/CSA-S16.1-94, Canadian Standards Association, Rexdale, Ont.

Kulak, G.L. and Wu, E.Y. 1997. Shear Lag in Bolted Angle Tension Members. ASCE Journal of Structural Engineering, 123(9): 1144-1152.

McKibben, F.P. 1906. Tension Tests of Steel Angles. Proceedings of the American Society for Testing and Materials, 6:267-274.

McKibben, F.P. 1907. Tension Tests of Steel Angles with Various Types of End Connections. Proceedings of the American Society for Testing and Materials, 7:287-295.

Nelson H.M. 1953. Angles in Tension. British Constructional Steelwork Association, Publication No. 7: 8-18.

Temple, M, C. 1998. Private Communication, University of Windsor, Windsor, Ontario.

VITA AUCTORIS

Born on October 4, 1974 in North Bay.

Moved to Sudbury in 1976 where I remained until attending University in Windsor in the fall of 1993.

Graduated in 1997 with a Bachelor's of Applied Science in Civil Engineering.

Began Master's of Applied Science in Structural Engineering in the fall of 1997.